IAHR AIRH

Supported by Spain Water and IWHR, China

IAHR 2017

37th IAHR WORLD CONGRESS

13-18 August, 2017

Kuala Lumpur, Malaysia

INLAND AND COASTAL LAKE MANAGEMENT

Proceedings of the 37th IAHR World Congress
August 13 – 18, 2017, Kuala Lumpur, Malaysia

STUDY ON CONTROL MEASURES OF WATER QUALITY OF LAKE YINGHU

CUICHAO PANG(1), JING TAO(2), XIAOHUI WU(3), WEI GONG(4) & FANGFANG WANG(5)

(1,2,3,4) Changjiang Institute of Survey, Planning, Design and Research, Shanghai Department, Shanghai, China,
pangcuichao@163.com; mizitong@126.com; ahxhwu@163.com; 52541764@qq.com
(5) Hydraulic Engineering Department, Nanjing Hydraulic Research Institute, Nanjing, China,
Wff08020102@163.com

ABSTRACT

Lake Yinghu located in Changjiang delta area is a planned manmade urban shallow lake. To maintain the water quality of lake, there are two main measures, one is establishing a perfect aquatic ecological system to purify and maintain the water quality of lake, and another is replacing lake water body with clear water. Lake Yinghu closely connects to surrounding river net, and has good condition of water diversion. Controlling the connection condition between lake and surrounding river net to regulate the period of replacing water body of Lake Yinghu is an important factor influencing effectiveness of improving the water environment of Lake Yinghu. The numerical models, MIKE11 and Delft3D, were used to investigate the effectiveness of two schemes of controlling connectivity (connection entrance complete opening scheme and connection entrance gating scheme) in regulating the period of replacing water body of Lake Yinghu. The numerical results show that in the complete opening scheme case the water replacing period is about 12 days in the condition of long term average tidal level, 18 days in the condition of low tidal level with the probability of once in 20 years, and 14 days in the condition of high tidal level with the probability of once in the 20 years. Therefore, the risk of occurrence of Cyanobacteria bloom is large according to the criteria that the Cyanobacteria bloom would occur if the water replacing period exceeds 15~18 days in the summer (temperature > 25°C). In gating scheme case, six operation alternatives were simulated. The results show that the water replacing period of the gate operation alternative (three gates are diverting water, two gates are discharging water) is 14~15 days regardless of tidal condition. This indicates that the risk of occurrence of Cyanobacteria bloom is small in the Lake Yinghu. Besides, gating scheme could also protect lake from water pollution accidents occurred in the surrounding river net.

Keywords: Shallow lake; eutrophication; diversion; period of replacing water body.

1 INTRODUCTION

The shallow lakes in plain area are mostly connected to river net. Nowadays, as the lakes are polluted, it is not possible to maintain water quality and purify water in lakes by constructing and improving aquatic bio ecological system simultaneously. Diversion of clear water through the river net which are connected to the lake is an efficient and important measure in improving water quality of shallow lake. The controlling connectivity of lake and river net is the key issue to regulate the period of replacing water body of lake, and is an important factor influencing water environment.

Yinhu Lake is a manmade landscape urban lake in Chenjia town of Chongming island of Shanghai, and the water area is 1.83 km^2. Maintaining good water quality is key point for a manmade landscape urban lake, and managing scheme of river net is one of the key factors influencing water quality of the lake. This paper investigates the managing scheme of the river net connecting to Yinghu Lake to provide the theoretical and technical support for design and construction purpose.

2 Schemes of drainage control

The density of river net of Chongming island is high, there are no gates inside the net, and the connectivity of rivers inside the net is good. At the connection entrance between river net and Changjiang River sets gate which is used for water resource dispatch, flood protection and drainage, (Gong, W. et al., 2015). The principle of water resource dispatch is so-called “water diversion from the west to the east”, and “withdraw from the north, drain away in the north”. In the water project plan, Yinghu Lake has 10 entrances connecting to surrounding rivers, and is included in water dispatch plan of Chenjia town area. Normal water level of Yinghu Lake is 2.8 m; the water level in surrounding rivers increased to 2.9 m during water diversion from rivers to Yinghu Lake; during drainage period, the water level of Yinghu Lake drops to 2.1 m before rain fall, and the highest water level of Yinghu Lake is 3.65 m.

Two schemes of drainage control, entrance opening and entrance gating, are considered and compared under the condition of low risk of occurrence of algal bloom.

Previous researches showed that the over growth of algae can be controlled effectively by controlling the period of replacing water. According to the guide of catchment integrated management by United Nations Environment Program (UNEP), the hydraulic retention time in the lake or reservoir does not exceed 30 days generally, (Tong, C.F.et al., 2012; XI, Y.P. et al., 2008). The researchers of Shanghai environmental research institute indicate according to water temperature, abundance of algae in Changjiang estuary that for the lakes or reservoirs in this area, the appropriate hydraulic retention time is about 15~18d in the summer time (> 25 C°), 25~30 d in the Spring and Autumn (<20 C°), (Tang, Y.Z. et al., 2011). Although the hydraulic retention time is different from the replacing period (the time needed for replacing certain amount of low quality water by better quality water) conceptually, here we still use the above proposed criterion for hydraulic retention time for reference to assess the goodness of drainage control scheme as the flow is relatively uniform, smooth and no dead zone existed in the Yinghu Lake. Therefore, in this paper, the risk of occurrence of algal bloom in Yinghu Lake is determined by the following criterion, that is, the risk of occurrence of algal bloom is small when the period of replacing water is less than 15~18 days in the summer, and less than 25~28 days in the Spring and Autumn (Pang, C.C. et al., 2012).

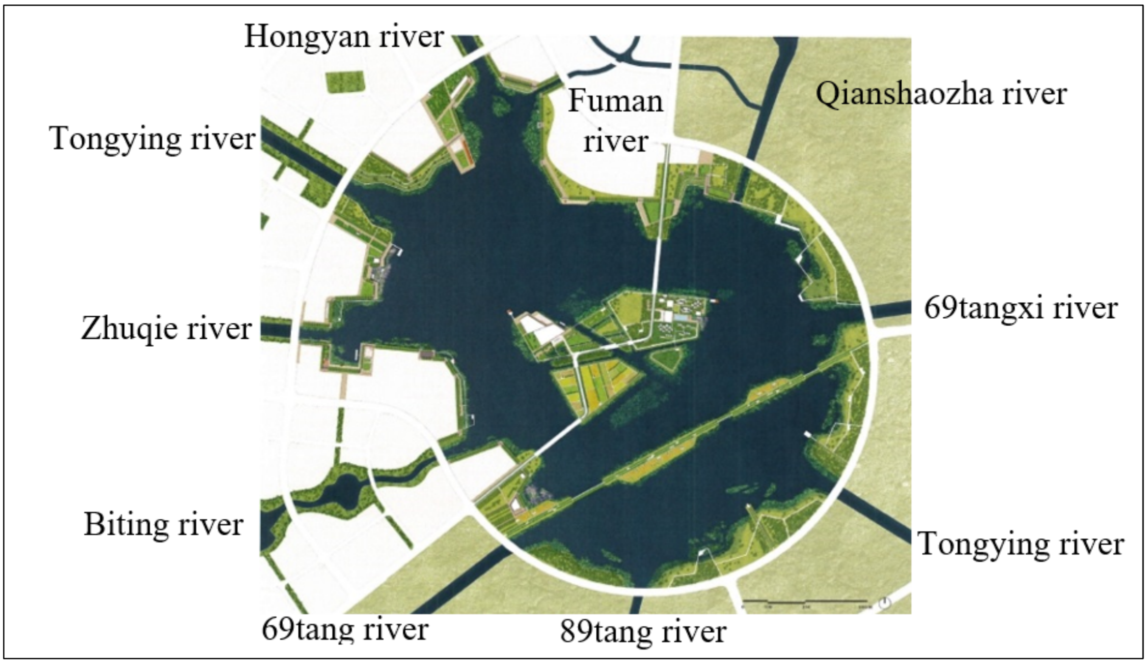

Figure 1. Lake Yinghu and surrounding rivers

3 COMPARISON OF THE EFFECTIVENESS IN WATER QUALITY CONTROL OF TWO SCHEMES

3.1 Entrance opening scheme

To compare the schemes, two numerical models were employed. One is MIKE11 model, HD module (DHI, 2012), which is used to simulate flow field of Chongming island river net during water resource dispatch process and provide the boundary conditions for 10 entrances of Yinghu Lake. Those boundary conditions are used for calculation of period of replacing water of Yinghu Lake. The period of replacing water was calculated by two dimensional version of Delft-3D model, Flow module (W L. Delft Hydraulics, 2010).

(a) Computational domain

Computational domain is the whole river net of Chongming island, Figure 2.

(b) Computational conditions

i. Boundary conditions

Hydraulic condition: typical tidal stencils of average annual tidal level, i.e. 00:00, 1997.08.05~00:00, 1997.08.25. At the connection entrance between river net and Changjiang river, the gated control conditions are listed in table 1.

Water quality condition: Here, conservative substance was used as tracer. The concentration of tracer is 1 mg/L.

ii. Initial conditions

Hydraulic condition: water level is 2.8 m, velocity is 0.0 m/s

Water quality condition: conservative substance concentration is 1.0 mg/L in river net, 0.0 mg/L in Yinghu Lake.

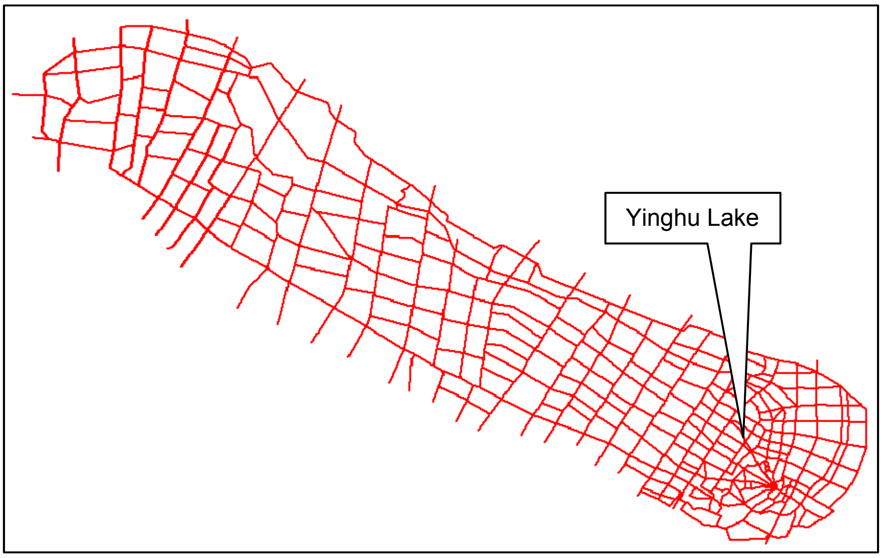

Figure 2. Schematized river net of Chongming island

iii. Roughness: 0.025~0.030

iv. Degration rate: Degration rate is assumed as 0.0 as tracer is conservative substance.

(c) Computation mesh

River net mesh: mesh size is 300 m, mesh size may be smaller in some river.

Yinghu Lake mesh: two dimensional orthogonal mesh, total 82*82 elements.

(d) Determination of the entering and exiting entrances of Yinghu Lake

Chenjia down diverts water 1~2 times a day, each diversion takes about 3~4 hours in the case of average annual tidal level. After calculation, the main entering entrances are Hongyan river, west part of Tongying river, Zhuque river, Biting river and 69tang river. The discharge ratios of these rivers are 1.7:3.0:2.7:3.6:1.0. The main exiting entrances are 89 Tang river, east part of Tongying river, 69 Tangxi river, Qianshaozha river and Fuman river. The discharge ratios of those rivers were 2.8:16.9:8.4:3.0:1.0.

Figure 3 shows the flow patterns of several typical diverting and draining cases.

(e) Computational results

According to water conservancy planning of Chongming island and sluices' dispatching scheme along the Changjiang river, the water replacing process was simulated. The changing process of conservative substance concentration with time is shown in Figure 4.

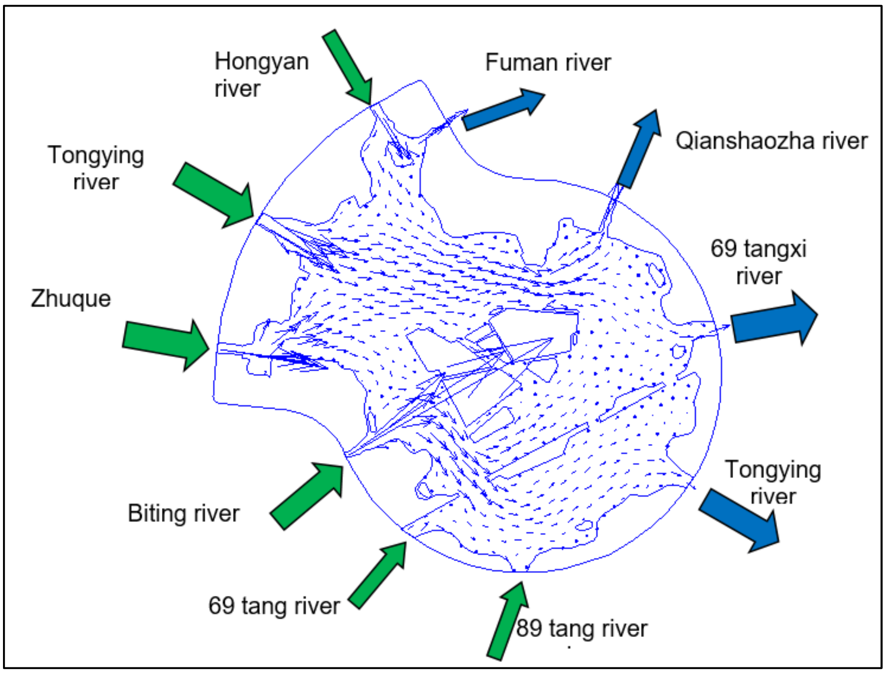

(a) Diverting case

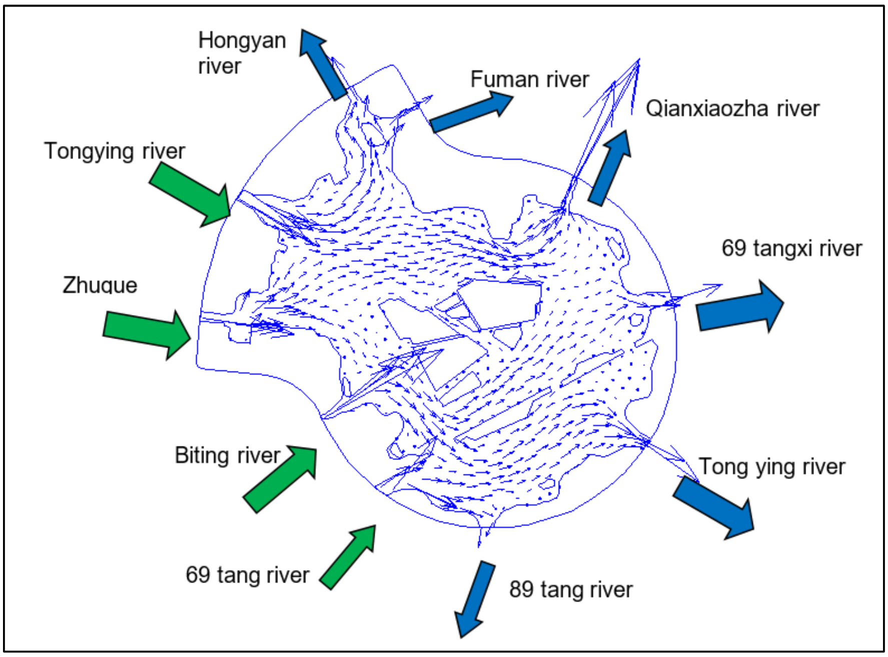

(b) Drain case

Figure 3. Flow pattern of two regulation cases.

Table 1. Regulation scheme

Type of regulation		Chongxi gate	Sanshahong gate	Other gates	Drain gate
Zinside max (Max. level inside gate, m ）		3.00	3.00	3.20	2.60
Z1outside (Level 1 outside gate, m）		3.50	3.50	3.80	2.00
Z2outside (Level 2 outside gate, m）		4.60	4.60	4.60	1.50
Gate opening（m）	Zoutside≤Zinsidemax and Zoutside>Zinside（diversion gate） Zoutside≥Zinsidemax and Zinside>Zoutside（drain gate）	Full open	Full open	Full open	Full open
	Zinsidemax＜Zoutside≤Z1outside（diversion gate） Z1outside＜Zoutside≤Zinsidemax（drain gate）	0.80	0.80	1.00	1.00
	Z1outside＜Zoutside≤Z2outside（diversion gate） Z2outside＜Zoutside≤Z1outside（drain gate）	0.30	0.30	0.50	0.50
	Zoutside＞Z2outside（diversion gate） Zoutside＜Z2outside（drain gate）	Close	Close	Close	Close

Note: subscript “outside” means Changjiang side, subscript “inside” means river side.

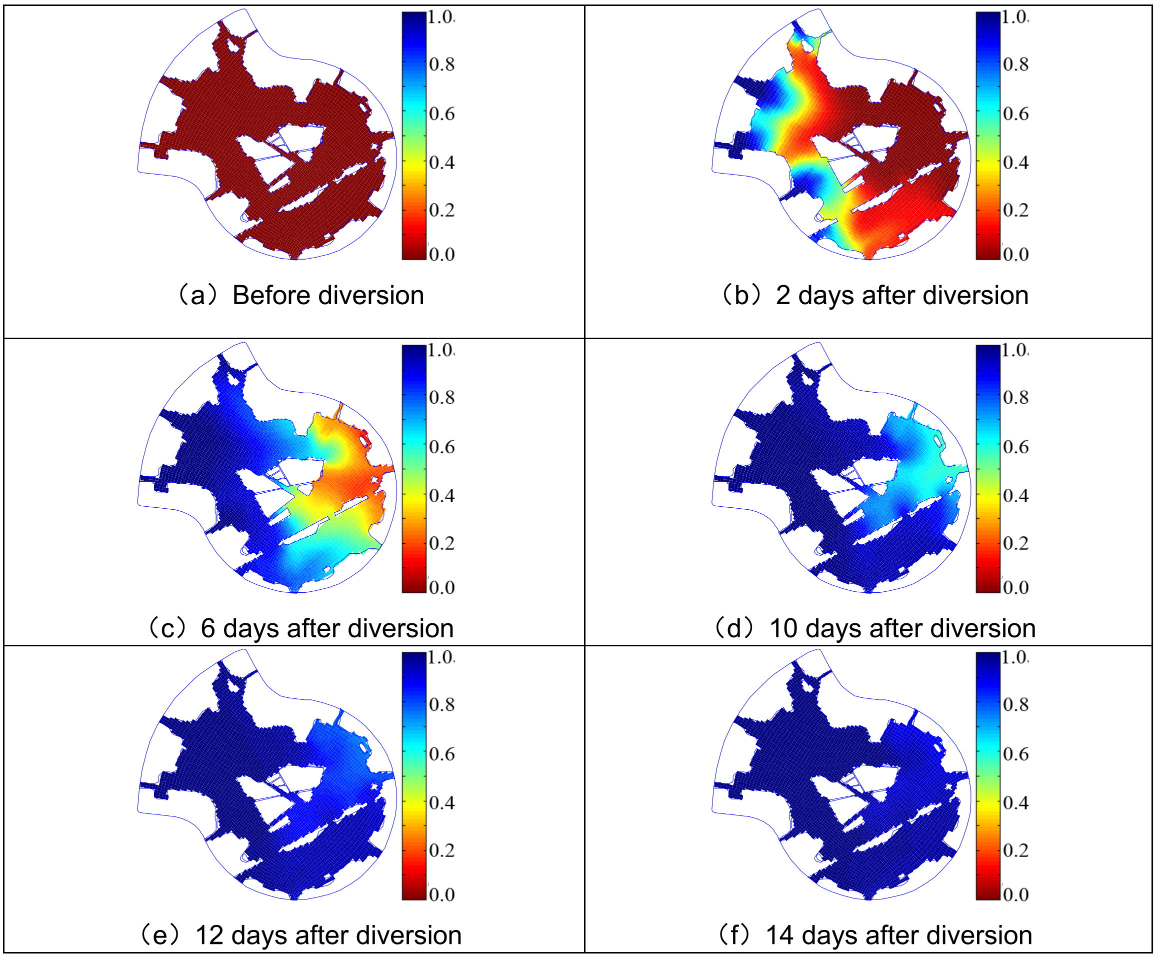

（a） Before diversion
（b） 2 days after diversion
（c） 6 days after diversion
（d） 10 days after diversion
（e） 12 days after diversion
（f） 14 days after diversion

Figure 4. The changing concentration of conservative substance with time (mg/L)

From the figure, several comments can be drown as following:

(a)The water is replaced gradually from southwest part to northeast part.

(b)The water in most part of the lake is replaced after 9~10 days. The water in the lake is almost replaced completely after 12 days, the difference of conservative substance concentration between surrounding river and Yinghu Lake is less than 1~5% at that time. Therefore, the period of replacing low quality water by clear water in Yinghu Lake is about 12 days in the average annual tidal level case.

(c) The periods of replacing water in low tidal level and high tidal level of probability of once in 20 years are 18 days and 14 days respectively, they are longer than that in average annual tidal level case. Therefore, the risk of occurrence of algal bloom is higher in summer time.

3.2 Gate regulating scheme

In the gating regulating scheme, the water level in lake can be raised to 3.2 m that makes better landscape of the lake. In this scheme, Yinghu Lake cannot have water exchange process simultaneously when water system in Chenjia down area operates water resource dispatching program as the water level in lake is higher than the water levels in surrounding rivers. In order to maintain the water quality in lake, the pumping stations are set in appropriate entrances, the water replacement is realized by operating those pumping stations.

3.2.1 Operation condition

The operation conditions of those pumping stations are as follows:

During May to October, pump stations are operated to reduce the risk of occurrence of algal bloom when water quality of river net in Chenjia town area is good and in Yinghu Lake is worse; Pump stations are not operated when pollution accident occurs in surrounding rivers to prevent lake from pollution. The pump stations would operate if the pollution accident is fully controlled, the water quality is improved, and the diversion is necessary for improvement of water quality in the lake.

During November to April of next year, the diversion does not realize the prevention of salt water from entering lake. The pumping station would operate to compensate water to lake keep water level at 3.2 m.

The water resources scheduling of Yinghu Lake: pumps are operating 24 hours per day, total diverting discharge is about 6.67 m^3/s (ecological water demand), several gates are selected to discharge the water, and the upstream water level of those gates are kept as 3.2 m.

3.2.2 Criterion of selecting entering entrances and exiting entrances

The criterions of selecting entering entrances and exiting entrances are as follows:

- Diversion entrance is near diversion gate of Chenjia down river net (Baxiaogang south gate and Xijiagang gate) to divert high quality water;
- The river connecting the diversion entrance should be main river, secondary main river, or the first grade branch of the river net in Chenjia town area in order to avoid large velocity occurred in the river during pumping;
- Small pools must be set in the rivers connecting to the diversion entrance. Those pools function as fore-reservoirs pretreating and regulating the water;
- The diversion and drain entrances are selected as similar as possible to entering and exiting entrances in the all entrance open case and agree well with the general flow direction of whole river net in Chenjia town area.
- The period of replacing water is as short as possible for certain diverting water quantity.

3.2.3 Entrance composite mode

There are 6 composite modes under consideration:

- One enter and one exit, i.e. one entrance diverting water and one entrance draining water. Here, Western part of Tongying river diverts water into lake, Eastern part of Tongying river drains water out of lake.
- One enter and two exits, i.e. one entrance diverting water and two entrances draining water. Here, Western part of Tongying river diverts water into lake, Eastern part of Tongying river and 69tangxi river drain water out of lake.
- One enter and three exits, i.e. one entrance diverting water and three entrances draining water. Here, Western part of Tongying River diverts water into lake, Eastern part of Tongying river, 69tangxi river and 89tang river drain water out of lake.
- Two enters and two exits, i.e. two entrances diverting water and two entrances draining water. Here, Western part of Tongying river and Biting river divert water into lake, Eastern part of Tongying river, and 69tangxi river drain water out of lake.
- Three enters and two exits, i.e. three entrances diverting water and two entrances draining water. Here, Western part of Tongying river, Hongyan river and Zhuque river divert water into lake, Eastern part of Tongying river and 69tangxi river drain water out of lake.
- Three enters and three exits, i.e. three entrances diverting water and three entrances draining water. Here, Western part of Tongying river, Hongyan river and Zhuque river divert water into lake, Eastern part of Tongying river, 69tangxi river and 89tang river drain water out of lake.

We used Delft-3D model to simulate the consequences of replacing water and period of replacing water for different water transfer manners under constant diversion discharge in order to select optimal water transfer manner.

3.2.4 Computational domain and computational conditions

a. Computational domain

Whole Yinghu lake.

b. Computational conditions

i. Boundary condition

Hydraulic condition: total diverting discharge is 6.67 m^3/s (6.67 m^3/s for one entrance in one enter case; 3.33 m^3/s for each entrance in two enters case; 2.22 m^3/s for each entrance in three enters case), diversion time is 24 hours per day, the water level is 3.2 m at draining entrances.

Water quality condition: conservative substance concentration is 1 mg/L.

ii. Initial condition

Hydraulic initial condition: water level is 3.2 m, velocity is 0.0 m/s,

Water quality initial condition: conservative substance concentration is 0 mg/L.

iii. Roughness: 0.025~0.030;

iv. Degradation rate: degradation rate assumes 0.0/day.

c. Mesh

82×82 elements.

d. Results and discussion

The computational results are shown in Figures 5 to 9.

It can be seen from the figures that water transfer mode, three enters and two exits (Western part of Tongying river, Hongyan river and Zhuque river divert water into lake, Eastern part of Tongying river and 69tangxi river drain water out of lake) replaces the water in Yinghu Lake most completely and efficiently. All the water in the lake was completely replaced by good quality water in 14~15 days. The international forum and business district is located nearby the western part of the lake, the requirement of landscape is high, therefore, the water transfer Modes, one entry and two entries, which are not efficient in replacing the water in western part of the lake are not appropriate Modes. Besides, among the water transfer Modes, the one with three exits discharges clear water out of lake before the low quality water in the lake is replaced completely. The Mode with one exit only cannot replace the low quality water in the lake fully, the low quality water in the area near central island and dyke cannot be replaced due to water remains in a standstill there.

It can be concluded that the Mode with three enters and two exits, i.e. Western part of Tongying river, Hongyan river and Zhuque river divert water into lake, Eastern part of Tongying river and 69tangxi river drain water out of lake, is the best Mode for replacing the low quality water of Yinghu lake.

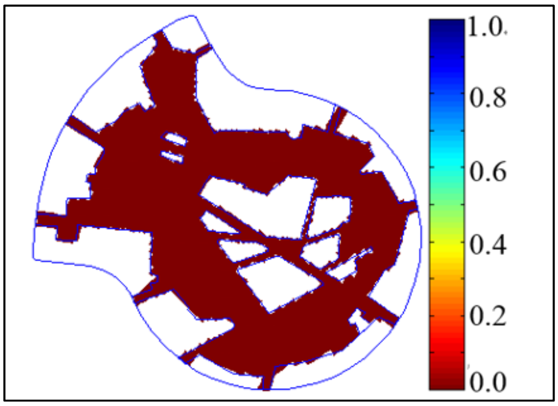

Figure 5. The concentration of conservative substance before diversion (mg/L)

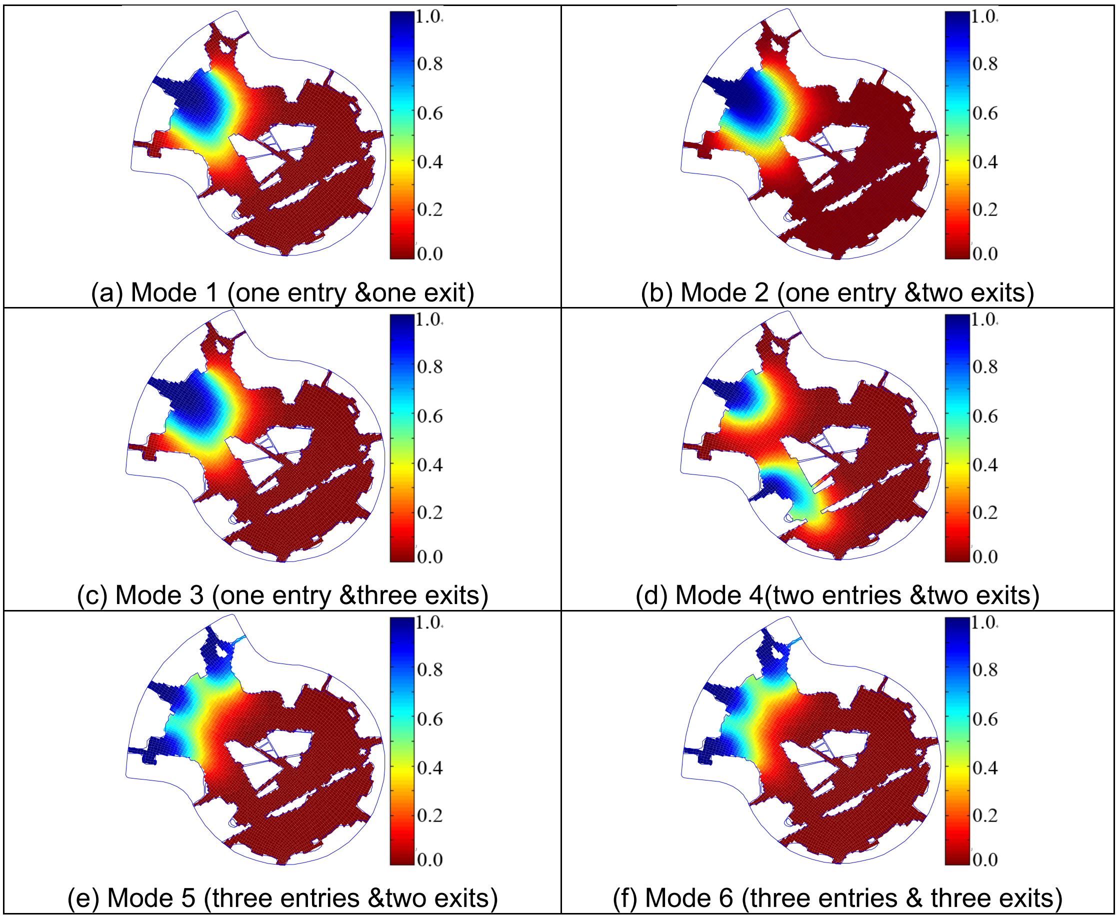

(a) Mode 1 (one entry &one exit)
(b) Mode 2 (one entry &two exits)
(c) Mode 3 (one entry &three exits)
(d) Mode 4(two entries &two exits)
(e) Mode 5 (three entries &two exits)
(f) Mode 6 (three entries & three exits)

Figure 6. Two days after diversion

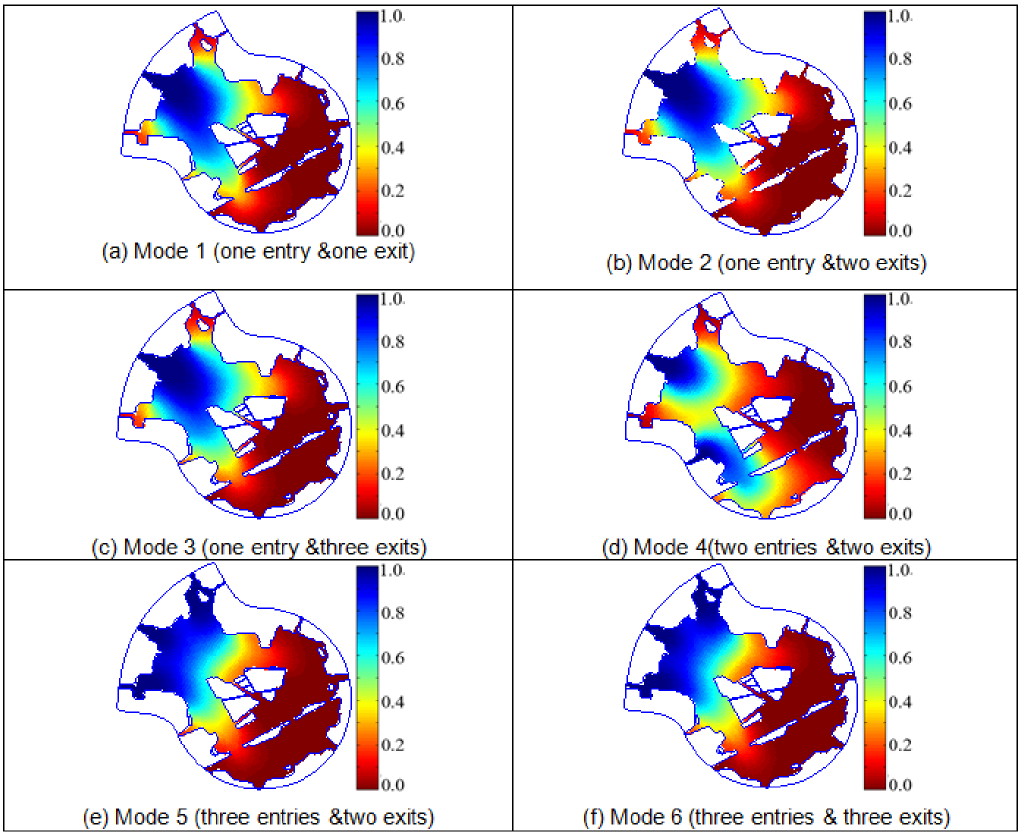

Figure 7. Four days after diversion

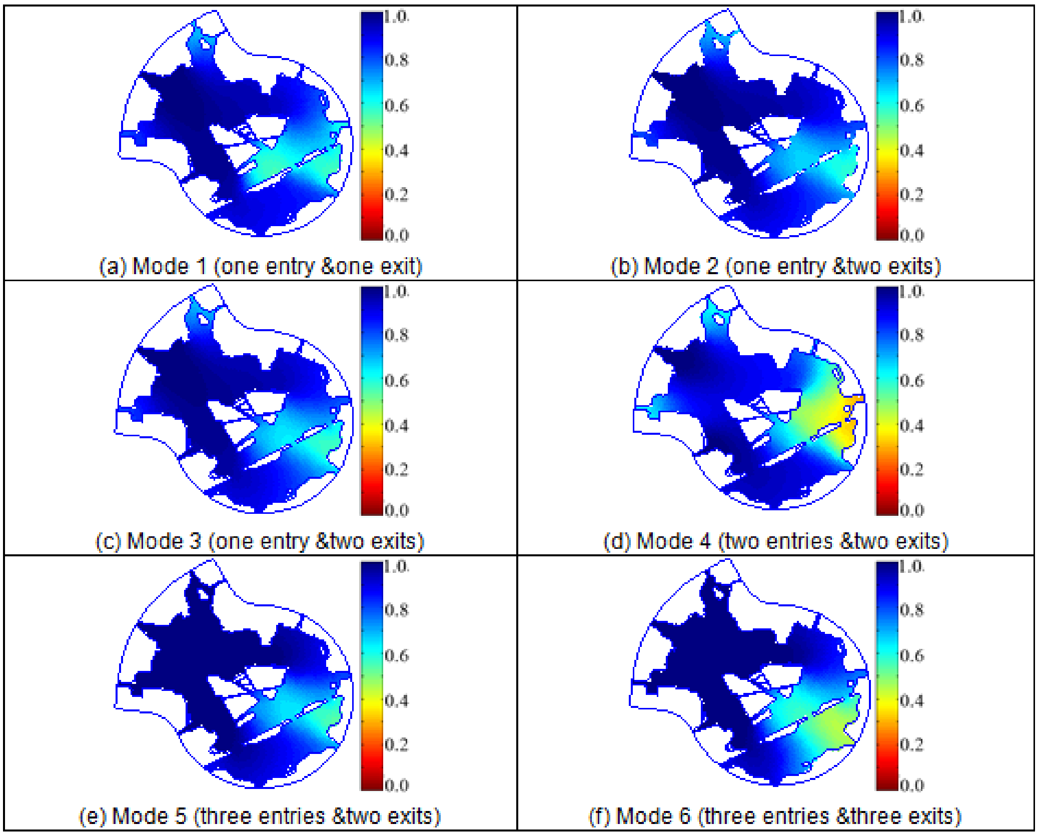

Figure 8. 14 days after diversion

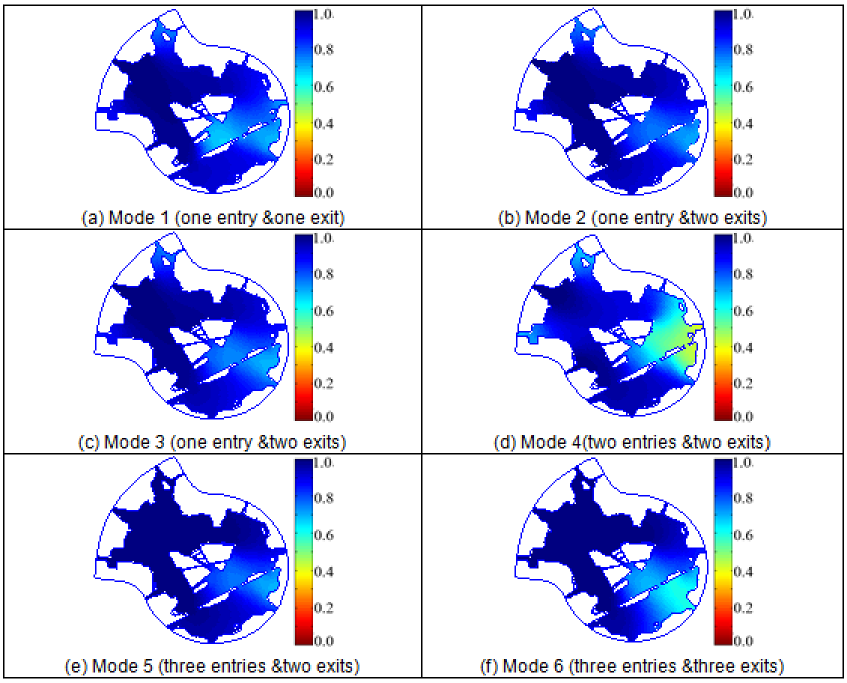

Figure 9. 16 days after diversion

4 CONCLUSIONS

After analysis with two dimensional numerical simulation, the following conclusions can be made. Gate-control scheme is better than open type scheme for water dispatching and water quality control of Yinghu Lake from the view point of reducing water replacing period and reducing the risk of occurrence of algal bloom. The gate-control scheme can also prevent lake from pollution caused by pollution accident occurred in surrounding river net as the lake can be isolated from surrounding river net during pollution accident. Besides, raising of water level in the lake can promote landscape sight of the lake.

ACKNOWLEDGMENTS

This work was supported by the National Natural Science Foundation of China (no. 51609143) and the foundation of Changjiang Institute of Survey, Planning, Design and Research (no. CX2016Z18. “Study on control factors of construction sponge town in changjiang delta area”).

REFERENCES

DHI (2012). *MIKE HYDRO User Guide*. DHI

Gong, W., Pang, C.C., Wu, X.H. & Tao, J. (2015). Effect of Comprehensive Ecological Management Engineering on Gated River Net Influenced Strongly By Tides: Case Study of Chenjia Town River Net In Chongming Island. *Environmental Science & Technology*, 38(2), 169-173.

Pang, C.C., Xu, J.P. & Wang, D.G. (2012). Research on Water Environmental Improvement Scheme of Water System in Western Area of Nanjing City through Water Diversion from Yangtze River. *Yangtze River*, 43(5), 76-79.

Tang, Y.Z., Xu, G.Q., Xu, H. & Ying, R.D. (2011). Study on clean water diversion tests of river network in Chongming Island. *Water Resources Protection*, 27(4), 70-73.

Tong, C.F., Yue, L.L., Hao, J.L., Shao, Y.Y., Yan, Y.X. & Liu, F.Y. (2012). Water Quality Simulation and Water Diversion Effect Analysis of External Qinhuai River in Nanjing. *Water Resources Protection*, 28(6), 49-54.

W L. Delft Hydraulics (2010). *Delft3D-Flow User Manual*. Delft Hydraulics

.XI, Y.P. & Pang, Y. (2008). Study on Improvement of Qinhuai River Water Environment By Transferring Shijiu Lake Water. *Jiangsu Environmental Science & Technology*, 21(4), 6-8.

AN UPDATED CATEGORISATION OF COASTAL EROSION AND VULNERABILITY INDEX ALONG MELAKA STATE

AHMAD KHAIRI ABD WAHAB [(1)], ROSITA SALAM [(2)] & DAENG SITI MAIMUNAH ISHAK [(3)]

[(1,3)] Center for Coastal and Ocean Engineering, Universiti Teknologi Malaysia, Kuala Lumpur, Malaysia,
akhairi@utm.my
[(1)] Faculty of Civil Engineering, Universiti Teknologi Malaysia, Johor Bahru, Malaysia,
akhairi@utm.my
[(2)] Department of Irrigation and Drainage, Kuala Lumpur, Malaysia,
salam.rosita@yahoo.com

ABSTRACT

Over a quarter of the coastlines of Malaysia are subjected to various stages of coastal erosion. A national study in 1985 categorised the degree of coastal erosion to signify Critical (1), Significant (2) and Acceptable (3) conditions. More than two decades later, a micro level coastline studies was conducted. The integrated approach took into account all the sectoral activities affecting the coastal areas and gave due consideration to economic, social, environmental and ecological issues. The state-level Integrated Shoreline Management Plan (ISMP) developed a management tool to harmonise all the activities in the coastal area. The ISMP for the state of Melaka was completed in 2010. Over the past 20 years, there were rapid development along its coast especially land reclamation, offshore sand mining and river outlet works. This paper assessed and update the findings of both these studies to compare evolution of erosion and to develop the Coastal Vulnerability Index (CVI) to sea level rise for the Melaka coastline. The CVI takes into account the past and ongoing developments along the coast and the projected rates of sea level rise. Data for sea level rise was obtained from a study completed in 2010. The findings include Category I (critical) erosion areas where previously there were none in 1985 and improvement to coastal stability in some areas. The United States Geological Survey (USGS) method was adapted to determine the CVI rankings. Comparison between the CVI scores of 1985 and 2015 showed that 64% (51.1km) of the Melaka coastline have increased vulnerability, 13% (10.7km) have decreased vulnerability and 22% (17.8km) were unchanged. The study provided a tool that may be adopted for other states in Malaysia.

Keywords: Coastal Vulnerability Index (CVI); coastal erosion; sea level rise; coastal zone management.

1 INTRODUCTION

Malaysia has a coastline of 4,809km. A pioneer nationwide coastal erosion study or the National Coastal Erosion Study (NCES), conducted in 1985 (EPU, 1985) reported that 1,313km or over 27% of the coastlines were affected by varying degrees of erosion. This study classified the erosion into three categories namely Critical (1), Significant (2) and Acceptable (3). The classification does not only consider the rate of land retreat at a particular coastal reach, but also how it would impact the economic, social and safety of coastal facilities and dwellers.

More than 90% of the Malaysian coast comprise of readily erodible alluvium. About half of the alluvial coast is sandy and the other half is clay and silt. The east coast of Peninsular Malaysia and the coast of Sarawak has about 91% and 76% sandy beaches respectively while the west coast of Peninsular Malaysia and the coast of Sabah consist mainly of clay and silt at 72% and 54% respectively. Even though it is within the relatively milder climate of the Melaka Straits, the west coast of Peninsular Malaysia is the most heavily populated and has many major facilities such as ports and power stations.

At the erodible alluvium coasts, the average rate of land retreat ranges from less than 1m per year to more than 100m per year. The NCES study suggested that coastal erosion seriously threatened important facilities along 140 kilometers of shoreline, while another 240 kilometers with important facilities may be vulnerable within the foreseeable future. This projection has yet to be proven quantitatively but this study would give a good indication of likely events.

The coastal reaches of Peninsular Malaysia was defined by the NCES as shown in Figure 1. The Melaka coastline is partially in the southern part of Reach 8W and the northern part of Reach 9W. The coastal process along this coast is shown in Figure 2. The net longshore sediment transport direction is southwards from Negeri Sembilan and northwards from Johor separated by the headland at Tg. Keling. A Coastal Erosion Inventory exercise was carried out by the Department of Irrigation and Drainage (DID, 2006) to update the status of erosion 20 years after the NCES study. Table 1 summarises the length of eroding coastlines for every states in Malaysia based on the type of erosion category. The table includes both data for 1985 and 2006. The 2006 Coastal Erosion Inventory data shows an increase in eroding coastlines by about 7% (92km)

  / ISSN 1562-6865 (Online) - ISSN 1063-7710 (Print)

throughout the whole country. What is further alarming is that there is a marked increase in category 1 (Critical) erosion for every states in Malaysia. This inadvertently indicated either a lack of monitoring and implementation of protection measures, poor planning of new coastal developments resulting in critical erosion spreading further along the coast or natural factors and recently identified phenomena such as adverse global climate or increase in the sea level. The distribution of coastal erosion based on erosion categories for each states according to the DID (2006) are shown in Figure 3(a) and 3(b) for Peninsular Malaysia, and for Sabah and Sarawak respectively.

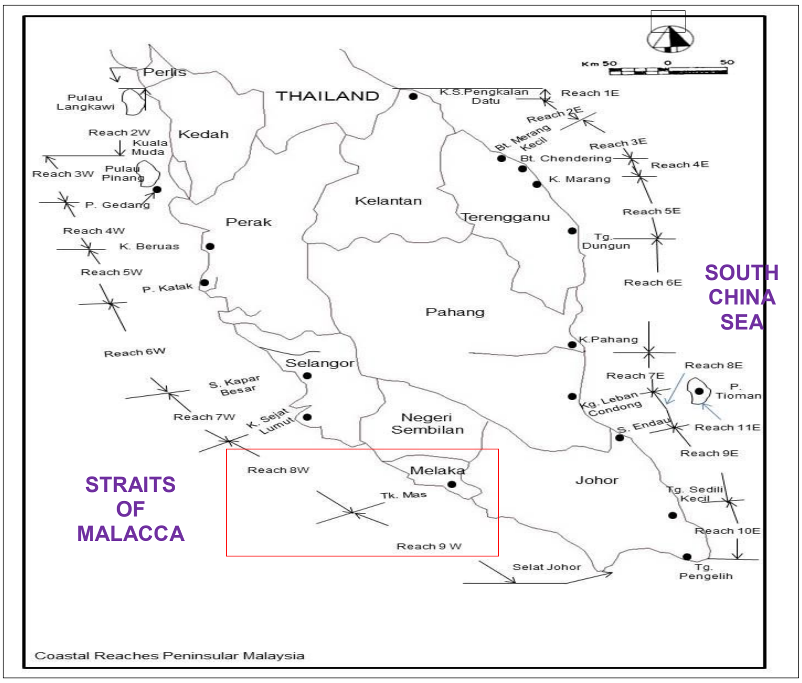

Figure 1. Coastal reaches of Peninsular Malaysia. Source: EPU (1985)

Table 1: Summary of eroding coastlines of Malaysia for 1985 and 2006.

States of Malaysia	Length of coastline (km)					Erosion Cat 1 (km)		Erosion Cat 2 (km)		Erosion Cat 3 (km)	
	Total Length	*Eroding 1985*	*Eroding 2006*	*+/- (km)*	*+/- (%)*	*1985*	*2006*	*1985*	*2006*	*1985*	*2006*
Perlis	20	14.3	14.5	0.2	1.4	4.4	4.4	3.5	3.7	6.4	6.4
Kedah	148	32.3	43.5	11.2	34.7	7.5	31.4	2.8	2.2	22.0	9.9
P Pinang	152	57.5	63.2	5.7	9.9	34.4	42.4	22.0	19.7	1.1	1.1
Perak	230	72.6	140.2	67.6	93.1	16.6	28.3	26.5	18.8	29.5	93.1
Selangor	213	160.5	141.9	-18.6	-11.6	58.9	63.5	32.5	22.3	69.1	56.1
N Sembilan	58	23.6	24.5	0.9	3.8	1.1	3.9	9.6	7.7	12.9	12.9
Melaka	73	29.6	36.7	7.1	24.0	-	15.6	28.6	15.1	1.0	6.0
Johor	492	234.9	234.8	-0.1	0.0	15	28.9	54.2	50.3	165.7	155.6
Pahang	271	117.8	125.4	7.6	6.5	0.3	12.4	5.9	5.2	111.6	107.8
Terengganu	244	149.2	152.4	3.2	2.1	8.0	20.0	12.2	10	129	122.4
Kelantan	71	50.5	52.1	1.6	3.2	1.0	5.0	11.9	9.5	37.6	37.6
FT Labuan	59	-	30.6	30.6	-	-	2.5	-	3.0	-	25.1
Sarawak	1035	36.7	49.2	12.5	34.1	8.0	17.3	15	22.3	13.7	9.6
Sabah	1743	333.4	295.5	-37.9	-11.4	5.7	12.8	17.5	3.5	310.2	279.2
Total	4809	1312.9	1404.5	91.6	7.0	160.9	288.4	242.2	193.3	909.8	922.8

Source of data: EPU (1985) and DID (2006)

In view of the above observations, there is an urgent need to update the status of the coastal erosion in Malaysia. The vulnerability of the coastlines to erosion should also be assessed to help to strategically plan, manage and prioritise mitigation measures. Such vulnerability assessments should include newly emerging factors such as sea level rise induced by global climate change and proliferation of coastal land reclamation and offshore sand mining. The main objective of this study is to pave the way for such tasks above to be implemented by developing a reliable tool that would allow the coastal zones to be better managed against erosion, clear cut indicators and up to date information at the fingertips of stakeholders.

TIDES	Elevation (m)
HAT	2.65
MHWS	2.10
MHWN	1.51
MSL	1.19
MLWN	0.88
MLWS	0.29
LAT	0.0

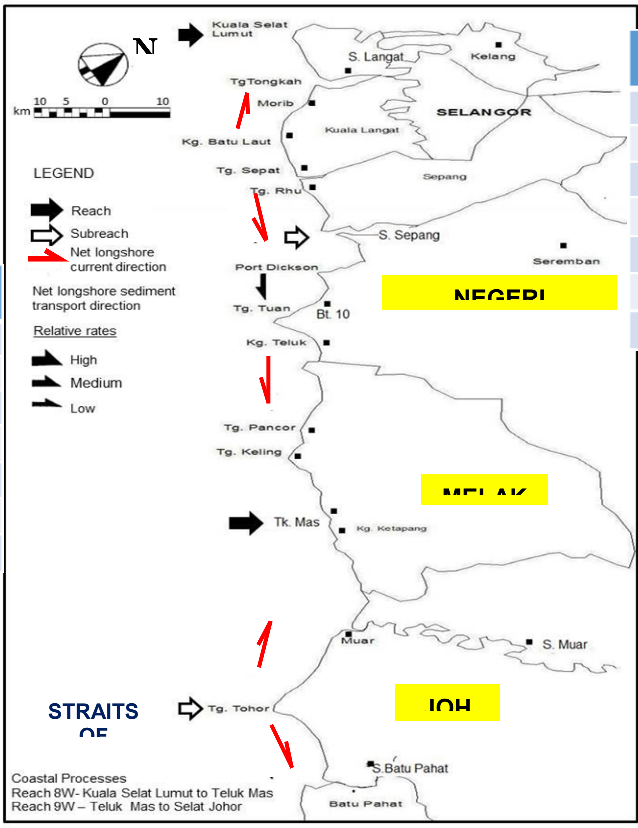

Wave Direction	Sig Wave Ht (m)
0°	0.73
30°	1.08
60°	0.97
90°	0.96
120°	0.84
150°	1.26
180°	0.95

Figure 2. Significant wave heights, tides and coastal processes along Melaka coastlines (Source: EPU (1985), NHC (2015) and DID (2010))

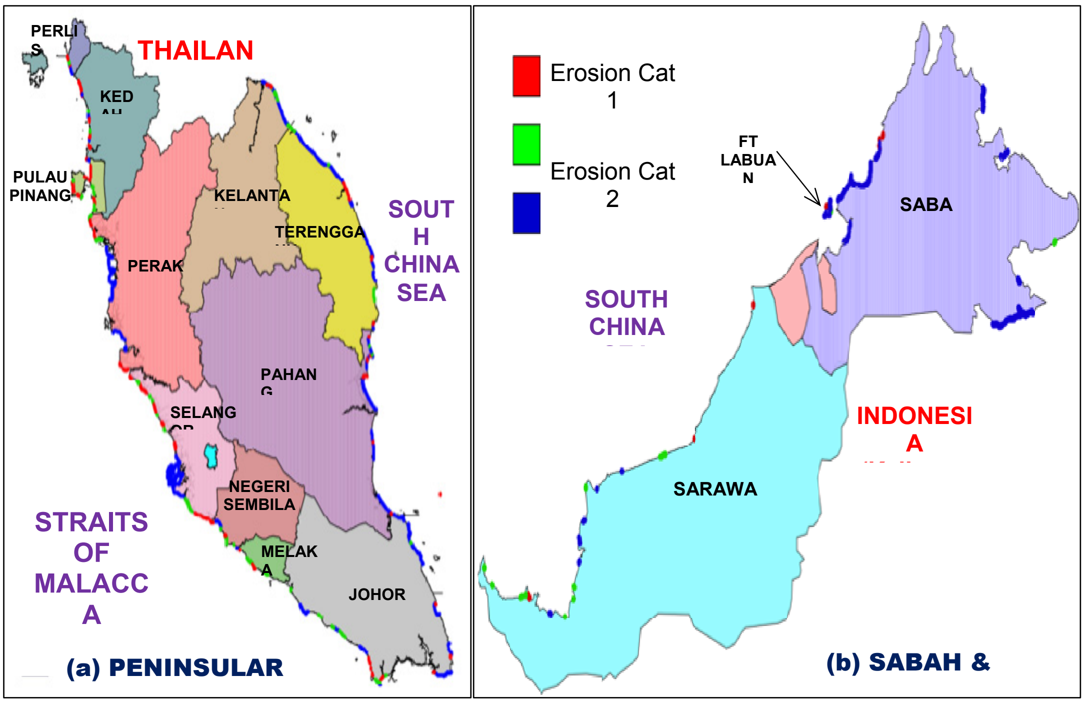

Figure 3. Distribution of coastal erosion and erosion categories for each states. Source: DID (2006)

2 THE STUDY AREA

Melaka is located at the west coast of Peninsular Malaysia and faces the Straits of Malacca. The state coastline extends from the boundary with Negeri Sembilan in the North and Johor in the South. The study area covers the entire shoreline of Melaka as shown in Figure 4 where the erosion categorisation for the 1985 study is also marked. Generally, only Category 2 was observed around the area of Tg. Keling while the whole coast to the south accretes. The Melaka coastline was chosen for this study due to its relatively short length of only 72km. It represents 1.5% of the total length of Malaysia's coastline. Despite that, Melaka is foremost in land reclamation compared to the other states. There was an acute shortage of land for future development. Over the past two decades, the state government approved numerous land reclamation and offshore sand mining projects to create more areas for economic generation in the state. There is an increase of 23% eroding beaches from about 30km in 1985 to about 37km in 2006. The category 1 erosion in 2006 is close to 16km compared to none in two decades earlier.

Besides the NCES (1985), another specific study on the Melaka coastline was the Integrated Shoreline Management Plan (ISMP) for Negeri Melaka (DID, 2010). The ISMP looked into the conditions of the coastal zone and the activities there. Melaka coastline was also selected based on the rapid development along coasts, in which approximately 25% of the total length experienced significant physical changes as a consequence of coastal reclamation for the construction of resorts, residential and commercial area. In fact, the ISMP recorded the coastline of Melaka in 2010 to be about 80km, an increase of 8km.

3 LITERATURE REVIEW

3.1 Coastal Erosion

Coastal erosion is a natural process involving the interactions between the ocean hydrodynamic forces and the shorelines. Many researchers have conducted studies on this. Gillie (1997) stated that the factors affecting shoreline retreat can be divided into two main categories: natural and human-induced. Van Rijn (2011) gave support by stating that coastal erosion is caused by natural effects as well as human activities at the same time. Human-induced causes include sand mining, construction of coastal structures, reclamation of shorefront lands and land subsidence due to construction (Hsu et al., 2007). The combined factors of natural and human activities drive coastal change and makes coastal regions and populations increasingly vulnerable (Williams et al., 2008). Komar (2010) stated that coastal erosion can also be the result of increasing local human alteration of the environment, particularly those that upset the sediment budget or obstruct the littoral sediment flow. Dam construction across rivers can cut off what has been a primary source of sediment flow.

Since many important economic and social activities are now taking place in coastal areas, the consequences of coastal erosion have increasingly become a serious concern. Coastal erosion and storms represent a source of risk for settlements and infrastructures along the coast. Impending increase in sea level due to climate change further exacerbate the problem. These will force coastal communities to apply drastic adaption strategies (Sano et al., 2011). Inundation of low-lying coastal regions due to higher water levels would create greater wave actions closer to the existing shore. This is particularly destructive in view of extreme weather events, which are nowadays increasing in frequency (Church et al., 2011). As a consequence of climate change, past information from tide gauges may have limited use because future sea levels is expected to differ significantly from that of the past and the present (Obeysekera et al., 2013).

In Malaysia, the National Coastal Erosion Study (EPU, 1985) deduced that community life, agriculture, transportation, and recreation are seriously affected by coastal erosion. More imminent damages can be seen on housing, coastal bunds, roads, and beaches important to those activities. Erosion along coastline is widespread. Consequently, coastal erosion is always a national issue that requires site specific local actions. As such, proper planning is needed to identify, prioritise and allocate funds to carry out mitigating measures. One such strategy undertaken by the NCES to handle the issue was to classify coastal erosion into categories to indicate their significance and priority for mitigations.

The Integrated Shoreline Management Plan (ISMP) for the state of Melaka was completed in 2010 (DID, 2010). In the ISMP, the solutions in addressing coastal issues such as coastal erosions are not only based on technical aspects, but also incorporates social, cultural, economic and environmental factors. The ISMP represents a long-term action of non-structural measures to overcome coastal erosion. It was formulated to be more specific and takes into account local factors, and represents a comprehensive management plan related to the management of coastal areas. A key component of the study is to incorporate stakeholders' consultations in order to ensure that local interests and issues are incorporated and given due attention. The main purpose is to control the coastal erosion in a sustainable manner and mitigate the risk of coastal flooding, to add value and improve the quality of the coastal tourism, preserve environment of the coast, history and archeology, as well as provide basic strategy and guidelines to ensure that the beach management is more effective, systematic and sustainable for the benefit of future generation.

3.2 Coastal Vulnerability Index (CVI) to sea level rise

Guidelines and methodologies to assess coastal vulnerability to sea level rise has been developed since 1990s. These were useful in determining the vulnerability of coastal infrastructures, individual structures, and the economic, environmental and societal factors to the impact of natural marine hazard. Several federal agencies in the United States such as USGS, NOAA, FEMA and USACE have produced their respective guidelines on vulnerability assessment methodologies. The most widely used method is the Coastal Vulnerability Index (CVI), first developed by the United States Geological Survey or USGS (Gornitz et al., 1997). This approach culminated in a map showing relative vulnerability of the area to sea level rise based on an indexed ranking system derived from geological and physical parameters of specific cells along the coastline. Examples of such mapping for various coastlines around the world can be seen from McLaughlin and Cooper (2010), Abuodha and Woodroffe (2010) and Yin et al. (2012). Such a technique has also been used to assess coastal vulnerability to floods (Balica et al., 2012), coastal erosion (Boruff et al., 2005) and tsunamis (Ismail et al., 2012). The USGS method, however, only ranks the CVI in terms of geological and physical parameters. The IPCC's Common Methodology technique (Kay et al., 1996), on the other hand, adapts both physical and socio-economic factors into an integrated CVI to produce a vulnerability profile.

For this study, only geological and physical parameters were considered where detailed site specific assessment was done for the coastline concerned. This gives a reliable means of predicting the most likely degree, pattern and rates at which sea level rise may impact on a particular coastal stretch. The integration of these data to produce a coastal behaviour model for the particular area is essentially a detailed hypothesis in response to both contemporary processes and projected sea level rise. Seven geological and physical parameters were defined. They are the coastal geomorphology, geologic material, the coastal slope, rate of shoreline change, relative sea level rise, nearshore waves and tidal ranges. The vulnerability value for each parameter were defined based on the USGS method but further refined to adapt to local physical ranges. The CVI for each coastal segment was then calculated and ranked according to their percentile values. Details of the computations is further explained in the study methodology.

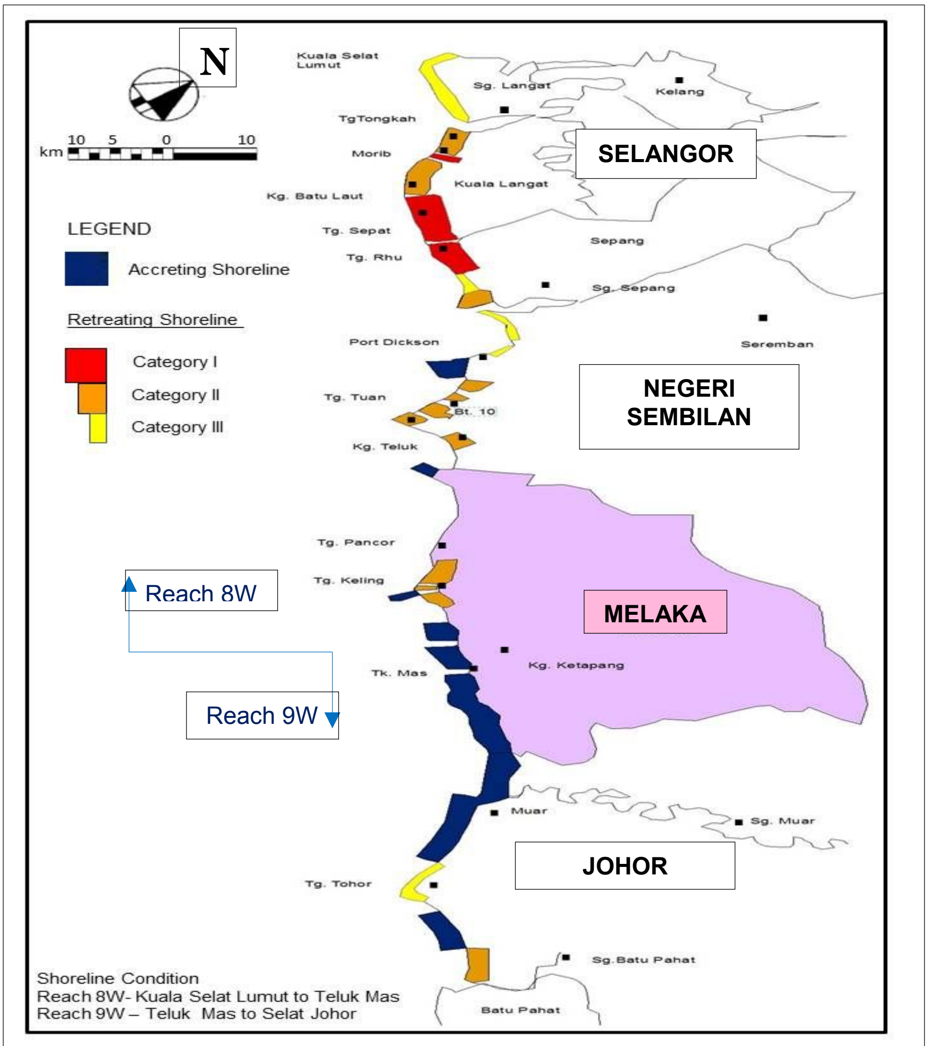

Adapted from: EPU (1985)

Figure 4. Melaka state (in blue) and its shoreline showing erosion categories in 1985.

4 STUDY METHODOLOGY

The study undertakes to carry out two objectives. The first objective is to update the status of coastal erosion in the state of Melaka from that reported by the NCES in 1985 to the recently concluded ISMP in 2010 with additional data from a field survey conducted in 2015. In order to further enhance the outcome of this objective, the categorisation of erosion is modified by introducing two new categories. This is necessary to take into account the various coastal protection measures and land reclamations works that in principal would create a relatively stable coastline and situation of accreting coastlines. Thus, Category 4 is for protected coastlines while Category 5 is for accreting coastline.

The second objective is to produce a Coastal Vulnerability Index (CVI) to sea level rise for the state of Melaka. Two CVI maps for 1985 and 2015 were produced to highlight the changes that has taken place over the two decades in Melaka and to demonstrate the versatility of such technique in helping to plan and execute the coastal management strategies.

4.1 Coastal segments for Melaka coastline

The coastline of Melaka is sub-divided into 51 coastal cells beginning from Cell 1 in the north, bordering with Negeri Sembilan (including Sg. Linggi) to Cell 51 in the south at the Johor state boundary (including Sg. Kesang) to make a systematic assessment and analysis. The extent of each cells is based on Management Units (MU) as defined by the ISMP Melaka sub-divisions. The properties of each coastal cells can be referred to in Table 2 and Figure 6. The analysis only covers the mainland of Melaka coastline and does not include islands in the state (Pulau Upeh and Pulau Besar) and Tg Tuan or Cape Rachardo, which is a part of Melaka state but is geographically located in Negeri Sembilan. In order to conduct the analysis based on a common site identification to allow direct comparison, the coastal reaches that was defined by the NCES is converted to the ISMP cell sub-division system.

4.2 Modified coastal erosion categorisation

The first coastal erosion assessment study was conducted in 1985 and defined 3 categories of erosion according to severity and imminence of economic and social consequences or threat to existing facilities. They are

1) **Category 1 (Critical erosion)** - Areas where rates of erosion are considered in conjunction with economic, agricultural, transportation, recreational and demographic value and with structures deemed valuable to be protected, with indication that action to halt erosion may be justified.
2) **Category 2 (Significant erosion)** - Areas where the erosion is not currently critical, but where the rates of erosion are considered in conjunction with economic, agricultural, transportation, recreational and demographic values and with intended structures deemed valuable to be protected, with indication that assessment of criticality should be reviewed periodically.
3) **Category 3 (Acceptable erosion)** - Areas where the rates of erosion are such that it is not a significant danger to economic, agricultural, transportation, recreational and demographic values and with intended structures deemed valuable to be protected, likely within the foreseeable future (say 10 to 15 years).

The current study proposes to create two additional categories. This is to take into account coastal land reclamation activities, construction of coastal structures and coastal protection systems along the shoreline. These developments and man-induced activities are quite abundant over the past 20 years. They are described as below

4) **Category 4 (Stable Coastline)** - Areas where there are no significant erosion or accretion due to the shoreline being protected or along reclaimed coastline with protection.
5) **Category 5 (Accreting Coastline)** - Areas showing accumulation of sediment by natural processes or triggered by man-made interference along neighbouring coastline.

4.3 CVI parameters, values and ranking

The USGS methodology (Thieler and Hammar-Klose, 1999) was adopted to assess the vulnerability of Melaka shorelines to coastal development and sea level rise. The resulting indicator is the CVI indices for each cells along the state coastlines. Seven variables were considered to have influence on the vulnerability assessments. They are made up of three geologic variables and four coastal process variables. These variables were aggregated according to an appropriate set of weights, of which the weighting factors were determined accordingly, depending on the characteristics of the particular site conditions and coastal settings. At the end of this stage, each coastal cell would be given a vulnerability ranking for each of the seven variables. Table 3 summarises the ranking for the coastal vulnerability weightage and weighting factors for the seven variables.

The vulnerability ranking for each input variable were combined and a CVI value calculated for each cells. The coastal vulnerability index (CVI) value was calculated using equation 1.

$$\text{CVI value} = \frac{\sqrt{a*b*c*d*e*f*g}}{7} \quad [1]$$

The CVI scores for the categorization of the shoreline were calculated based on percentile values from a statistical analysis which are divided into quartile ranges for the five (5) vulnerability categories, as indicated in Figure 5.

VERY LOW	≤ 20th percentile
LOW	20th percentile ≤ CVI ≤ 40th percentile
MODERATE	40th percentile ≤ CVI ≤ 60th percentile
HIGH	60th percentile ≤ CVI ≤ 80th percentile
VERY HIGH	≥ 80th percentile

Figure 5. The CVI value for each of the defined coastal cell were then transferred to the CVI map that shows the vulnerability assessments along the study coastline.

5 RESULTS AND DISCUSSIONS

5.1 Updated and modified coastal erosion categorisation for the state of Melaka

The results of the coastal erosion update to the 2015 condition for the state of Melaka is presented in Table 2 alongside the NCES output. (EPU, 1985). Two important features that were implemented here are the redefinition of coastal reaches into smaller units of coastal cells and the modification of the coastal erosion categorisation. The Melaka coastline were subdivided into 51 coastal cells. The erosion category for each cells are in column *(7)* for year 1985 and column *(8)* for year 2015. Generally, in 1985, most of the coastal cells were either stable or accreting while the rest (18 cells with a total of 24.3km length) were with category 2 erosion. As a result of vigorous coastal developments that took place over the past 20 years, a drastic change was observed. Some 29 out of 51 cells has undergone some form of change in their categorisation. Most notable are the four cells that has degraded from stable to critical. They are cells 7, 9, 12 and 16 at Kg. Tengah, Kg. Sg. Baru, Kg. Teluk Gong and SMK Tg. Bidara respectively. On the other hand, nine cells have improved from having significant erosion to becoming stable. These cells lie mainly within newly reclaimed section of the coast.

5.2 Coastal Vulnerability Index (CVI) for the state of Melaka

The vulnerability of the Melaka coastlines to sea level rise was investigated using the CVI methodology developed by the USGS. The analysis considered the seven variables that would be affected in various degrees by the sea level rise phenomenon. Melaka has a relatively short distance of coastline that are exposed to common hydrodynamic factors arising from the Strait of Malacca. Thus, similar characteristics were applied along the whole coastline for the mean significant wave height and the mean tidal range. Wave and tidal analysis produced a common value of 1.26m and 1.50m for the significant wave height and mean tidal range respectively. The rate of sea level rise was referred to a study by NAHRIM (2010) for the whole of Malaysia. This study was assisted by the California Hydrological Laboratory where the spatial variation of sea level change was estimated by assimilating the global mean sea level rise projection from the AOGCM simulations to the satellite altimeter observations along the coastlines. The mean sea level rise was projected for stations along the west coast of Peninsular Malaysia. Based on the NAHRIM study, the rates of sea level rise along the coast of Melaka were shown in column *(6)* of Table 2. The shoreline changes were calculated using the Digital Shoreline Analysis System (Thieler et al., 2008). Two sets of data from 1998 SPOT and 2007 SPOT satellite images were used. The shoreline changes for cells along the Melaka coast are shown in column *(4)* of Table 2. The average coastal slope values are shown in column (5) of Table 2. They were derived from Malaysia bathymetry charts MAL 521 and MAL 532.

Using data from the NCES (EPU, 1985) and the Melaka ISMP (DID, 2010) supplemented by recent field works in 2015, a comparative CVI map for 1985 and 2015 were developed. The comparative CVI map for Melaka is shown in Figure 6. Comparison between the CVI scores of 1985 and 2015 showed that 64% (51.1km) of the Melaka coastline have increased vulnerability, 13% (10.7km) have decreased vulnerability and 22% (17.8km) were unchanged. At the northern coastlines, areas around cells 1 to 3 showed increased vulnerability (Figure 6A). The effect of land reclamation seem to reduce the vulnerability as can be seen around cells 30 and 31 at Pantai Klebang (Figure 6D). Generally, there is an increase in vulnerability towards the south of the state.

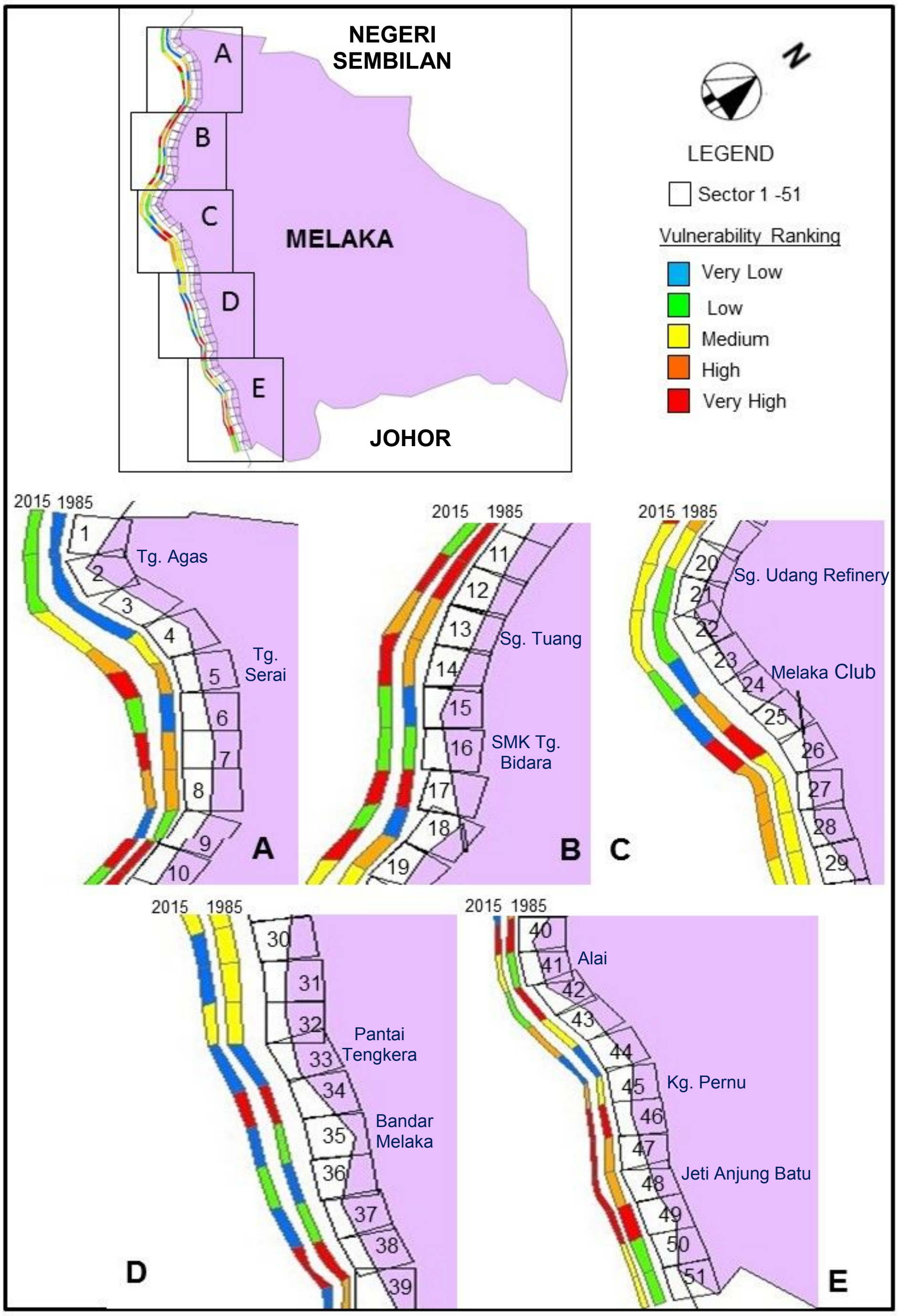

Figure 6. The Coastal Vulnerability Index (CVI) map for Melaka with 2015 (left) and 1985 (right) values.

Table 2. Sub-division of Melaka coast into 51 coastal cells and some descriptions

(1) Cell	(2) Name	(3) Length (km)	(4) Shoreline change (m/yr)	(5) Average Coastal Slope (%)	(6) Sea Level Rise (m)	(7) Erosion Category NCES (EPU,1985)	(8) 2015 Modified Erosion Category	(9) Remarks
1	Kg. Nelayan	1.0	5.27	0.75	1.98	4	4	River mouth
2	Tg. Agas	0.6	3.76	0.38	1.98	5	4	
3	Bg Che Amar (BCA)	1.8	2.68	0.14	1.98	4	3	
4	BCA-Tg. Serai	0.7	-0.55	0.77	1.98	4	4	
5	Tg. Serai	0.5	-1.87	0.9	1.98	4	4	
6	Kg. Tg. Dahan	1.9	-1.64	1.68	1.98	4	3	Protected
7	Kg. Tengah	4.9	-1.59	0.55	1.97	4	1	
8	Kuala Sg. Baru	0.2	-1.32	0.82	1.97	4	4	River mouth
9	Kg. Sg. Baru	0.7	-1.30	0.99	1.97	4	1	
10	Kg. Teluk Belanga	1.7	-1.97	0.6	1.97	4	4	
11	Tk Gong Power Stn	0.5	-4.65	0.76	1.97	4	4	Reclaimed
12	Kg. Teluk Gong	1.3	-1.65	0.39	1.97	4	1	
13	Sg. Tuang	0.1	-0.35	0.39	1.97	4	4	Protected
14	Pengkalan Balak	3.8	-1.82	0.54	1.97	4	4	Protected
15	Sg. Air Hitam	0.5	-1.71	1.62	1.97	4	4	Protected
16	SMK Tg. Bidara	0.8	-3.41	1.43	1.97	4	1	
17	Tg. Bidara Beach	1.2	-3.66	0.63	1.97	4	4	Protected
18	Kem Terendak	2.7	-1.19	1.41	1.97	4	4	
19	Kem Terendak (2)	2.8	-1.22	0.9	1.94	2	3	Protected
20	Sg. Udang Refinery	2.5	-0.71	0.68	1.94	2	4	Reclaimed
21	Pantai Putri	3.0	-3.92	1.26	1.94	2	2	
22	Jetty Tg. Beruas	1.1	-2.02	1.63	1.94	4	3	
23	Kg. Tg. Keling	1.1	-1.42	1.88	1.92	2	4	Protected
24	Melaka Club	0.2	-0.52	0.57	1.92	5	4	Reclaimed
25	Shah Beach Motel	0.7	-4.07	0.54	1.92	5	4	Protected
26	Taman Spring	0.6	-0.27	0.63	1.92	2	3	Protected
27	Sg. Lereh	0.1	-0.9	0.65	1.92	2	2	
28	Btg. Tiga	1.2	0.52	0.69	1.92	2	2	
29	Klebang Outlet	0.1	-0.93	0.67	1.92	2	4	River mouth
30	Pantai Klebang	0.7	1.09	0.67	1.92	2	4	Protected
31	Pantai Klebang (2)	1.0	6.49	0.71	1.92	2	2	Reclaimed
32	Sg. Seri Melaka	0.1	0.2	0.74	1.92	2	2	River mouth
33	Pantai Tengkera	6.3	69.70	1.57	1.92	2	2	Reclaimed
34	Sg. Melaka	0.5	-2.73	0.61	1.92	4	4	River mouth
35	Bandar Melaka	2.8	1.66	1.04	1.92	4	4	Reclaimed
36	Taman Melaka Raya	0.3	1.47	1.03	1.92	4	5	
37	Kg. Portugis	1.0	1.87	0.52	1.92	2	4	Reclaimed
38	Sg. Parit China	0.1	-1.11	0.59	1.92	2	4	Reclaimed
39	Padang Temu	2.0	-0.35	0.5	1.92	2	4	Reclaimed
40	Sg. Duyong	0.2	-3.16	0.74	1.92	2	4	River mouth
41	Alai	1.8	-8.55	1.28	1.92	2	3	
42	Taman Teluk Mas	0.8	-2.77	0.71	1.92	2	3	Reclaimed
43	Tg. Ketapang	1.0	0.07	0.61	1.92	4	4	
44	Henry Gurney Sch	1.2	-0.88	1.62	1.92	4	4	Protected
45	Kg. Pernu	1.1	-0.14	0.62	1.92	5	4	
46	Sg. Umbai	0.7	-3.4	0.26	1.92	5	4	River mouth
47	Umbai	2.0	-0.27	0.48	1.92	5	4	
48	Jetty Anjung Batu	3.9	-1.35	0.67	1.92	5	2	
49	Sg. Serkam	0.1	-4.88	0.34	1.88	5	3	
50	Kg. Permatang Pasir	13.5	9.16	0.21	1.88	5	5	Protected
51	Sg. Kesang	0.2	5.97	0.17	1.88	5	4	River mouth

Table 3. List of seven variables with their ranking for the coastal vulnerability assessment due to sea level rise.

Ranking Index -> Variables	Very Low 1	Low 2	Moderate 3	High 4	Very High 5
Geomorphology	Rocky cliffed coast	Medium cliffs, indented coasts	Low cliff, alluvial plains	Cobble beaches estuary, lagoons	Barrier beaches, mud flats, sand beaches, deltas, mangrove, coral reef
Coastal Slope (%)	>1.2	1.20 – 0.90	0.90 – 0.60	0.60 – 0.30	<0.30
Relative Sea Level Rise (mm/year)	<1.80	1.80 – 2.50	2.50 – 3.00	3.00 – 3.40	> 3.40
Mean Significant Wave Height (m)	<0.55	0.55 – 0.85	0.85 – 1.05	1.05 – 1.25	>1.25
Shoreline Change Rate (m/year)	>2.0	1.0 – 2.0	-1.0 – 1.0	-2.0 - -1.0	< -2.0
Mean Tidal Range (m)	>6.0	4.0 – 6.0	2.0 – 4.0	1.0 – 2.0	<1.0
Geological Materials	Old erosion of Resistant Rocks (crystalline interlocking) and stronger metamorphic rocks (recrystallisation): • Igneous volcanic (basalt, rhyolite, andesite, etc) • Gneous plutonic (granite, granodiorite, etc) • Metamorphic high-grade (gneisses, marble, quartzite, etc)	Sedimentary Rocks (cemented, granular, weak minerals) and weak metamorphic rocks (distinctive mineral arrangement, slaty): • Shale • Siltstone • Sandstone • Conglomerate • Limestone • Metamorphic low-grade to medium-grade (schist and slate) • Eolianite (calcite-sand) Mixed or varied lithology	Unconsolidated sediments (loose, uncemented): • Mud, clay • Silt • Sand • Gravel, conglomerates • Calcareous sediments Mixed or varied lithology	Recent Volcanic Materials: • Lava • Volcanic Ash • Composite	Coral reef

Source*:* Thieler and Hammar-Klose (1999)

6 CONCLUSIONS

The coastal erosion categorisation from the 1985 National Coastal Erosion Study (NCES) was updated to the more recent coastline in the state of Melaka. In order to enhance the classification, it was modified to include two additional categories to indicate a stable condition and an accreting condition. The study observed that there was an increase in the degree of erosion for Melaka state over the past two decades where conditions of critical erosion can be detected.

A vulnerability of Melaka state to sea level rise was derived based on the 1985 and 2015 records. A comprehensive analysis is not carried out in this paper due to space constraints but generally there was an increase in vulnerability around the southern coastal region of the state. On the other hand, the northern region and reclaimed areas showed reduced vulnerability.

One of the important benefits to be derived from this study is the pinpointing of specific critical areas along the coast that need immediate attention. These problematic cells were already designated as coastal cells that are characteristically small and manageable. This would enable the authorities to draw out specific plans to respond and mitigate, organise budget and identify the agencies responsible.

Continuous monitoring and updating of the erosion and CVI maps can easily be carried out by the state to be shared and disseminated to the general public, stakeholders and responsible agencies. Thus, an up-to-date database will always be available not only to serve as a management tool but also as a transparent and accessible public awareness system that would enhance self-regulation of the coastal and environmental resources within the state. The methodology adopted here could also be extended in other states in Malaysia where data is available.

The next stage of the CVI should be the inclusion of environmental and socio-economic parameters that would produce a vulnerability assessment from coastal developments and sea level rise directly on to the various layers of stakeholders and local community such as the tourism, fishing and aquamarine industries, the general population and other related parties in the state.

REFERENCES

Abuodha, P.A.O. & Woodroffe, C.D. (2010). Assessing Vulnerability to Sea-Level Rise Using a Coastal Sensitivity Index: A Case Study from Southeast Australia. *Journal of Coast Conservation*, 14, 189-205.

Balica, S.F., Wright, N.G. & Van Der Meulen, F. (2012). A Flood Vulnerability Index for Coastal Cities and its Use in Assessing Climate Change Impacts. *Natural Hazards*, 64, 73-105.

Boruff, B.J., Emrich, C. & Cutter, S.L. (2005). Erosion Hazard Vulnerability of US Coastal Counties. *Journal of Coastal Research*, 21, 5, 932-942.

Church, J. A., N. J., White, L. F., Konikow, C.M., Domingues, J.G., Cogley, E., Rignot, J.M., Gregory, M.R., Van, D. Broeke, A. J., Monaghan. & I. Velicogna (2011). Revisiting The Earth's Sea-Level and Energy Budgets from 1961 to 2008. *Geophysical Research Lett*er, 38, 1-8.

DID (2006). *Coastal Erosion Inventory*, Coastal Engineering Division, Department of Irrigation and Drainage Malaysia, Ministry of Natural Resources and Environment.

DID (2010). *Integrated Shoreline Management For Melaka*, Department of Irrigation and Drainage Malaysia, Ministry of Natural Resources and Environment.

EPU (1985). *National Coastal Erosion Study*, Report Submitted To The Economics Planning Unit (EPU), Prime Minister's Department, Government Of Malaysia By Stanley Consultants Inc.

Gillie, R.D. (1997). Causes of Coastal Erosion In Pacific Island Nations. *Journal Of Coastal Research*, Special Issue No. 24, Pp173-204.

Gornitz, V.M., Beaty, T.W. & Daniels, R.C. (1997). *A Coastal Hazard Data Base For The U.S. West Coast*, Pub. #4590, Environmental Sciences Division, Office Of Biological And Environmental Research, U.S. Department Of Energy, Prepared By Carbon Dioxide Information Analysis Center, Oak Ridge National Laboratory, Oak Ridge, Tennessee.

Hsu, T.W., Lin, T.Y. & Tseng, I.F. (2007). Human Impact on Coastal Erosion in Taiwan. *Journal of Coastal Research*, 23, 4, 961-973.

Kay, R.C., Eliot, I., Caton, B., Morvell, G. & Waterman, P. (1996). A Review Of The Intergovernmental Panel On Climate Change's Common Methodology For Assessing The Vulnerability Of Coastal Areas To Sea-Level Rise. *Coastal Management*, 24, 165-188.

Komar, P.D. (2000). Coastal Erosion—Underlying Factors and Human Impacts. *Shore and Beach*, 68, 1, 3–16.

Mclaughlin, S. & Cooper, J.A.G. (2010). A Multi-Scale Coastal Vulnerability Index: A Tool for Coastal Managers. *Environmental Hazards*, 9(3), 233-248

NHC (2015), *Tide Tables Malaysia 2015 Volume 1*, National Hydrographic Centre, Royal Malaysian Navy.

Obeysekera, J., Park, J., Irizarry-Ortiz, M., Barnes, J. & Trimble, P. (2013). Probabilistic Projection of Mean Sea Level and Coastal Extremes. *Journal of Waterway, Port, Coastal, and Ocean Engineering*, 139, 2, 135-141.

Sano, M., Jimanez, J.A., Medina, R., Stanica, A., Sanchez-Arcilla, A. & Trumbic, I. (2011). The Role of Coastal Setbacks in the Context of Coastal Erosion and Climate Change'. *Ocean & Coastal Management*, 54, 12, 943-950.

Thieler, E.R. & Hammar-Klose, E.S. (1999). *National Assessment of Coastal Vulnerability to Sea-Level Rise; U.S. Atlantic Coast*, United States Geological Survey, Open-File Report 99-593.

Thieler, E.R., Himmelstoss, E.A., Zichini, Z.L. & Ergul, A. (2008). *The Digital Shoreline Analysis System (DSAS) Version 4.0 - An Arcgis Extension For Calculating Shoreline Change*, United States Geological Survey, Open-File Report 2008-1278.

Van Rijn, L.C. (2011). Coastal Erosion and Control. *Ocean & Coastal Management*, 54, 12, 867-887.

Williams, S.J., Gutierrez, B.T., Thieler, E.R. & Pendleton, E. (2008). Geologic Effects and Coastal Vulnerability to Sea-Level Rise, Erosion and Storms*, Solution to Coastal Disasters Congress 2008,* ASCE.

Yin, J., Yin, Z., Wang, J. & Xu, S (2012). National Assessment of Coastal Vulnerability to Sea-Level Rise for the Chinese Coast, *Journal of Coast Conservation*, 16, 123-133.

RESPONSES OF HYDRODYNAMIC AND WATER EXCHANGE TO THE TIDAL INLET WIDTH OF QILIHAI LAGOON WETLAND

ZHI-CHAO DONG(1), CUI-PING KUANG(2), YUE MA(3) & JIE GU(4)

(1) Department of Hydraulic Engineering, Tongji University, Shanghai, China,
228dongzc@tongji.edu.cn; cpkuang@tongji.edu.cn; mayue_mavis@tongji.edu.cn; jgu@shou.edu.cn

ABSTRACT

Qilihai lagoon, located in Changli Gold Coast nature reserve, Qinhuangdao city, Hebei province, is one of the most typical and representative wetland lagoon in China. The tidal inlet of Qilihai lagoon is like an open channel with the length of 1700m and the geometry of tidal inlet is one of the key control factors of the lagoon system. Due to that, its changes will influence the system's hydrodynamic characteristics. Studying the influence of tidal inlet width on current and water exchange is carried out so that a hydrodynamic and conservation substance transport model can be established by MIKE21 to simulate four scenarios with different tidal inlet widths, i.e., 100m, 200m, 300m and 400m respectively. Computed tracer mass is dealt with Eulerian method based on solving the convection-diffusion equation and least-squares method to fit nonlinear curve. Then the residence time is obtained to analyze water exchange capacity, which can provide a scientific basis for the tidal inlet design. The numerical results indicate that: 1) there is an anti-clockwise circulation inside Qilihai lagoon near the tidal inlet and the area of circulation is the largest for the moment of flood slack; 2) with the increase of inlet width, both flood and ebb discharge increase and the range of water level turns larger, however, the mean current speed from the tidal inlet into lagoon becomes smaller; 3) widening inlet width will reduce water residence time and enhance the water exchange capacity in the lagoon.

Keywords: Qilihai lagoon; tidal inlet; hydrodynamic; water exchange; residence time.

1 INTRODUCTION

A large number of nutrient and contaminant have been discharged into sea by increment of human development. There is no doubt that it is aggravated by the offshore water environment problem with oil spilling and hazardous chemicals emerge occasionally at the same time. From the long-term exploration and study on the water environment, it can be found that pollutant in the water is interplayed by physics, chemistry and biology process (Ntengwe, 2006). The improvement of water ecological environment will finally end the domination of pollutants (Suffet, 1977). The precondition and basic of analysis of pollutant fate is quantifying the process and law of water transport. The strength of water exchange reflects the capacity of water self-purification which has a virtual significance of water environment improvement.

Water exchange had been studied in the early through computed rate of water exchange (Parker et al., 1972) from a measured indicator concentration (Davies, 1984; Bi et al., 2000). With the development of computer technology, numerical model performs an effective role in water exchange study and several studies have been conducted by particle tracking model (Kawasaki et al., 2008) and convection-diffusion model (Luo et al., 2011). There are two major methods to study the water exchange by numerical simulation which are Lagrangian method and Eulerian method. Lagrangian method is based on particle tracking while the diffusion of the water has been neglected. Eulerian method describes spatial substance movement over time based on convection-diffusion equation and reflects the characteristics of the local residual current.

Qilihai lagoon, located in Changli Gold Coast nature reserve, Qinhuangdao city, Hebei province, is one of the most typical and represented lagoon wetland in China. The tidal inlet of Qilihai lagoon is like an open channel with the length of 1700m and the average width of 150m. However, with the effect of human activities, the problems of water area reduction and lagoon deposition become serious. So, the lagoon restoration project is imperative. The initial planning scheme includes widening tidal inlet for water exchanging, center island construction for the requirement of lake landscape and bird habitat and dredging for water depth reaches of 1.5m. For lagoon restoration project, the capacity of water exchange has been studied by solving the convection-diffusion equation based on Eulerian method. The geometry of tidal inlet is one of key control factors of the lagoon system. Due to that its changes will influence the system's hydrodynamic characteristics. Hence, the influence of tidal inlet width on current and water exchange is focused in this study through a 2D hydrodynamic numerical model based on MIKE 21.

2 METHOD

A two-dimensional finite volume model based on MIKE21 Flow Model (FM) and Transport Model developed by the DHI Group (DHI, 2014) was established to study water exchange of Qilihai lagoon. The

MIKE21 FM adopts a flexible unstructured mesh and has been widely used for applications in coastal and estuarine environments. The system was based on the numerical solution of the two-dimensional incompressible Reynolds-averaged Navier-Stokes equations with the assumptions of Boussinesq and hydrostatic pressure.

A three-level unstructured triangular mesh system was set up as shown in Figure 1. The large mesh (Level 1) covers the whole Bohai Sea to ensure a correct tidal flow field, and the middle mesh (Level 2) is intermediate covering Qinhuangdao coastal water, including tidal inlet of Qilihai, which can provide the water level and current boundary to the small mesh (Level 3). The small mesh is a fine grid of Qilihai lagoon to provide a high-resolution flow field for the study area. The large, middle and small meshes have 14183, 7670 and 1416 nodes with 23419, 14440 and 2477 elements respectively.

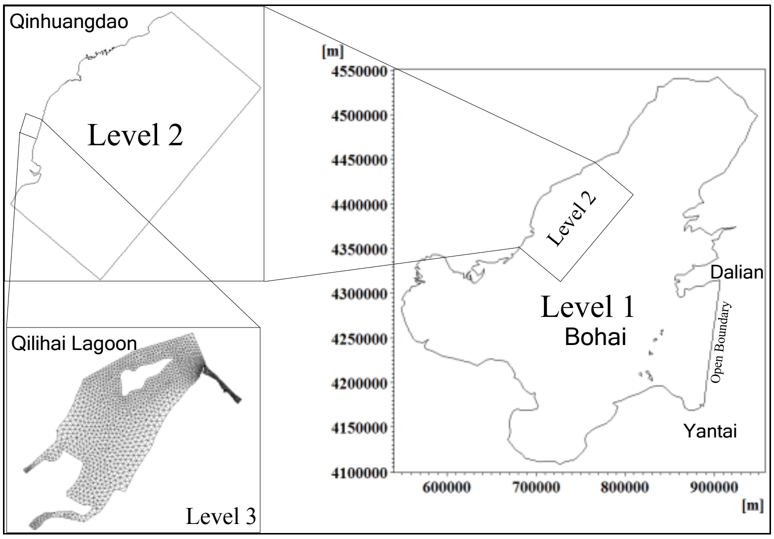

Figure 1. Study Area and Computational Mesh.

The open boundary in Level 1 located through the Bohai Strait and the open boundary condition were given based on the tidal tables of Dalian and Yantai provided by National Marine Data and Information Service of China. Model bed resistance is determined by Manning number and relation between the Manning number, water depth and the bed roughness can be estimated using the following (DHI, 2014):

$$M = \frac{2.5\sqrt{g}\,\ln(\frac{30h}{k_s e})}{h^{1/6}} \qquad [1]$$

M and h are Manning number and water depth, e is the Napierian base, g is the acceleration of gravity, k_s is the Nikuradse bed roughness which is generally defined as 2.5 times the diameter of the sediment. The average sediment diameter was 0.268 mm and average water depth was 1.5m. The calculated value for Manning number was 74 $m^{1/3}/s$ which had been used previously in the study of hydrodynamics and pollutant transport in Qinhuangdao coastal water (Kuang et al., 2015).

The model adopts wet-dry dynamic boundary processing technology, and the critical water depths of dry and wet points were 0.005 m and 0.05 m respectively. The computational time step was in the range of 0.1-30s and adjust themselves to meet the Courant number to be less than 1 in the model calculation process. The horizontal eddy viscosity coefficient uses Samagorinsky model to calculate the grid scale and Samagorinsky coefficient was 0.28. The initial velocity and water level were 0 m/s and 0 m respectively.

Residence time indicating the timescales of water exchange from a water body is a widely-used index for assessment of water quality which is defined as the time required for the mass of a conservative constituent in the water body reducing to a given percentage of its initial mass (Pan et al., 2014). The given percentage, or cutoff percentage, was taken as different values by different researchers and agencies, e.g., 10% (Huang et al., 2011) and 1/e (Abdelrhman, 2005; Asselin and Spaulding, 1993). Considering that the study area is a lagoon and the water exchange was relatively slow, 1/e was taken as the cutoff percentage to calculate the residence time. For studying water exchange in Qilihai lagoon, conservation substance transport model was established, and computed tracer mass was dealt with Eulerian method based on solving the convection-diffusion equation and least-squares method to fit nonlinear curve, then the residence time is obtained to analyze water exchange capacity, which can provide a scientific basis for the tidal inlet design. Numerical tracer test determines the residence time. Firstly, the studied water should be dyed to unit-concentration tracer agent, then convection-diffusion equation of water and the tracer concentration should be solved and the rest of the tracer mass comes out. Tracers in the model were released at the lowest water level for residence time so that we can have a conservative estimate. Variation of the rest of the tracer mass can be expressed by attenuation formula (Kuang et al., 2009).

$$M_t / M_0 = \beta e^{-kt} + C \quad [2]$$

M_t and M_0 are tracer mass at t moment and initial moment respectively, β, k and C are parameters those can be obtained by least-squares method.

3 RESULTS

A 2D hydrodynamic model in Level 3 has been established drive by water level and current speed from Level 2 model. The flow fields at four different typical moments under 200m tidal inlet width scenario are shown in Figure 2. It can be seen that the magnitude of current speed in tidal inlet was relatively large while it was small in the lagoon, and the current speed in the north of Central Island was bigger than that in the south. During the flood period, there is an anti-clockwise circulation near the tidal inlet, and the circulation area reaches the largest at the moment of flood slack.

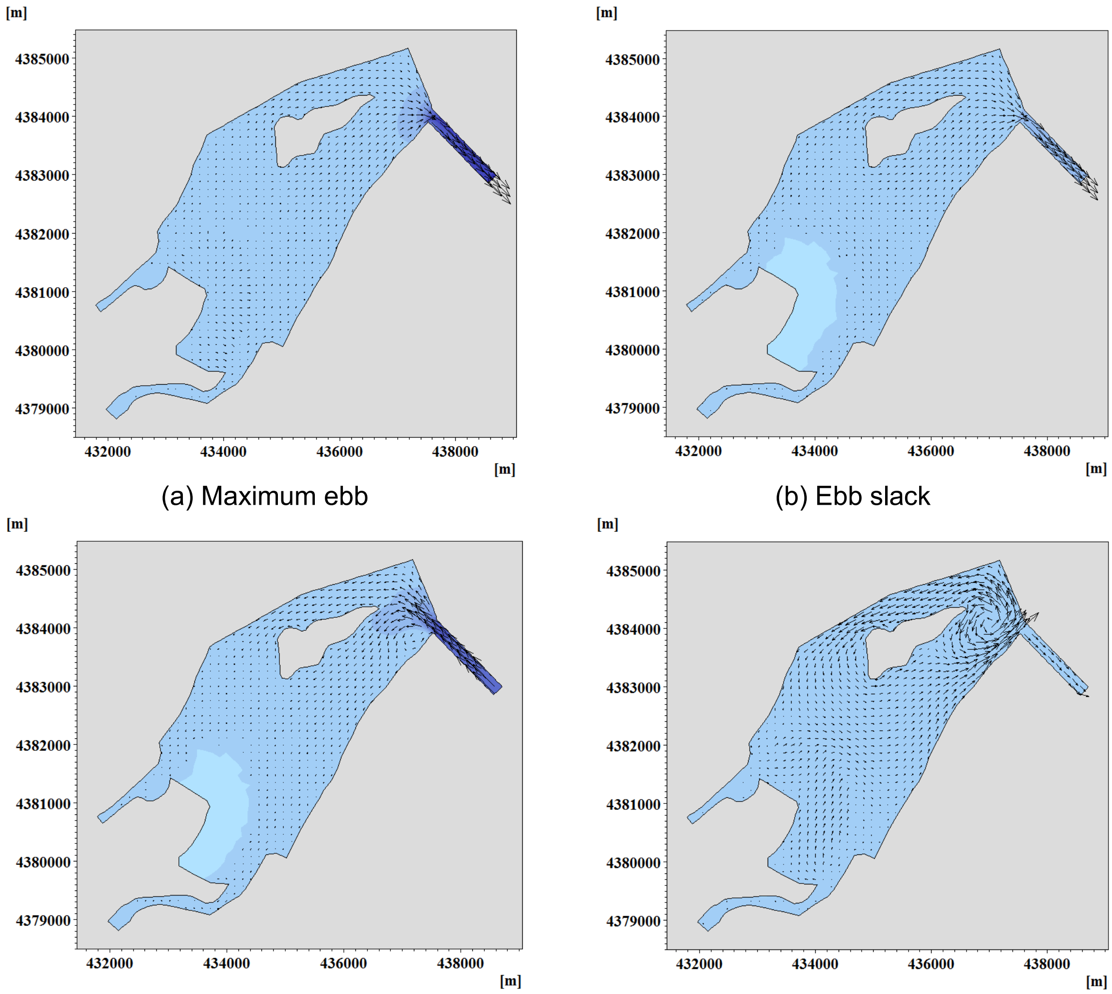

(a) Maximum ebb (b) Ebb slack

(c) Maximum flood (d) Flood slack

Figure 2. Flow fields at four different typical moments under 200m tidal inlet width scenario.

To compare and analyze the influence of tidal inlet width on hydrodynamic and water exchange, the simulation of four scenarios with different tidal inlet widths, i.e., 100m, 200m, 300m and 400m respectively, had been done. The comparisons of discharge, water level and current speed at inlet under four scenarios are given in Figure 3. The shape of tide shows two peaks and two troughs in a tidal cycle and high water level last longer than low water level, i.e., the tide is an asymmetry semi-diurnal tide. With the increase of inlet width, both flood and ebb discharges increases, the quantity of flow exchange in the lagoon becomes larger. The range of water level turns into larger and the mean current speed from the tidal inlet into lagoon becomes smaller.

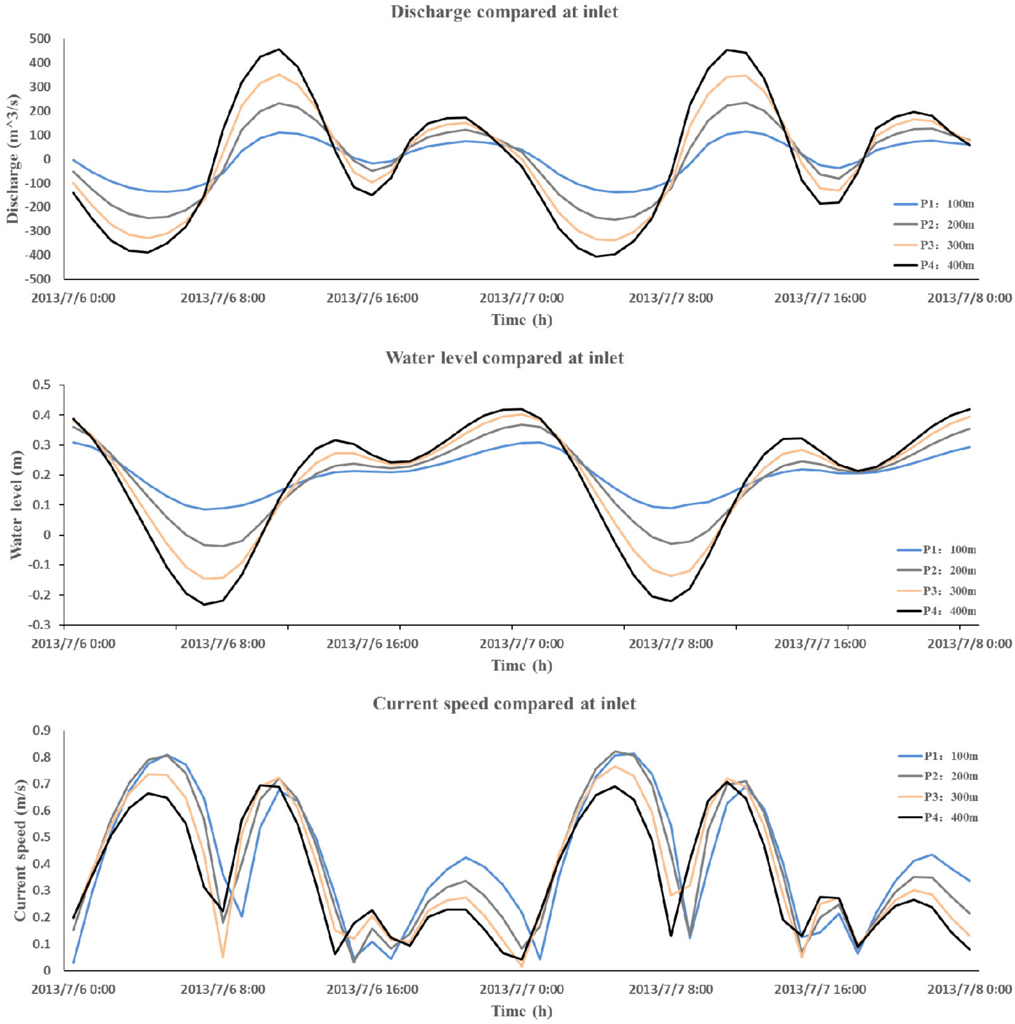

Figure 3. Comparisons of discharge, water level and current speed at inlet under four scenarios (100m, 200m, 300m and 400m of tidal inlet width).

For studying the water exchange in Qilihai lagoon, convection-diffusion equation was solved and a nonlinear curve was fitted by least-squares method as shown in Figure 4. Tracer mass increases during flood period and decreases during ebb period and the total variation trend over time were decreasing, which are illustrated by the 200m tidal inlet width scenario in Figure 4(a). The residence time was determined as the cutoff percentage of 1/e to evaluate the water exchange capacity and residence time of four scenarios. The residence times were 887h, 551h, 468h and 445h for the tidal inlet widths of 100m, 200m, 300m and 400m, respectively. Correspondingly, the reduction ratios of residence time from 100m to 200m, 200m to 300m and 300m to 400m were 37.9%, 15.1% and 4.9% respectively. Due to low residence time, this means high water exchange capacity occurred where the scenario of 200m tidal inlet width had the most effective improvement in the water exchange.

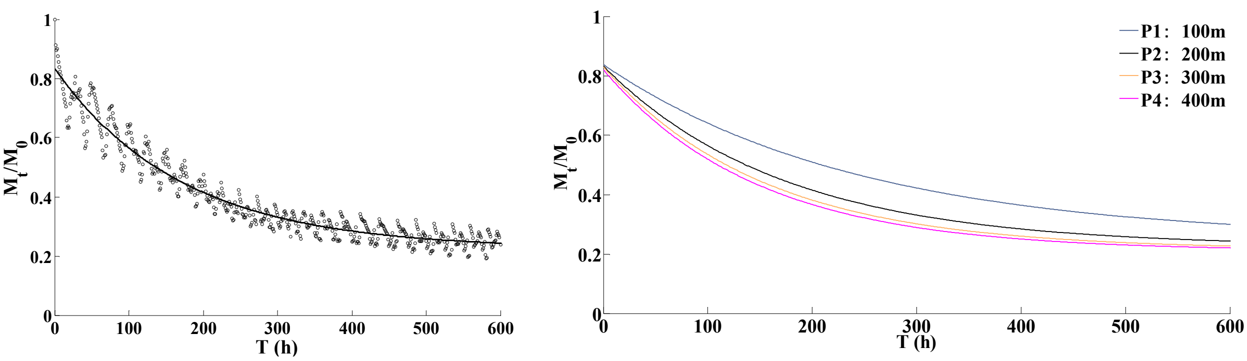

(a) 200m tidal inlet width (b) four tidal inlet widths

Figure 4. (a) Variations of tracer mass over time in 200m tidal inlet width scenario; (b) Best-fitted curve of tracer mass variation under four scenarios (100m, 200m, 300m and 400m of tidal inlet width).

4 CONCLUSIONS

Based on 2D hydrodynamic and transport model, four different tidal inlet widths of Qilihai lagoon have been simulated. Variation of hydrodynamic and water exchange capacity is compared and analyzed where main results can be concluded that:

(1) The current speed in tidal inlet is larger than that in lagoon, and there is an anti-clockwise circulation near the tidal inlet during flood period and the circulation area reaches the largest at the moment of flood slack.

(2) With the increase of tidal inlet width, flood and ebb discharges, the range of water level increase, while the mean current speed decreases at the inlet.

(3) With the increase of inlet width, the residence time decreases. While the tidal inlet width is 200m, the improvement of water exchange has been the most effective.

REFERENCES

Abdelrhman, M.A. (2005). Simplified Modeling of Flushing and Residence Times in 42 Embayments in New England, USA, With Special Attention to Greenwich Bay, Rhode Island. *Estuarine Coastal & Shelf Science,* 62(1–2), 339-351.

Asselin, S. & Spaulding, M.L. (1993). Flushing Times for the Providence River based on Tracer Experiments. *Estuaries and Coasts,* 16(4), 830.

Bi, Y., Liu, H., Jiang, S., Xue, K. & Wang, N. (2000). Primary Study on Seawater Exchange and Environment Forecast in Xiaoyao Bay. *Marine Environmental Science,* 19(3), 40-43.

Davies, A.M. (1982). Meteorologically Induced Circulation on the North-West European Continental Shelf: from A 3-Dimensional Numerical-Model. *Oceanologica Acta,* 5(3), 269-280.

DHI. (2014). *Hydrodynamic and Transport Module Scientific Documentation.* DHI.

Huang, W., Liu, X., Chen, X. & Flannery, M.S. (2011). Critical Flow for Water Management in a Shallow Tidal River based on Estuarine Residence Time. *Water Resources Management,* 25(10), 2367-2385.

Kawasaki, K., Murakami, T., Toda, K. & Okubo, Y. (2008). Particle Tracking Analysis on Seawater Exchange and Soil Transport in Ise Bay Area at Tokai Heavy Rain. *Doboku Gakkai Ronbunshuu B,* 55, 986-990.

Kuang, C.P., Lee, J.H.W. & Liu, S.G. (2009). Effect of Large Scale Reclamation on Hydrodynamic Circulation in Victoria Harbour of Hong Kong. *Journal of Tongji University (Natural Science),* 437(2), 176-181.

Kuang, C.P., Hu, C.F., Mao, X.D. & Gu, J. (2015). Numerical Simulation of Hydrodynamics and Pollutant Transport in Qinhuangdao Coastal Water in the Flood Season. *Journal of Tongji University (Natural Science),* 43(9), 1355-1360.

Luo, F., Liao, G.H., Yang, C.H. & Xu, X.H. (2011). Study on the Features of Water Exchange in Yueqingwan Bay. *Journal of Marine Sciences,* 2, 011.

Ntengwe, F.W. (2006). Pollutant Loads and Water Quality in Streams of Heavily Populated and Industrialised Towns. *Physics & Chemistry of the Earth Parts A/B/C,* 31(15–16), 832-839.

Pan, Y., Kuang, C.P., Gu, J., He, L.L., Zhang, Y., Yang, Y.X., Qiu, R.F. & Zhang, J.B. (2014). Assessment of a Measure for Water Exchange Strengthening of Artificial Headland Bays based on Shoreline Change and Flushing Time. *Journal of Coastal Research,* 295(3), 615-628.

Parker, D.S., Norris, D.P. & Nelson, A.W. (1972). Tidal Exchange at Golden Gate. *Journal of Sanitary Engineering Division,* 98(2), 305-323.

Suffet, I.H. (1977). *Fate of Pollutants in the Air and Water Environments. Part 1. Mechanism of interaction between environments and mathematical modeling and the physical fate of pollutants.* (No. CONF-750410-P4). John Wiley and Sons, Inc., New York, NY.

BIOAVAILABILITY AND BIO ACCESSIBILITY OF HEAVY METALS IN SURFACE AND SUB-SURFACE SEDIMENTS IN INTERNATIONAL WETLAND OF ZARIVAR, IRAN

AMIR HAJNOROOZI[1], ABDOLREZA KARBASSI[2], SADEGH PARTANI[3], FATEMEH TORABI[3] & KACHOOSANGI[4]

[1,3] Civil Engineering Department, Faculty of Engineering, Islamic Azad University, Central Tehran Branch (IAUCTB), IRAN,
amirnoroozy1981@gmail.com; sadegh_partani@yahoo.com
[2,4] Faculty of Environment, University of Tehran, Tehran, IRAN ,
fatemeh.torabi@gmail.com

ABSTRACT

This paper has attempted to do an in-situ research based on new data generation due to structured field sampling and laboratory measurement in finding out the pollution and contamination risk of bioavailability and bio-accessibility of heavy metal in Zarivar wetland. This research aims to figure out the heavy metal contamination level and evaluate the risk of its pollution in human life cycle. Structures regular rout sampling plans was considered for two different locations of wetland. Surface and subsurface sediment samples were taken and transported to laboratory in standard method. Total concentration of 26 trace elements were measured within inductively coupled plasma atomic emission spectroscopy (ICP-AES) techniques. To determine the bioavailability and bio accessibility, Ethylenediaminetetraacetic acid (EDTA) and Glycine digestion were applied for the same samples to estimate the bioavailability and bio accessibility of trace elements. The results showed high levels of Lead (Pb), Nickel (Ni), Copper (Cu), Cadmium (Cd), Arsenic (As), and Silver (Ag) in raw sediment samples. Bioavailability tests were carried out on leached extracted samples and declared the dramatic amount of Aluminium (Al), Ag and Zinc (Zn) in sediments. There were significant difference in concentration of elements in surface and sub-surface samples. Pore water laboratory analysis on the same heavy metals revealed 70% of bioavailability analysis but current root tissues of floating plants samples were drastically different from them. Therefore, the suggestion of water cycle and reservoir hydraulic flow could be assigned for this phenomenon. However, little pollution and low level of trace metal contamination were obtained during the research while there is no river which is terminated in the wetland. It seems that the agricultural activities might be the main source of pollution. Pollution indices and original pollution analysis declared that the pollution might goes toward the anthropogenic variety more than the natural one which may cause by agricultural activities.

Keywords: Heavy metals; bioavailability; bio accessibility; international wetland of zarivar; sediment sample.

1 INTRODUCTION

Bioavailability of Heavy Metals (HMs) may be considered in an aquatic ecosystem in bottom and suspended sediments. Industrial or domestic sewage, storm runoff, leaching from landfills, shipping and harbor activities and atmospheric deposits (Jafari et al., 2014) are effective factors in distribution patterns of HMs (Tabatabaei et al., 2014). HMs' Geochemical availability of bottom sediment has been an important challenge recently, and transportation and adsorption of HMs are effected by different geochemical process (Alhashemi, et al., 2011).

Sediment HMs studies in coastal areas (Hervé et al., 2010; Udayakumar et al., 2014), salt marshes and river basins (Siddique and Aktar, 2012) and estuaries (Karbassi et al. 2016) were taken to find out the pollution and dynamics of HMs.

Sometimes mining and agricultural activities influence on the heavy metal concentration in sediment and water. The toxicity of heavy metals has long been of great concern since it is very important to the health of people and ecology (Feng et al. 2008). Heavy metal pollution was reported for Mengkabong Lagoon as a result of human activities (Praveena et al., 2008). They concluded that the top 5 cm of aquatic sediment is very reactive.

Water, which can be dispersed and accumulated in plants and taken in by humans through consumption (Wcisłoa et al., 2002). Sediments, which play both the source and sink roles, are very important in evaluating the pollution level of heavy metals (Al-Juboury and I. 2009; Zhipeng et al., 2009). Despite the differences in toxic effects of the metals, their concentrations are reliable indicators of ecosystem health (Jain et al., 2005). Aquatic organisms can bioaccumulate, biomagnificate or bio transfer certain metals to concentrations high enough to bring about harmful effects (J. Naimo 1995; Opuene et al., 2008) in the aquatic environment, and sediments have a high storage capacity for contaminants. In the hydrological cycle, less than 0.1% of the

  / ISSN 1562-6865 (Online) - ISSN 1063-7710 (Print)

metals are actually dissolved in the water and more than 99.9% are stored in sediments and soils (Karbassi et al., 2007; Pradit et al., 2010).

They act as carriers and possible sources of pollution due to the fact that heavy metals are not permanently fixed by them and can be released back to the water by changes in environmental conditions, therefore they may become sufficiently polluted to disrupt natural biological communities. Contaminated sediments are known to be responsible for degradation of water quality in the natural waters especially in the shallow and enclosed water systems (Toluna et al., 2001; Venugopal et al., 2009).

Also, most of the researchers have now realized that the toxicity of heavy metals has much to do with the bioavailability and not total concentration (Li Feng et al., 2008). In this study, Zarivar wetland is selected for determination of trace elements in sediments and identification of natural and anthropogenic sources shares because of trace elements transfer in upper levels of food chains that can contribute to toxic levels. For this purpose, Chromium (Cr), Ag, Cu, Pb, Al, As, and Cd were measured in the study area. The estuaries are complex systems which receive inputs from different sources like land derived material through river, banks, marine, atmosphere etc. The river waters that mix with sea water in estuaries vary with the rate of freshwater discharge from the drainage basin and with the geological and geochemical characters of each drainage basin (Alhashemi et al., 2011). Therefore, the sedimentation in estuaries is within three distinguishable regimes viz. estuarine fluvial, estuarine brackish and estuarine marine. Fine sedimentary deposits or mud are a characteristic feature of estuaries. The most significant sorting is the coarse (gravel and sand), which are found in the more energetic areas and fine (silt and clay) sediments, which accumulate in low energy conditions or quiet waters. It is also necessary to mention here that the sediments are composed of different geochemical phases such as clay, silt, and sand, organic material, oxides of iron and manganese, carbonate and supplied complexes that act as potential binding sites for metals. In the sediments, metals can be present in various forms and generally exhibit different physical and chemical behavior in terms of chemical interactions, mobility, biological availability and potential toxicity. Therefore, the fate of various metals, in the natural environment is of great concern. Metals may be partitioned into six fractions: dissolved, exchangeable, carbonate, iron-manganese oxide, organic, and crystalline. The metal bioavailability includes metal species that are bio-accessible and are absorbed or adsorbed by an organism with the potential for distribution, metabolism, elimination, and bioaccumulation (Alhashemi et al., 2011).

2 METHODOLOGY

2.1 Study area

Zarivar wetland is one of the most important wetlands that is located in northwest of Iran within Kurdistan Province of western Iran. Figure 1 shows (S1, 35°31'51.89"N, 46° 7'17.13"E - S2, 35°32'9.19"N, 46° 7'59.74"E) the location of stations and sediment samples in the study area. It has a length of 5 km (3.1 mi) and a maximum width of 1.6 km (0.99 mi). The lake's water is fresh and has a maximum depth of 6 meters (20 ft) (Sobhanardakani and Jafari, 2014), but due to the field survey of this research, some spots were revealed to have more than 7 meters in depth. Zerivar Lake is a major touristic attraction in the region. Zarivar is fed by a seasonal river and its water is provided by the precipitation dominantly (Asadi et al., 2014).

2.2 Field study

Some research declared that old HMs has most resistance to dilution and washing courant (Hervé et al., 2010). Macro Scale Parameters (MSPs) which may be origin of some HMs, such as erosion (Hervé et al., 2010) and land use (Mwalusepo et al., 2017) are considered in this research as surrounding land use and land cover that are dominated by agricultural activities (Sobhanardakani et al., 2014).

Sediments samples were collected from Lake Zarivar on 26 of August 2016 at two sampling stations (here in after appeared by letter "S" and followed by 1 or 2 as station number), and in two routes, which are in the center of Lake and far from Lake Coast. In each of these routes, two samples as surface (here in after followed by "S" in tables) and deep (here in after followed by "D" in tables) samples were taken.

2.3 Sampling process

Sediment and water sampling was done during summer, 2016. Surface sediment was collected manually. Subsurface sampling of the sediments was carried out in 20 cm of sediment depth using diver and tubes of the polyethylene pipe. Sediment samples were preserved at 4 ° C (Jain et al., 2005). US EPA water sampling preservation and transferred to Inductively Coupled Plasma Mass Spectrometry (ICP) laboratory. Water samples were added by acidic to reduce pH and stored at 4 ° C(Jain et al., 2005). Physic-chemical analysis involving grain size fraction (Allen, 1989), pH, electrical conductivity (EC) and total organic matters (Alhashemi et al., 2011) was performed in sediment samples.

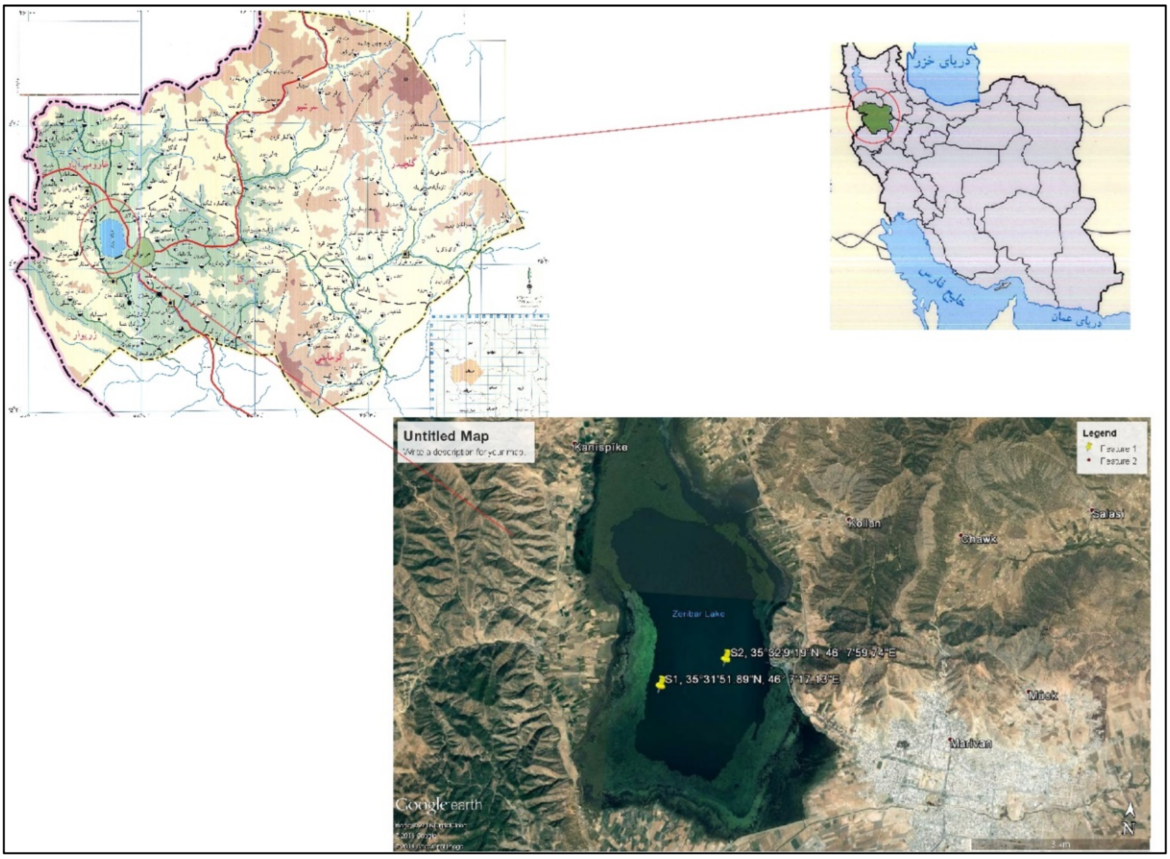

Figure 1. Study Area and Sampling Stations.

2.4 Laboratory Measurements

The first step of HMs analysis was ICP-OES mechanisms. Four-Acid method were employed to digest and prepare the sediment samples (Agency, 1994) for ICP-OES analysis. The powdered raw samples were leached using per chloric acid, Nitric acid and Hydrochloric acid each to a certain level, at the temperature of 220 ° C for four hours in Hot Box.

The second step was the simulation of bio adsorption to find bio-availability. The chemical simulation was applied to samples using Glycine and EDTA (EPA, 2000; Quevauviller et al, 1997) digestion process. Then, the prepared samples went on ICP-MS device (Model: ICP-MS Agilent series 4500) for residual HMs measurements.

2.5 Preliminary data validation tests (QA/QC)

Normality tests was applied to all data and outliers were removed due to cook's distance. Quality control and quality assurance procedure were performed in two stages. Field sampling (ref. 6/24, US EPA 2001) and laboratory measurements (Eaton et al., 1999)

3 ANALYSIS METHODS

In this method, a solution of 0.05 mg EDTA ($C_{10}H_{16}N_2O_8$) and the ratio of 1:10 was used to precipitate soluble. The time required for a time was considered shakers. Also, centrifuge for 20 minutes at 30 rpm was used. The results of this test can simulate the amount of heavy metal uptake (Quevauviller et al., 1997). The 0.04 glycine was dissolved to simulated gastric digestion solution which is used to simulate the bioavailability of heavy metals for organisms. The glycine solution and the ratio of deposits to the solution of 1: 100 was used. After centrifugation, the samples were performed with an intensity of 30 rpm (Table 1).

4 RESULTS AND DISCUSSION

Heavy metals could be found naturally according to earth’s crust concentration (Mcdonougha and Sun., 1995). Chemical composition of the upper crust is thus important to find out the relative potential contamination of continental crust surface soil (Bu et al., 2016). Most of HMs contamination are resulted from agricultural activities and domestic (Omole et al., 2006). Comparative assessment on measured samples and earth's crust background (Hu and Gao. 2008; Mcdonougha and Sun. 1995) is illustrated in figure 2. As it can be seen, concentration of Pb, Ni, Cu, Cd, As and Ag have upper level amount versus earth's crust value.

As mentioned before, in vitro digestion to extract the bio-availability of HMs was carried out using EDTA and Glycine and the results are presented in figure 3. The differences between the two digestion methods in samples demonstrated that there are no significant variances between two deeps samples while the differences of the two digestion method were considerable. Zn, Al and Ag have recognizable amounts of bio-availability contention. Another suggestion is referable according to pore water ICP analysis (Table 2). Negligible and small amounts of HMs in water samples allow the research consideration to reveal and disapproval point of view on high level of bio-availability.

Table 1. The results of analysis inductively coupled plasma optical emission spectrometry (ICP-OES), Four-Acid method, EDTA and Glycine. (mg/kg)

Element	Unit	S1-D	S2-D	S2-S	S1-D EDTA	S2-D EDTA	S1-D GLYCINE	S2-D GLYCINE
Ag	PPM	0.22	0.22	0.19	0.04	0.04	0.04	0.04
Al	PPM	16962	21740	20600	1.18	0.93	2.36	3.16
As	PPM	5.7	5.7	8	0.04	0.04	0.04	0.04
Cd	PPM	0.29	0.32	0.32	0.04	0.04	0.04	0.04
Cr	PPM	34	20	22	0.04	0.04	0.09	0.04
Cu	PPM	20	14	33	0.04	0.04	0.22	0.04
Fe	PPM	12087	13762	13489	1.83	1.91	9.14	8.62
Mn	PPM	924	762	767	0.72	1.39	1.37	1.85
Ni	PPM	35	33	33	0.04	0.04	0.04	0.04
Pb	PPM	49	25	48	0.05	0.11	0.25	0.22
V	PPM	20	27	27	0.04	0.04	0.04	0.04
Zn	PPM	38	33	43	0.16	0.35	0.74	0.64

Table 2. The results of analysis ICP-OES water. (mg/kg)

Element	Unit	Station 1	Station 2
Ag	PPM	0.04	0.04
Al	PPM	0.09	0.09
As	PPM	0.04	0.04
Cd	PPM	0.04	0.04
Cr	PPM	0.04	0.04
Cu	PPM	0.04	0.04
Fe	PPM	0.09	0.09
Mg	PPM	17.14	17.01
Mn	PPM	0.34	0.09
Pb	PPM	0.04	0.04
V	PPM	0.04	0.04
Zn	PPM	0.04	0.04

Correlation between some HMs is important as a hint of source estimation (Bu et al., 2016). For example, in Iran, taking Iran continental earth's crust as the base of the study area, Vanadium and Nickel are indices of oil resources (Tabatabaei et al., 2014). Cluster analysis followed by hierarchical dendrogram was employed to find the Pearson linkage correlation. Following dendrograms show correlated HMs in same clusters. In total concentration and bio-availability extracted samples, Fe-Al and Mn-Fe-Al appeared in same cluster respectively in figure 4.

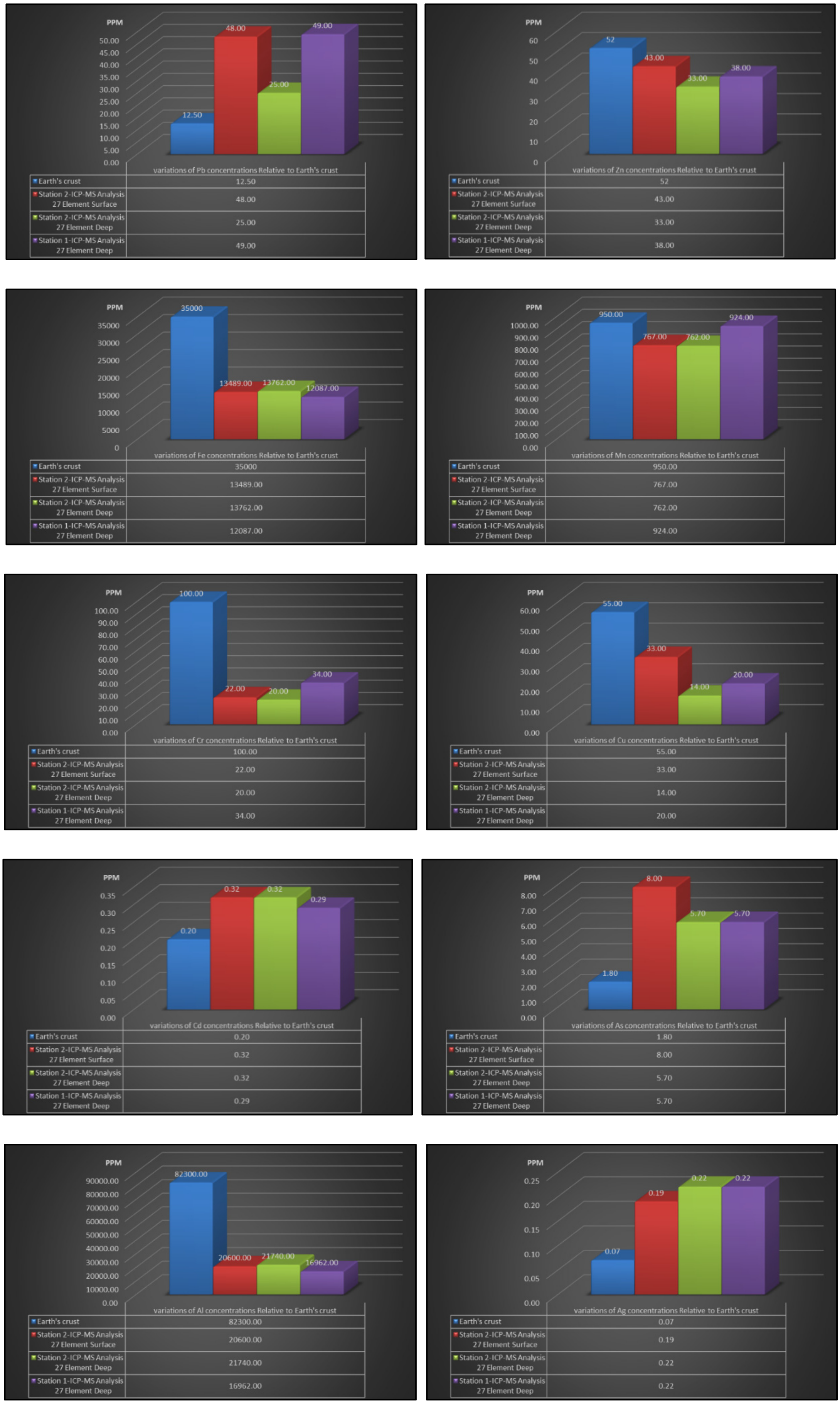

Figure 2. Variations of heavy metal concentrations Relative to Earth's Crust.

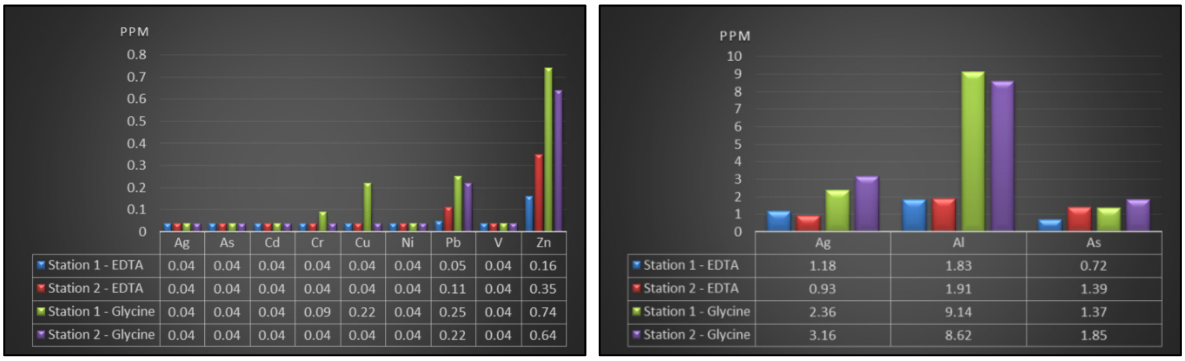

Figure 3. Variations of heavy metal concentrations in EDTA Relative to Glycine.

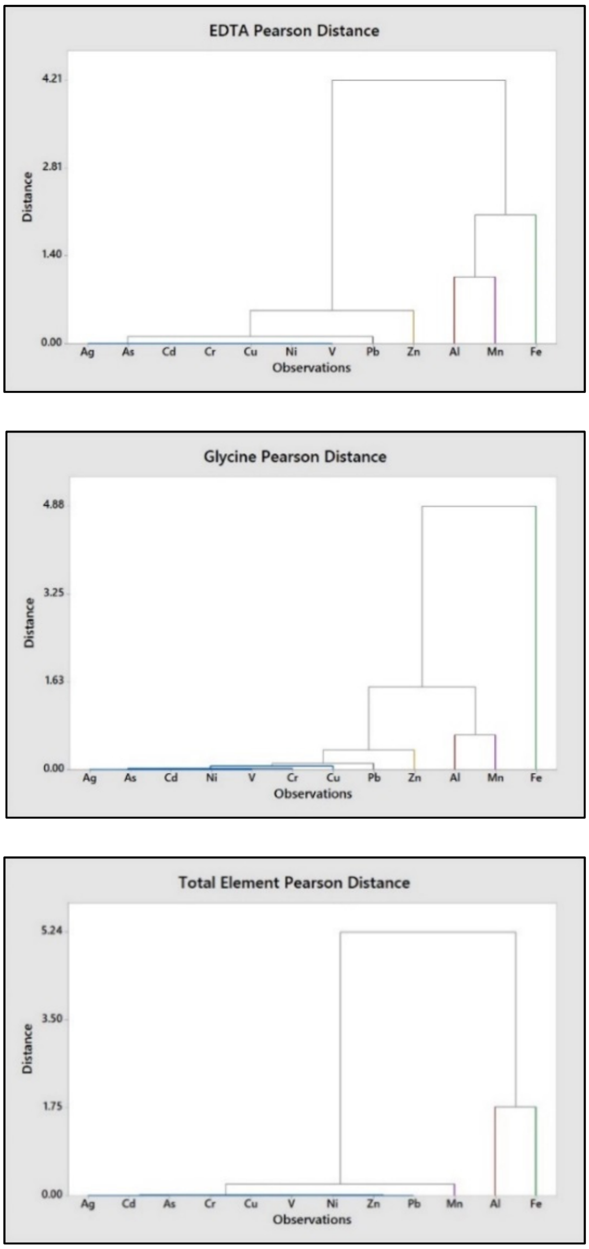

Figure 4. Dendrogram of cluster analysis amongst heavy metals, EDTA and Glycine in Zarivar wetland bed sediments.

There is a considerable variation in how the impact of anthropogenic pollution in a study area is estimated. To figure out the geo-chemical pollution level, some popular sediments indices were calculated. A known approach to estimate the human activities impact on marine sediments is to calculate a normalized enrichment factor (EF) for metal concentrations above uncontaminated background levels (Abrahim and Parker. 2008). Enrichment factor which is proposed by Sutherland (Likuku et al. 2013) was used as follows.

The EF was calculated according to the following equation:

$$EF = (M_x \times Fe_b) / (M_b \times Fe_x) \quad [1]$$

EF<2 is deficiency to minimal enrichment
EF 2-5 is moderate enrichment
EF 5-20 is significant enrichment
EF 20-40 is very high enrichment
EF>40 is extremely high enrichment

where M_x and Fe_x are the sediment sample concentrations of the heavy metal and Fe (or other normalizing element), while Mb and Feb are their concentrations in a suitable background or baseline reference material (Karbassi et al. 2006; Karbassi et al. 2008). Only Ag, As, Cd and Pb exhibit moderate to significant enrichment. However, on the basis of comparison between methods, there are considerable differences in EF values for Cu, Cr and Zn. I_{geo} as a geochemical accumulation index was calculated for laboratory results according to the following equations;

$$I_{geo} = Log_2\left[\frac{Cn}{Bnx1.5}\right] \quad [2]$$

$$I_{Poll} = Log_2\left[\frac{Cn}{Bn}\right] \quad [3]$$

where Cn is the metal concentration in sediment and Bn is the metal concentration in shale (Mediolla et al., 2008). I_{Poll} is the pollution index, an optimized form of I_{geo} (Asaah and Akinlolu, 2005). Seven contamination ranges have been determined to assess the metal pollution status (Martin et al., 1979).

$I_{geo} \le 0$ means unpolluted
$0 < I_{geo} < 1$ means unpolluted to moderately polluted
$1 \le I_{geo} < 2$ means moderately polluted
$2 \le I_{geo} < 3$ means moderately to strongly polluted
$4 \le I_{geo} < 5$ means strongly to very strongly polluted
$I_{geo} \ge 5$ means very strongly polluted another

Heavy metals are that it is unpolluted to moderately polluted and unpolluted except Cd, and Pb average are infected (Karbassi et al., 2011). The results of figure 3 confirmed the availability of heavy metals that were digested and extracted by Glycine. This kind of availability can strengthen the hypothesis of human availability of heavy metals more than phyto-availability (Likuku et al., 2013) (Table 3).

Table 3. Comparison of I_{geo} and EF values for metals in sediments of Zarivar wetland.

Element	Igeo			EF		
	S1-D	S2-D	S2-S	S1-D	S2-D	S2-S
Ag	-3.0324	-3.0324	-3.2439	11.9609	10.5051	9.2562
Al	-2.2377	-2.4646	-2.5423	0.7844	0.8829	0.8536
As	-1.3959	-1.9809	-1.4919	12.0515	10.5847	15.1564
Cd	0.5361	0.0931	0.0931	5.5183	5.4643	5.4563
Cr	-1.4044	-2.7549	-2.6174	1.2940	0.6685	0.7502
Cu	-1.1699	-2.2695	-1.0324	1.3839	0.8508	2.0461
Fe	-1.9592	-2.3569	-2.3858	1.0000	1.0000	1.0000
Mg	-0.2129	-0.5929	-0.6683	2.4627	2.4932	2.4141
Mn	0.1204	-0.7426	-0.7332	3.7016	2.6811	2.7533
Pb	1.2928	-0.2630	0.6781	14.9185	6.6851	13.0951
V	-2.5850	-2.7370	-2.7370	2.1747	2.5785	2.6307
Zn	-1.3219	-2.1104	-1.7286	2.0660	1.5758	2.0948

4 CONCLUSION

Assessment of pollution by heavy metals in Zarivar wetland sediments revealed the high contamination potential of Al, Pd, Zn, Ag and As which the bioavailability of As, Al and Zn were dramatically higher than others. These elements were evaluated using enrichment factors, geo-accumulation index. Degree of enrichment was examined by comparing present day sediment metal contents obtained using actual metal concentrations with standard earth material obtained from literature. In aggregation differences between

heavy metals concentration were significant but most of them appeared lower than critical pollution amount. The important problem that attracted all points of views was the high human-based bioavailability index in some dangerous trace elements such as As and Zn. The suggestions on this phenomenon can be put forward on the type of pesticides and herbicides which are popularly used in agricultural activities of drain area of wetland. Detecting this amount in the depth of middle of wetland may be caused by long term discharge there. However, increasing the concentration in depth can approve the hypothesis.

Although the nature of calculating geo-accumulation indices (I_{geo}) is somewhat different from pollution calculation methods discussed in other studies and bioavailability investigations will also be needed to be carried out by other extraction solvents to figure out the exact amount of HMs in water body.

ACKNOWLEDGMENTS

The authors are gratefully acknowledging the support of the Modares Environmental Research center (MERC) of Tarbiat Modares University of Iran for cooperation in sample preparation. The authors also highly appreciate the works done by Mr. Abueian, master student of mining engineering and Mrs. Mazrouei, master student of civil engineering for providing assistance with sampling and extraction process.

REFERENCES

Abrahim, G. M. S. & Parker, R. J. (2008). Assessment Of Heavy Metal Enrichment Factors And The Degree Of Contamination In Marine Sediments From Tamaki Estuary , Auckland , New Zealand. *Environmental Monitoring Assesment*, 136, 227–238.

Agency, U. S. E. P. (1994). B. Methods For Assessing The Toxicity Of Sediment Associated Contaminants With Estuarine And Marine Amphipods. *Narragansett, RI.EPA-600/R94-025*.

Al-Juboury, & I., A. (2009). Natural Pollution By Some Heavy Metals In The Tigris River ,. *International Journal Of Environmental Research*, 3(2), 189–198.

Alhashemi, A. H., Karbassi, A. R., Kiabi, B. H., Monavari, S. M. & Nabavi, M. B. (2011). Accumulation And Bioaccessibility Of Trace Elements In Wetland Sediments. *African Journal Of Biotechnology*, 10(9), 1625–1636.

Allen SE. (1989). *Chemical Analysis Of Ecological Materials, 2nd Ed., Blackwell Scientific Publ., Oxford.*

Asaah, & Akinlolu. (2005). Heavy Metal In Cattle Market Soils Of Ibadan , Southwestern Nigeria . Is There Any Environmental Risk. *The Arabian Journal For Science And Engineering*, 31(2A), 147–158.

Asadi, M., Ghaderzadeh, H., Chapi, K. & Rezaie, F. (2014). IBWRD Estimation Of Willingness To Pay For Conservation Of Zarivar Wetland , Iran : A Contingent Valuation Approach. *Internationa Bulletin Of Water Resources & Developmet*, *1*(2), Online Publish Edition.

Bu, J., Sun, Z., Zhou, A., Xu, Y., Ma, R. & Wei, W. (2016). Heavy Metals In Surface Soils In The Upper Reaches Of The Heihe River , Northeastern Tibetan. *International Journal Of Environmental Research And Public Health*, 247(13), 1–19.

Eaton, D., A., Clesceri, S., L. & Greenberg, E. A. (1999). *Standard Methods For The Examination Of Water And Wastewater Part 4000 INORGANIC NONMETALLIC CONSTITUENTS Standard Methods For The Examination Of Water And Wastewater*, Standard Methods For The Examination Of Water And Wastewater.

EPA. (2000). *Appendix To Bioacculation Testing And Interetation For The Purpose Of Sediment Quality Assessment Status And Needs Chemical-Specific Summary Tables*. *Environmental Protection*.

Hervé, R. P., Andriamalala, R., Yves, M., Marcellin, R., Christine, R. & Andriamandimbisoa, N. (2010). Assessment Of Heavy Metals Concentrations In Coastal Sediments In North-Western Cities Of Madagascar. *African Journal Of Environmental Science And Technology*, 4(2), 51–60.

Hu, Z. & Gao, S. (2008). Upper Crustal Abundances Of Trace Elements : A Revision And Update. *Chemical Geology Journal*, 253, 205–221.

J. Naimo. (1995). A Review Of The Effects Of Heavy Metals On Freshwater Mussels. *Ecotoxicology*, 4(6), 341–362.

Jafari, Milad, Seyed, Sobhanardakani, & Soheil. (2014). Determination Of Heavy Metal (Cu , Pb And Zn) Concentrations In Muscle Tissue Of Hypophthalmichthys Molitrix , Cyprinus Carpio And Ctenopharyngodon Idella Caught From Zarivar Wetland , Western Iran. *Current World Environment*, 9(3), 923–931.

Jain, Singhal, & Sharma. (2005). Metal Pollution Assessment Of Sediment And Water In The River Hindon, India. *Environmental Monitoring And Assessment*, 105(1), 193–207.

Jean-Marie Martin, Meybeck, & Michel. (1979). Elemental Mass-Balance Of Material Carried By Major World Rivers. *Marine Chemistry*, *7*(3), 173–206.
Karbassi, A. R., Bayati, I. & Moattar, F. (2006). Origin And Chemical Partitioning Of Heavy Metals In Riverbed Sediments. *International Journal Of Environmental Science And Technology*, 3(1), 35–42.
Karbassi, A. R., Tajziehchi, S. & Adib, N. F. (2016). Role Of Estuarine Natural Processes In Removal Of Trace Metals Under Emergency Situations. *Global Journal Of Environmental Science And Management-Gjesm*, 2(1), 31–38.
Karbassi, A. R., Torabi, F., Ghazban, F. & Ardestani, M. (2011). Association Of Trace Metals With Various Sedimentary Phases In Dam Reservoirs. *International Journal Of Environmental Science {&} Technology*, 8(4), 841–852.
Karbassi, A., Saeedi, M. & Amirnejad, R. (2008). Historical Changes Of Heavy Metals Content And Sequential Extraction In A Sediment Core From The Gorgan Bay, Southeastern Caspian Sea. *Indian Journal Of Marine Sciences*, 37(3), 267–272.
Karbassi, Nouri, & Ayaz. (2007). Flocculation Of Cu , Zn , Pb , Ni And Mn During Mixing Of Talar River Water With Caspian Seawater. *Graduate Faculty Of Environment*, 1(1), 66–73.
Li, F., Wen, Y. M. & Zhu, P. T. (2008). Bioavailability And Toxicity Of Heavy Metals In A Heavily Polluted River, In PRD, China. *Bulletin Of Environmental Contamination And Toxicology*, 81(1), 90-94.
Likuku, A. S., Mmolawa, K. B., & Gaboutloeloe, G. K. (2013). Assessment Of Heavy Metal Enrichment And Degree Of Contamination Around The Copper-Nickel Mine In The Selebi Phikwe Region , Eastern Botswana. *Environment And Ecology Research*, 1(2), 32–40.
Mcdonough, W. F. & Sun, S. S. (1995). The Composition Of The Earth. *Chemical Geology*, 120(3-4), 223-253.
Mediolla, Domingues, & Sandoval. (2008). Environmental Assessment Of An Active Tailings Pile In The State Of Mexico(Central Mexico). *International Journal Of Environmental Science*, 2(3), 197–208.
Mwalusepo, S., Muli, E., Faki, A. & Raina, S. (2017). Land Use And Land Cover Data Changes In Indian Ocean Islands: Case Study Of Unguja In Zanzibar Island. *Data In Brief*, *11*, 117–121.
Omole, D. O., Eng, B., Rusyniak, D. E., Arroyo, A., Acciani, J., Froberg, B. & Furbee, B. (2006). Molecular, Clinical And Environmental Toxicology. *Nih*, *100,* (June), 365–396.
Opuene, Okafor, & Agbozu. (2008). Partitioning Characteristics Of Heavy Metals In A Non-Tidal Freshwater Ecosystem. *International Journal Of Environmental Research*, 2(3), 285–290.
Pradit, S., Wattayakorn, G., Angsupanich, S., Baeyens, W. & Leermakers, M. (2010). Distribution Of Trace Elements In Sediments And Biota Of Songkhla Lake, Southern Thailand. *Water, Air, And Soil Pollution*, 206(1), 155-174.
Praveena, Ahmed, Radojevic, Abdullah, & Aris. (2008). Heavy Metals In Mangrove Surface Sediment Of Mengkabong Lagoon , Sabah : Multivariate And Geo-Accumulation Index Approaches. *International Journal Of Environmental Research*, 2(2), 139–148.
Quevauviller, P., Rauret, G., Rubio, R., López-Sánchez, J. F., Ure, A., Bacon, J. & Muntau, H. (1997). Certified Reference Materials For The Quality Control Of EDTA-And Acetic Acid-Extractable Contents Of Trace Elements In Sewage Sludge Amended Soils (Crms 483 And 484). *Fresenius' Journal Of Analytical Chemistry*, 357(6), 611-618.
Siddique, M. A. M. & Aktar, M. (2012). Heavy Metals In Salt Marsh Sediments Of Porteresia Bed Along The Karnafully River Coast, Chittagong. *Soil And Water Research*, 7(3), 117–123.
Sobhanardakani & Jafari (2014). Heavy Metals Contamination In Silver, Common And Grass Carp Caught From Zarivar Lake , Western Iran. *European Online Journal Of Natural And Social Sciences*, *3*(2), 344–350.
Tabatabaei, T., Karbassi, A. R., Moatar, F. & Monavari, S. M. (2014). Geospatial Patterns And Background Levels Of Heavy Metal In Deposited Particulate Matter In Bushehr, Iran. *Arabian Journal Of Geosciences*, 1–13. Http://Doi.Org/10.1007/S12517-013-1241-6
Toluna, Okaya, Gainesb, Tolayc, Tüfekçia & Kıratlıd. (2001). The Pollution Status And The Toxicity Of Surface Sediments In İzmit Bay (Marmara Sea), Turkey. *Environment International*, 26(3), 163–168.
Udayakumar, P., Jose, J. J., Krishnan, K. A., Kumar, C. S. R., Manju, M. N. & Salas, P. M. (2014). Heavy Metal Accumulation In The Surficial Sediments Along Southwest Coast Of India. *Environmental Earth Sciences*, 72(6), 1887–1900.
Venugopal, Giridharan, Jayaprakash & Department. (2009). Characterization And Risk Assessment Studies Of Bed Sediments Of River Adyar-An Application Of Speciation Study. *International Journal Of Environmental Research*, *3*(4), 581–598.
Wcisłoa, E., Iovenb, D., Kucharskia, R. & Szdzuja, J. (2002). Human Health Risk Assessment Case Study: An Abandoned Metal Smelter Site In Poland. *Chemosphere*, 47(5), 507–515.
Zhipeng, Jinming, Naixing, Peng & Yayan. (2009). Variation Characteristics and Ecological Risk of Heavy Metals in The South Yellow Sea Surface Sediments. *Environ*, 157, 515–528.

3D WIND EFFECTS ON HYDRODYNAMICS AND TRANSPORT IN A BRAZILIAN BAY

ELENA MATTA[(1)], FLORIAN SELGE[(2)], GÜNTER GUNKEL[(3)] & REINHARD HINKELMANN[(4)]

[(1, 4)] Chair of Water Resources and Modeling of Hydrosystems, Technische Universität Berlin, Germany
elena.matta@wahyd.tu-berlin.de
[(2, 3)] Chair of Water Quality Control, Technische Universität Berlin
florian.selge@tu-berlin.de

ABSTRACT

Many water bodies throughout the world are currently facing more frequent extreme events driven by climate change (e.g. droughts or floods), water quality problems (e.g. periodically nutrients overload) and conflicts over water uses. This is likewise the case of Icó-Mandantes bay, located in Itaparica reservoir, São Francisco River, Northeast Brazil. Multiple uses of water (e.g. fishery, irrigation agriculture), long drought periods and intense rain events, as well as high water level variations (up to 5 m/y) and a new water infrastructure project (i.e. water diversion to nearby watersheds) are some of the existing challenges. Furthermore, the bay is quite isolated by the reservoir's main stream and characterized by low flow velocities (order of mm/s). The wind has an important role in the bay, being one of the main drivers of water movement and exchange, as shown in previous research using two-dimensional (2D) models. In the current paper, the effects of mean and extreme wind on water flow and on passive transport of nutrients (i.e. emissions from fish farming) were investigated with TELEMAC-3D, observing results over the water column and over time. The aim was to explore the capabilities of the 3D modeling, in order to understand whether 2D is satisfactory enough for water management. The outcomes of this work showed that the answer is complex and cannot be given a priori, since it is highly dependent on the objective and the conditions of the study, e.g. extreme wind yields not non-negligible 3D effects in shallower areas of the bay. Further studies are needed and currently focusing on 3D density-induced flow and heat exchange with atmosphere.

Keywords: TELEMAC-3D; numerical simulation; tracer transport; wind; Itaparica reservoir.

1 INTRODUCTION

Finding innovative technologies environmentally sustainable and adapted to climate change for lake management in semi-arid Northeast Brazil is one of the principal challenges of the INNOVATE project (2017), a joint interdisciplinary research between German and Brazilian institutions (e.g. TU Berlin, Germany and UFPE Recife, Brazil), to which this work belongs (Siegmund-Schultze et al., 2015; 2017). The Itaparica reservoir (Figure 1) covers an area of approximately 828 km^2 (CHESF, 2017) and is part of a reservoir cascade located in the Sub-Middle São Francisco River. It was completed in 1988 with the resettlement of 10,400 households and the main purpose of hydropower production (HPP), but nowadays it is used for multiple uses, as irrigation agriculture and aquaculture production (Hagel et al., 2014; Gunkel and Sobral, 2013).

Besides the conflicts and the management plans regarding the various water uses, climate change also plays a crucial role in the area, which is suffering from a severe drought since end of 2012 (Marengo et al., 2016). The rare and intense rain events represent one of the main contamination sources of the peripheral bays of the reservoir, which are prone to nutrient overloads. In those areas, the yearly water level variations up to 5 m, caused by HPP and high evaporation rates, is considered responsible of algae bloom, including cyanobacteria and mass development of submerged macrophytes i.e *Egeria densa* (Keitel et al., 2015; Lima and Gunkel, 2015). The reservoir is also in the interest of aquaculture production and it is feared that further extensions to its branches may increase the phosphorus contents and the potential of eutrophication (Gunkel et al., 2015; Selge et al., 2016). Furthermore, water abstraction for human and animal supply, as well as for irrigation agriculture are located in a specific bay of the reservoir called Icó-Mandantes, where the eastern channel of the controversial Transposition project (Castro, 2011) was built, with the aim to divert water to nearby watersheds, i.e. the wild regions of Pernambuco and Paraíba.

Out of the abovementioned reasons, Icó-Mandantes bay (Figure 1) is the main focus of previous modeling studies (Matta et al., 2014; 2016; 2017; Selge et al., 2016), being a lively challenge for land and water management. Computational Fluid Dynamics (CFD) is nowadays a well-known powerful tool, being able to simulate various scenarios correspondent to different flow conditions or water uses. Often, two- and three-dimensional (respectively 2D and 3D further on) models are preferred for lakes and reservoir management and the choice between them depends on whether the vertical variability of velocities, tracer profiles and stratification are significant.

This paper presents further investigations of the Icó-Mandantes bay's hydrodynamics, using a 3D model, set up with the software TELEMAC-3D (Hervouet, 2007). The aim of this work was to understand whether the stresses induced by wind relevantly influenced the results over the water column (vertical) and, if so, whether it is necessary to avoid the use of 2D models for future studies in Icó-Mandantes bay. In fact, physical forces as wind are applied on the free surface of a water body and transferred along the water depth by turbulence in the vertical plane, thus the depth-averaged approximation is more limiting for wind-driven flows than for gravity-driven ones, such as rivers (Fenocchi et al., 2016). In particular, no wind, mean and extreme wind conditions were considered for the simulations, and the effects were observed on the bay's hydrodynamics in the first place and on transport of a mass-conservative (passive) tracer afterwards, simulating nutrient emissions from a net cage aquaculture system hypothetically located inside the bay. The daily accumulation of total dissolved phosphorus in water was implemented, considering a small fish production and defining a made-up scenario. The outcomes of this work lead to a deeper knowledge of a complex system, presenting suitable modeling tools, to support water management and research at the local scale, e.g. to identify in the future locations and capacity limits for aquaculture systems and, thus, preventing potential eutrophication processes. The methodology used can be applied in similar reservoirs in semi-arid areas.

2 MATERIAL AND METHODS

2.1 Study region

Icó-Mandantes bay is a small branch of Itaparica reservoir of approximately 25 km^2, located in the semi-arid state of Pernambuco, Northeast Brazil (Figure 1). The bay itself is surrounded on one side by the natural biome Caatinga, a dry forest ecosystem, and irrigation agriculture on the other side (Selge and Gunkel, 2013). The reservoir is formed by the Luiz Gonzaga dam, in the sub-middle part of the São Francisco river basin. The installed power capacity of the turbines counts ca. 1.480 MW in total, the mean water discharge is 2,060 m^3/s, regulated by the upstream Sobradinho reservoir, and the mean water elevation 302.8 m a.s.l., with a maximum variation of about 5 m (CHESF, 2017). The area is affected by high temperatures, strong wind and a mean annual precipitation of about 475 mm/y, usually between January and April (Selge et al., 2016).

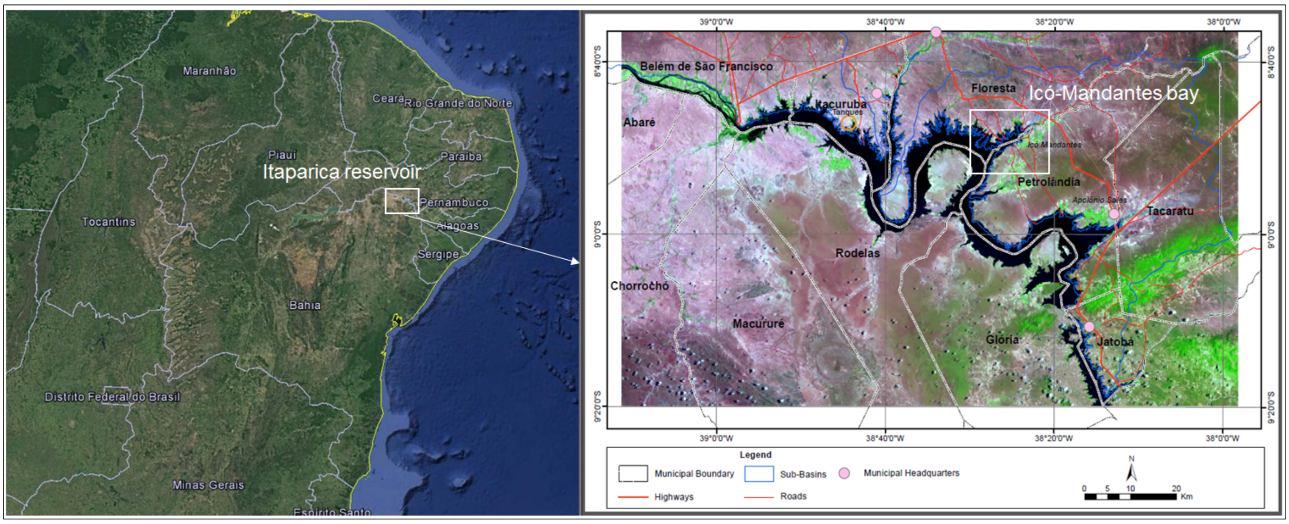

Figure 1. Location of the study area: Northeast Brazil (*left*), and capture of Itaparica reservoir and Icó-Mandantes bay (*right*). Adapted by the author from Google Earth (2016) and Lopes et al. (2013).

2.2 Modeling tools

A three-dimensional (3D) model of Icó-Mandantes bay was set up with the TELEMAC modeling system, using the unstructured triangular grid created for TELEMAC-2D in Matta et al. (2016) with the software Janet (Smile Consult GmbH), which covers the whole bay and part of the river, the so-called main stream. TELEMAC-3D creates the 3D mesh out of the existent 2D grid, multiplying it on different layers imposed by the user, in here, 14 layers were chosen. The resulting mesh columns consist of 13 prisms with a variable height, depending on the water column.

The 3D simulations were performed with the computational code TELEMAC-3D, as mentioned above, which solves the free surface Navier-Stokes and tracer transport equations, describing the velocity field, the water depths and the tracer concentrations at each time step (Hervouet, 2007). Since the code has no graphical interface, the results were analyzed with different open-source data analysis and visualization applications, such as POSTEL-3D and Rubens (integrated in the TELEMAC modeling system), Blue Keneu (Canadian Hydraulics Centre of the National Research Council, Ottawa) and ParaView (Ayachit, 2015).

2.3 Theoretical background

The governing equations are the 3D shallow water and transport equations, obtained by the hydrodynamic Navier Stokes equations, assuming a free surface changing in time, an incompressible fluid, the hydrostatic pressure hypothesis and the Boussinesq approximation for the momentum (Hinkelmann, 2005; Hervouet, 2007). The 3D shallow water system consists of the continuity and momentum equations, reported in Eq. [1] and [2], [3], [4], respectively in x-, y-, z-directions. The tracer transport equation is reported in Eq. [5]:

$$\frac{\partial u}{\partial x}+\frac{\partial v}{\partial y}+\frac{\partial w}{\partial z}=r \quad [1]$$

$$\frac{\partial u}{\partial t}+u\frac{\partial u}{\partial x}+v\frac{\partial u}{\partial y}+w\frac{\partial u}{\partial z} = -g\frac{\partial z_s}{\partial x}+\nu_{th}\frac{\partial^2 u}{\partial x^2}+\nu_{th}\frac{\partial^2 u}{\partial y^2}+\nu_{tv}\frac{\partial^2 u}{\partial z^2}+f_x \quad [2]$$

$$\frac{\partial v}{\partial t}+u\frac{\partial v}{\partial x}+v\frac{\partial v}{\partial y}+w\frac{\partial v}{\partial z} = -g\frac{\partial z_s}{\partial y}+\nu_{th}\frac{\partial^2 v}{\partial x^2}+\nu_{th}\frac{\partial^2 v}{\partial y^2}+\nu_{tv}\frac{\partial^2 v}{\partial z^2}+f_y \quad [3]$$

$$p = p_{atm}+\rho_0 g(z_s-z)+\rho_0 g\int_z^{z_s}\frac{\Delta\rho}{\rho_0}dz \quad [4]$$

$$\frac{\partial c}{\partial t}+u\frac{\partial c}{\partial x}+v\frac{\partial c}{\partial y}+w\frac{\partial c}{\partial z}=\nu_{t,th}\frac{\partial c}{\partial x}+\nu_{t,th}\frac{\partial c}{\partial y}+\nu_{t,tv}\frac{\partial c}{\partial z}+q \quad [5]$$

where,

h (m) is the water depth,
u, v, w (m/s) are the three-dimensional components of velocity,
c (mg/L) is the tracer concentration,
z_s (= z_b + h) (m), is the free surface elevation, where z_b (m) is the bottom depth,
t (s) is the time,
p, p_{atm} (mbar) is the pressure and the atmospheric pressure, respectively,
ρ, ρ_0 and Δρ (kg/m^3) are the density, the reference density and the density difference, respectively,
v_{th}, v_{tv} (m^2/s) are the horizontal and vertical turbulent viscosity, respectively,
$v_{t,th}$, $v_{t,tv}$ (m^2/s) are the horizontal and vertical turbulent tracer diffusion coefficients, respectively,
f_x, f_y (m/s^2) are the momentum source terms (i.e. surface and bottom shear stresses),
r (m/s^2), q (mg/L/s) are the source or sink terms for flow and tracer, respectively.

The bottom and surface frictions (i.e. wind stress) expressed by the terms f_x, f_y (m/s^2) are calculated by empirical laws. The Strickler's law (1923) was used to evaluate the first, with a roughness coefficient assumed equal to 30 $m^{0.33}$/s, according to values calibrated in previous work by Cirilo (1991). For the second, the wind shear stress is determined in function of the wind speed, the density of the air and a dimensionless empirical coefficient, calculated according to the formula used by the Institute of Oceanographic Sciences (United Kingdom) after Flather (1976) (Hervouet, 2007). Information about wind values used in the simulations are given in the next paragraph. Zero-equation turbulent models were applied for the horizontal and vertical direction: the constant viscosity and the mixing length Prandtl model (Hervouet, 2007; Hinkelmann, 2005), respectively, giving nearly same results of more complex models (e.g. k-ε), but faster and less CPU (Central Processing Unit) consuming. No flow measurements were available in the study area. For this reason, we conducted sensitivity analyses for different values of turbulent viscosity (range 10^{-1} ÷ 10^{-6} m^2/s; the latter is the TELEMAC default value) and the results showed negligible changes. Thus, we assumed the horizontal turbulent viscosity v_t equal to 10^{-4} m^2/s, in the range of literature values and of the results of k-ε model, and we set it equal to the horizontal turbulent diffusivity of Eq. [5] (Jourieh 2015; Hervouet, 2007).

3 RESULTS AND DISCUSSIONS

3.1 Setup of the cases

As initial conditions, a constant initial water elevation of 302.8 m a.s.l., a zero initial velocity and zero tracer concentration were imposed. The boundary conditions prescribed at the inflow and outflow boundaries (Figure 2) represent the reservoir under normal operating conditions: respectively a flow discharge released from Sobradinho upstream to Itaparica reservoir of 2,060 m^3/s and a water elevation of 302.8 m a.s.l. measured at the dam outlet (CHESF, 2017).

The cases simulated took into account the mean flow conditions and specifically:

i. Hydrodynamics in absence of wind (further called HYDREF)
ii. Hydrodynamics with constant mean and extreme wind (HYDMW and HYDEW, respectively)
iii. Tracer transport in absence of wind (AQNW)
iv. Tracer transport with constant mean and extreme wind (AQMW and AQEW, respectively)

Mean and extreme wind velocities were chosen to be equal to 5.5 m/s and 20 m/s, respectively, both with a wind direction of 140° (from Southeast to Northwest). Wind data were statistically analyzed in previous work (Matta et al., 2014), out of historical data collected in a weather station located in Floresta (Figure 1, right), a municipality about 30 km from Icó-Mandantes bay, and available on the Brazilian database SINDA (INPE 2016).

The tracer transport was investigated defining a made-up scenario, meant to simulate the release of nutrients from fish net cages hypothetically located in the bay. The values of nutrient emissions used for this case were measured with a multi parameter device (i.e. EXO water quality sonde, YSI, Yellow springs, OH, USA) in other aquaculture systems existent in the reservoir (Gunkel et al., 2015). A small fish productivity of 130 t/y was assumed for the simulations, having a daily accumulation of total dissolved phosphorus (namely DP) of 1.302 kg/d (Matta et al., 2016). Only phosphorus was considered, since it is often the eutrophication-limiting nutrient in reservoirs (Zamani et al., 2016). A passive (mass-conservative) tracer source was implemented in the model in a specific location. Here, the term *passive* means that the tracer is only transported in the domain without influencing the flow. The tracer source was set at 1.7 m water depth from the surface, i.e. reasonable depth of nutrients emissions. A mass-conservative explicit distributive scheme was chosen to solve the tracer advection step (Hervouet, 2007).

Results of the hydrodynamics and transport were analyzed over the 14 layers of the 3D model and in different sections (100-300 m width) of the computational domain. This allowed us to observe the changes of the 2D flow circulations on each plane, as well as cutting vertical sections in the near field of specific interesting areas: in the main stream (namely s1), in the bay (s2) and at the tracer source (s3), shown in Figure 2-5 in the next paragraph.

3.2 Hydrodynamic simulations (HYDREF, HYDMW, HYDEW)

The simulation without wind and without transport (HYDREF) serves as reference and as initial condition for the next scenarios. It was computed until steady state was reached in the entire domain (after few days). The flow field of the HYDREF case is characterized by a clearly separated main current in the reservoir main stream, with mean velocities of ca. 0.023 m/s, oriented from the inflow to the outflow (Figure 2, *left*). Figure 2 (*middle*) shows the vertical velocity profile plotted over s1, having the typical course of open channels. Otherwise, inside the bay, the water is almost stagnant (velocity range lower than 0.2 mm/s), in agreement with Özgen et al. (2013) and Matta et al. (2014). Plotting the results over the water column, the velocity vertical profile in the central bay (s2, Figure 3) is rather constant with the depth, with values close to zero.

Starting from HYDREF, the HYDMW and HYDEW cases were simulated as well until the attainment of steady state conditions (ca. 5 days). Wind induces water movement in the bay and increases flow velocities. The results in s1 and s2 of HYDMW and HYDEW are reported in Figure 2-5. Inside the bay, flow velocities range approximately 0.001 – 0.015 m/s for HYDMW, while up to mean values of 0.092 m/s for HYDEW. In the main stream, mean values increased up to ca. 0.024 m/s and 0.179 m/s for HYDMW and HYDEW, respectively. Wind direction is oriented against the flow both in the main stream (s1) and in the central bay (s2). Thus, over the vertical, we observe the decrease of the velocities in the first surface layers, compared to the lower ones. In the bay, where water depth is lower (i.e. about 10 m in s2 and 6 m in s3), this is occurring at a higher extent and higher velocities are encountered nearer to the bottom with maximum values of approximately 0.016 m/s for HYDMW and 0.034 m/s for HYDEW in s2. Nevertheless, wind-driven flow is not strong enough to create vertical circulations in the deeper parts of the domain (s1 and s2), even for the extreme case. However, for instance, in the shallow parts along the shores (s3), a vertical anti-clockwise circulation occurs when wind is taken into account (HYDMW and HYDEW): water moves from the bottom to the surface layers, from higher to lower velocities (Figure 5). Figure 5 captures the flow field under extreme wind conditions (HYDEW) in s3, whose results differ for the HYDMW scenario only in regards of velocities magnitudes (higher for stronger wind, as we observed in Figure 3, 4).

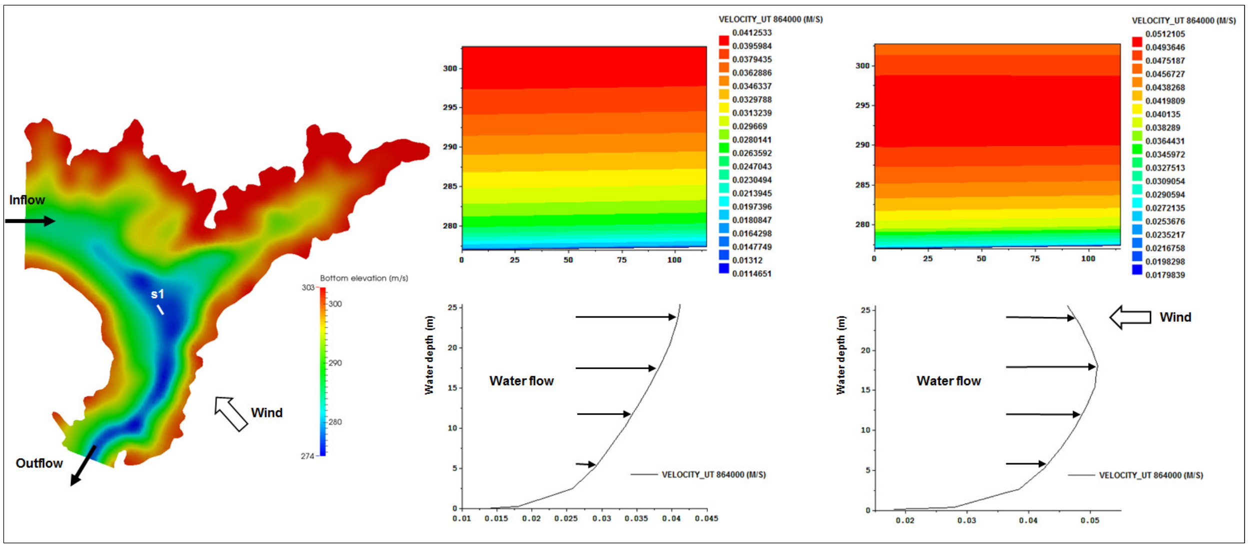

Figure 2. Vertical section of the flow field (*up*) and vertical velocity profiles (*down*) in section s1 in the reservoir main stream (*left*) without wind (*middle*) and with mean wind (*right*).

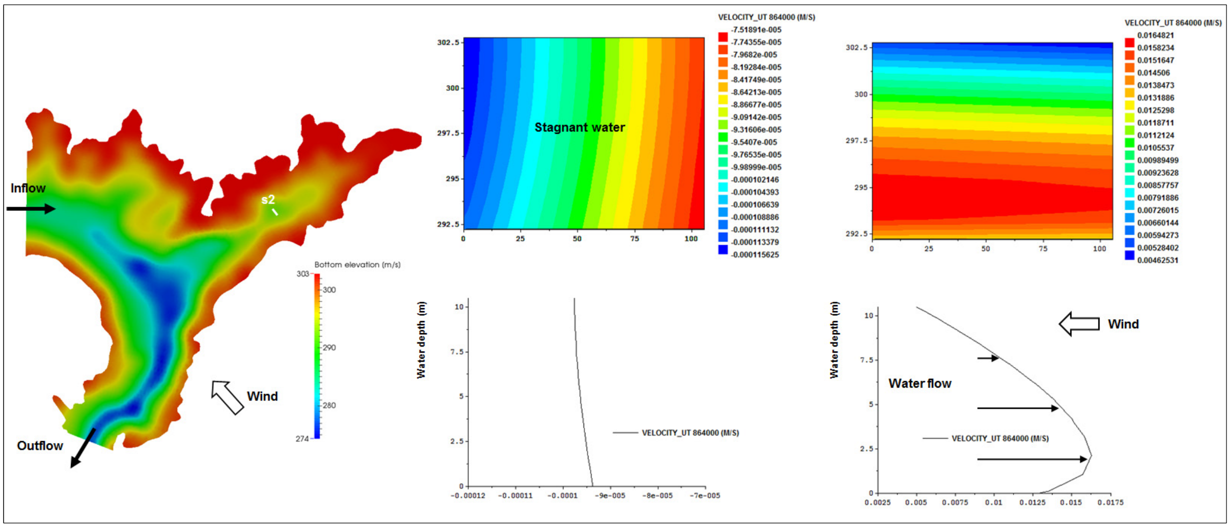

Figure 3. Vertical section of the flow field (*up*) and vertical velocity profiles (*down*) in section s2 in the bay (*left*) without wind (*middle*) and with mean wind (*right*).

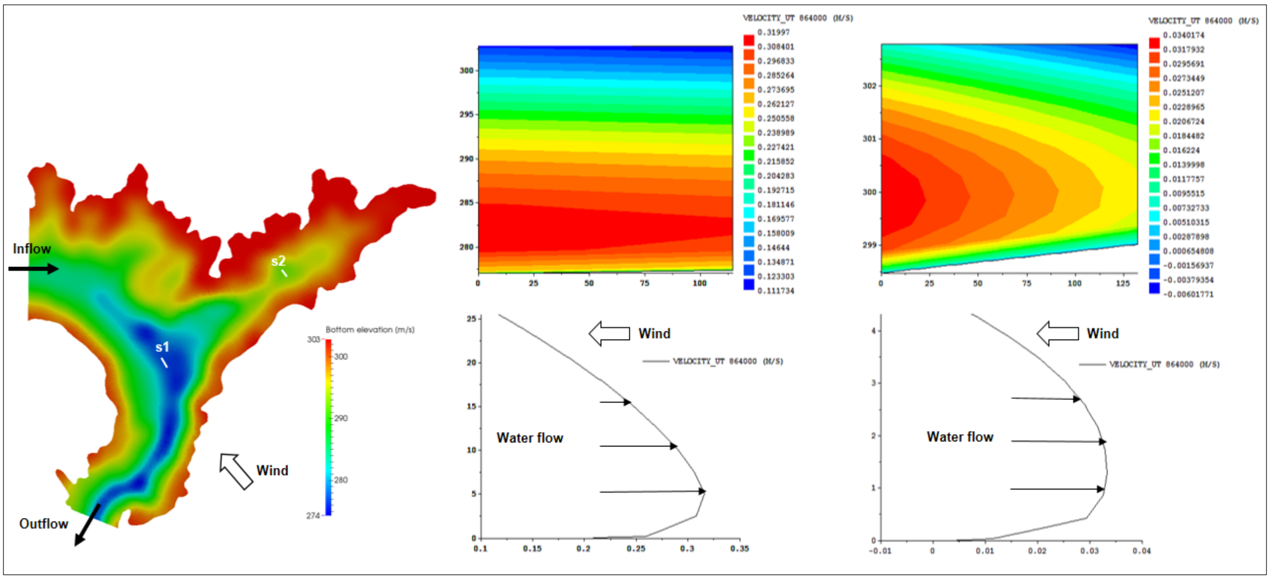

Figure 4. Vertical section of the flow field (*up*) and vertical velocity profiles (*down*) in sections s1 (*middle*) and s2 (*right*), for extreme wind conditions.

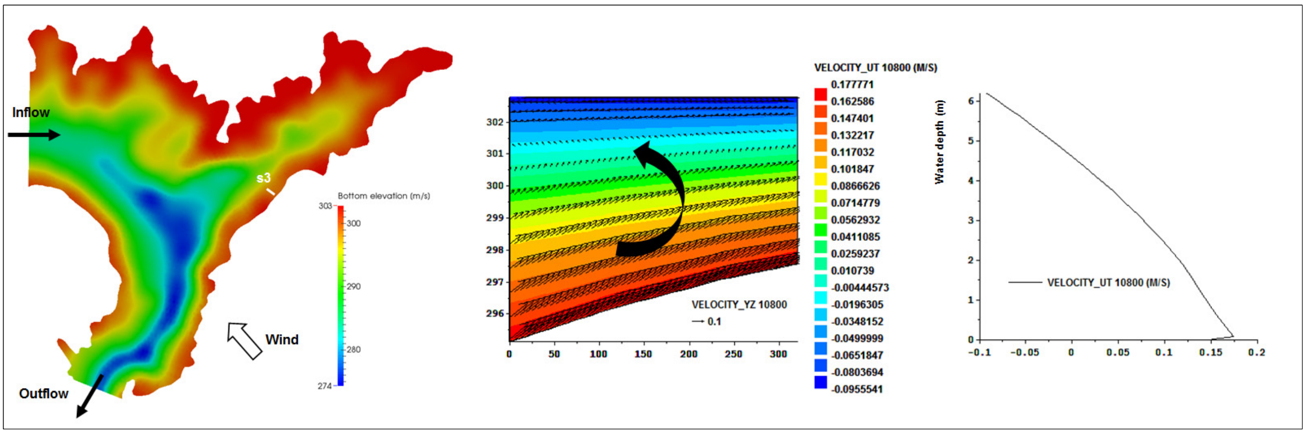

Figure 5. Vertical section s3 in the bay near the shore (*left*) of the flow field (*middle*) and vertical velocity profile (*right*), for extreme wind conditions.

3.3 Transport simulations (AQNW, AQMW, AQEW)

The point of injection of the tracer source (see methods in 3.1) was chosen in the same location of the section s3, where we observed higher 3D effects in the hydrodynamic simulations (see Figure 5). For the purpose of this paper, the results were observed on the short term (some hours), in order to reveal the effects of the different wind forces on the tracer spreading, both in the horizontal and in the vertical plane. Thus, the focus here is not on the magnitude of the emissions, in terms of, for instance, eutrophication limits, but on the 3D effect of the different wind intensities.

Figure 6 reports the results after 3 h on the 12th layer (location of the tracer source) for AQNW, AQMW and AQEW. We noticed that the mean wind has a lower influence compared to the extreme wind, looking at the concentrations in the horizontal plane. Besides, the concentrations of DP are lowest for AQEW, as expected, because the higher water turbulence enhances the faster spreading of the tracer. In the AQNW and AQEW scenarios, concentrations are nearly zero in the layers near the bottom beneath the injection point. In fact, the tracer did not yet reach the lower planes in the former, because of stagnant water, while it is already diffused by the turbulent water movement in the latter. Otherwise, for AQMW the values near the bottom are not negligible (ca. 0.4 10^{-3} mg/L).

In order to analyze the spreading of the tracer over the vertical direction, tracer concentrations were observed in section s3, same location as the source of emissions. The hydrodynamics were presented in 3.3: in particular, Figure 5 shows the velocity vertical profile in s3 under extreme wind conditions. Figure 7-9 report the results of DP concentrations over the water column, correspondent to AQNW, AQMW and AQEW after 0.5 h and 3 h. The results of AQNW and AQMW are similar on the short term (3 h), with maximum respective values at the tracer source of ca. 1.4 10^{-3} and 1.0 10^{-3} mg/L, while lower maximums of 0.1 10^{-3} mg/L are found for AQEW. In the AQNW scenario, the spreading of the tracer is due exclusively to diffusion (ca. 10^{-9} m^2/s), since wind is neglected and water is almost stagnant. Thus, the highest concentrations are reached in the near field of the source. On the contrary, the AQEW showed the lowest values in the same location, because the extreme wind stimulates water movement and mixing, transporting the tracer faster to the bottom. Nevertheless, the spreading's width is still smaller than 300 m after three hours simulation.

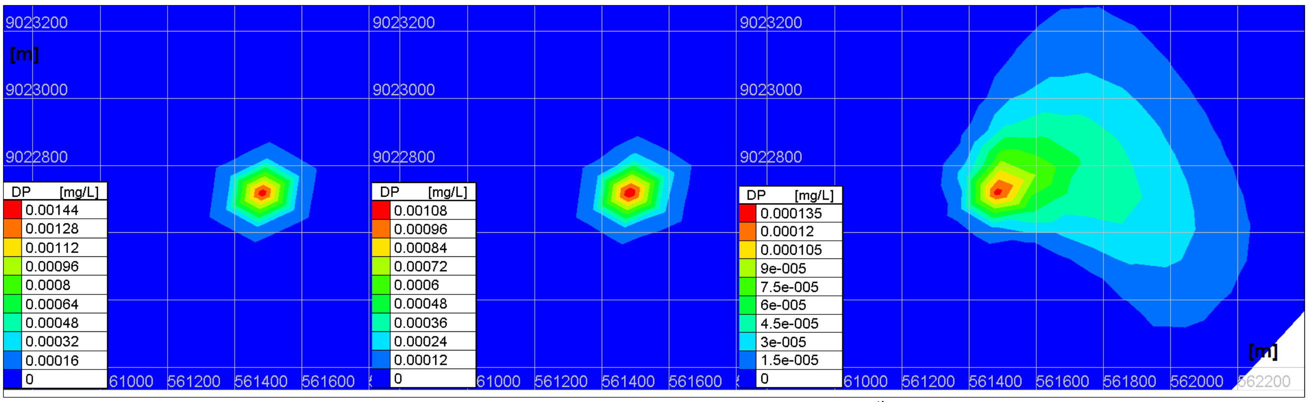

Figure 6. Capture of DP spreading (passive tracer) after 3 h on layer 12th (301.1 m a.s.l.) for AQNW (*left*), AQMW (*middle*) and AQEW (*right*).

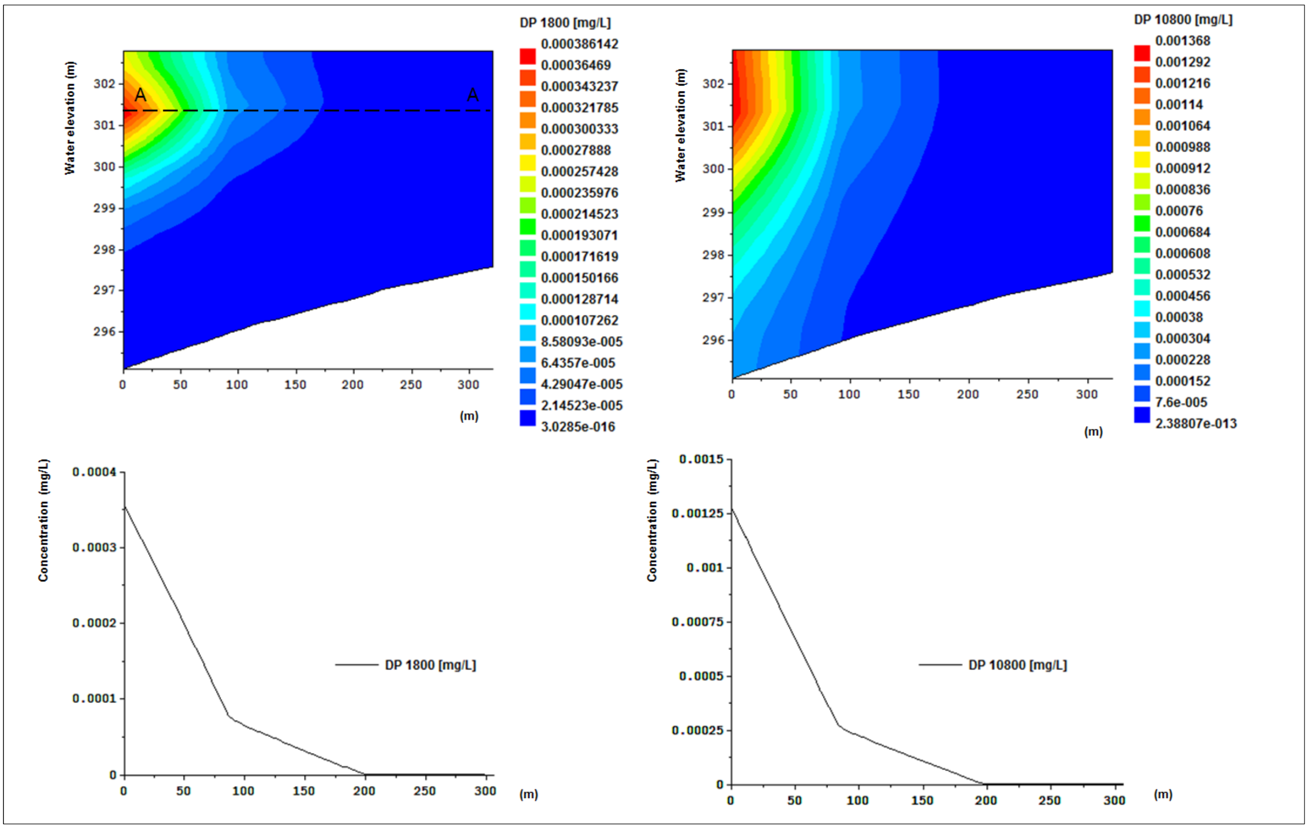

Figure 7. Vertical section s3 capturing DP concentrations (passive tracer) for AQNW after 0.5 h (*left*) and 3 h (*right*) over the water column (*up*) and tracer variations at different times (s) over the section width A-A (m) (*down*).

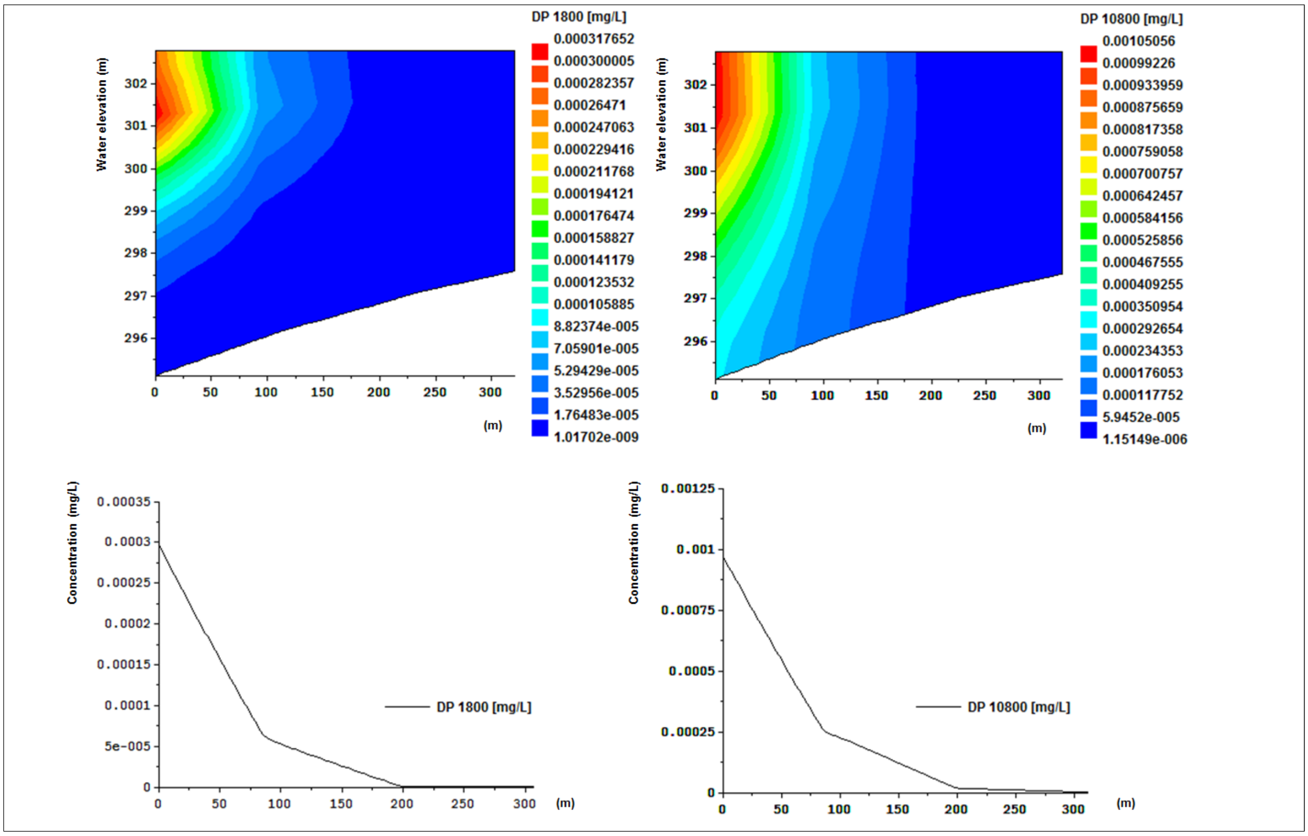

Figure 8. Vertical section s3 capturing DP concentrations (passive tracer) for AQMW after 0.5 h (*left*) and 3 h (*right*) over the water column (*up*) and tracer variations at different times (s) over the section width A-A (m) (*down*).

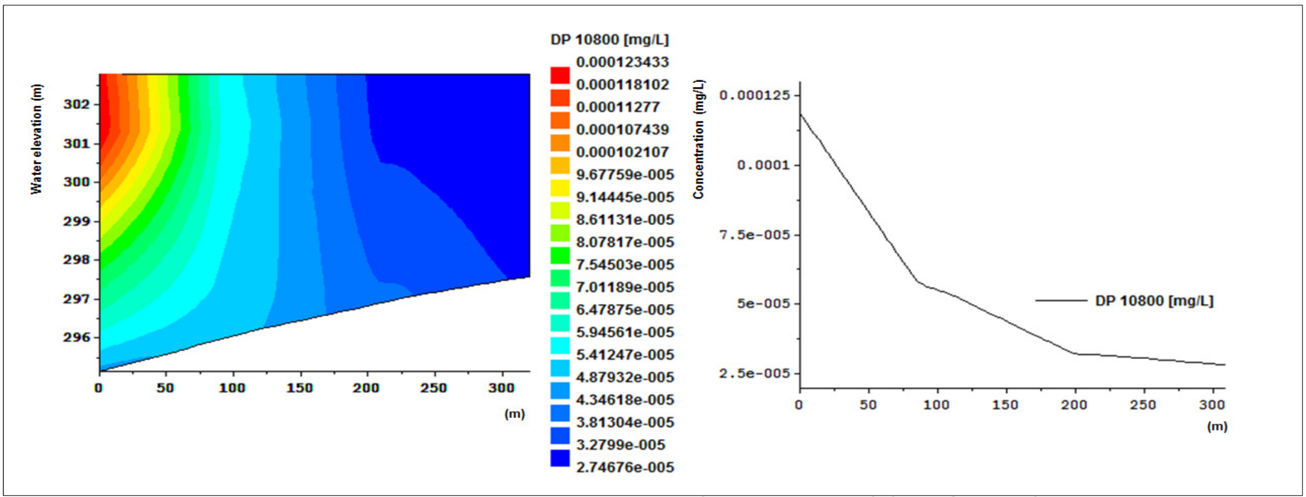

Figure 9. Vertical section s3 capturing DP concentrations (passive tracer) for AQEW after 3 h over the water column (*left*) and tracer variation over the section width A-A (m) (*right*).

3.4 Discussions

The cases presented in this paper explored some capabilities of a 3D hydrodynamics and transport model and the additional value given in comparison to two-dimensional depth averaged analyses. On the one hand, we observed that magnitudes and directions of flow velocities are strongly wind dependent, as stated in regards of 2D analyses in Matta et al. (2014), in particular, inside the bay, where water is otherwise almost stagnant. On the other hand, the simulations performed with TELEMAC-3D lead us to a deeper knowledge of the water system, in particular, concerning the shallower areas in the bay and when strong wind is taken into account. Indeed, the analyses of vertical sections and profiles in strategic points (e.g. fish net cages, water abstraction for multiple uses, see Matta et al., 2017 for more detail) reveal the course of currents and circulation patterns, as well as specific zones where velocities are more intense. This, together with the simulation of tracer transport, can refine relevantly the fate and effects analyses. This is highly relevant for water management regarding, for instance, the accumulation of nutrients. The results can be analyzed at different water depths in response to specific questions, e.g. the time needed by the specific substance to reach the bottom and in which amount, in order to evaluate the availability of nutrients for algae or macrophytes growth with the tropholytic zonation.

4 CONCLUSIONS

The dynamics of surface water bodies such as lakes and reservoirs are often reproduced by two- or three-dimensional (2D, 3D) models. Understanding the most suitable modeling tool according to the specific scenario is of extreme importance, in order to save time and resources. External forces such as wind, play a big role, being one of the main drivers of water movement, particularly in isolated peripheral bays, where velocities are very low (Özgen et al., 2013; Matta et al., 2014). The focus of this study was Icó-Mandantes bay, branch of Itaparica reservoir in the Sub-Middle São Francisco River, Northeast Brazil. We analyzed the hydrodynamics and the transport of a passive tracer using a 3D high-resolution model set up with TELEMAC-3D for Icó-Mandantes bay and part of the reservoir main stream, under variable wind conditions. The aim of the work was to explore the capabilities of the 3D modeling presenting different scenarios of flow and transport. The choice between 2D and 3D models for water management in the Icó-Mandantes bay was also discussed.

The results showed that the wind had an impact on the velocity intensities and directions, but only in some specific parts of the bay (e.g. in the shallow areas near the shores) in regards of the vertical direction (i.e. over the water column). In that location, a scenario was defined, simulating the emissions of total dissolved phosphorus from a hypothetical aquaculture system. A mass-conservative tracer source was implemented and the results were observed under variable wind forces. Under extreme wind conditions, the transport of the plume showed relevant changes over the water column, while more similar results were obtained in absence of wind or with weaker wind.

In a complex system as Icó-Mandantes bay, stressed e.g. by climate change and water multiple uses (Matta et al., 2017), the choice between 2D or 3D needs a scenario-oriented approach, being highly dependent on the purpose of the study in the first place. The 2D results are considered satisfactory for a general understanding of the system and in the case of absence of wind or for mean wind conditions. For extreme wind scenarios, with or without transport, 3D studies are more accurate, in particular for water management in specific areas of the bay (e.g. near the shallow shores were intakes for irrigation are located, s. Matta et al., 2017).

Currently, we are investigating density-induced flow, vertical mixing and stratification in the bay using TELEMAC-3D, in order to consider the eventual impacts of the significant daily air temperature changes (range ± 20°C) on the water and transport dynamics.

ACKNOWLEDGEMENTS

This work, as part of the INNOVATE project, was financially supported by the German Federal Ministry of Education and Research (BMBF).

REFERENCES

Ayachit, U. (2015). *The ParaView Guide: A Parallel Visualization Application*. Kitware, NY, 233.

CHESF, Companhia Hidroelétrica do São Francisco (Hydroelectric company of the São Francisco River) (2017). Sistemas de Geração: Luiz Gonzaga. URL: https://www.chesf.gov.br/, [Accessed 11 January 2017].

Flather, RA. (1976). *Results from Surge Prediction Model of the North-West European Continental Shelf for April November and December 1973*. Report (24), Institute of Oceanography (UK), 1-37.

Gunkel, G. & Sobral, M. (2013). Re-Oligotrophication as a Challenge for a Tropical Reservoir Management with Reference to Itaparica Reservoir, São Francisco, Brazil. *Water Science and Technology,* 67(4), 708-714.

Gunkel, G., Matta, E., Selge, F., Nogueira da Silva, G.M. & Sobral, M. (2015). Carrying Capacity Limits of Net Cage Aquaculture for Brazilian Reservoirs. *Revista Brasileira Ciencias Ambientais* 36, 127-144.

Hagel, H., Hoffmann, C. & Doluschitz, R. (2014). Mathematical Programming Models to Increase Land and Water Use Efficiency in Semi-arid NE-Brazil. *International Journal on Food System Dynamics*, 5(4), 173-181.

Hervouet, J.M. (2007). *Hydrodynamics of Free Surface Flows: Modelling with the Finite Element Method*. John Wiley & Sons, 366.

Hinkelmann, R. (2005). *Efficient Numerical Methods and Information-Processing Techniques for Modeling Hydro- and Environmental Systems*. Springer Science & Business Media, Berlin, 306.

INNOVATE, (2017). Interplay Among Multiple Uses of Water Reservoirs via Innovative Coupling of Substance Cycles in Aquatic and Terrestrial Ecosystems. URL: http://www.innovate.tu-berlin.de/. [Accessed 26 January 2017].

INPE, Instituto Nacional de Pesquisas Espaciais (2016). *SINDA,* Sistema Integrado de Dados Ambientais, URL: http://www.sinda.crn2.inpe.br/. [Accessed 5 July 2016].

Jourieh, A. (2015). *Multi-dimensional Numerical Simulation of Hydrodynamics and Transport Processes in Surface Water Systems in Berlin*. Dissertation. Technische Universität Berlin, Germany, 1-204.

Keitel, J., Zak, D. & Hupfer, M. (2015). Water Level Fluctuations in a Tropical Reservoir: the Impact of Sediment Drying, Aquatic Macrophytes Dieback, and Oxygen Availability on Phosphorus Mobilization. *Environmental Science and Pollution Research,* 23(7): 6883–6894.

Lima, D. & Gunkel, G. (2015). Controlling the growth of Egeria densa in Itaparica Reservoir, Brazil. *Conference proceedings of 17th IWA International Conference on Diffuse Pollution and Eutrophication (DIPCON), Berlin.*

Lopes, H.L., Sobral, M.C., Gunkel, G., Candeias, A.L. & Melo, G.L. (2013). *First Approach to Retrieve Chlorophyll-a using Remote Sensing Techniques in Itaparica Reservoir, Semiarid of Pernambuco, Brazil*. In: Gunkel G., Silva J.A.A. de, Sobral M. do C. - Sustainable Management of Water and Land in Semiarid Areas. Ed. UFPE, Recife, 41-59.

Marengo, J.A., Torres, R.R. & Alves, L.M. (2016). Drought in Northeast Brazil-Past, Present, and Future. *Theoretical and Applied Climatology,* 1-12.

Matta, E., Koch, H., Selge, F., Simshäuser, M.N., Rossiter, K., Nogueira da Silva, G.M., Gunkel, G. & Hinkelmann, R. (2017) High Resolution Two-Dimensional Modeling of Flow and Transport in Icó-Mandantes Bay to Support Water Management. *Reg. Environ. Change*. Submitted.

Matta, E., Selge, F., Gunkel, G., Rossiter, K., Jourieh, A. & Hinkelmann, R. (2016). Simulations of Nutrient Emissions from a Net Cage Aquaculture System in a Brazilian bay. *Water Science and Technology* 73(10), 2430-2435.

Matta, E., Özgen, I., Cabral, J., Candeias, A.L. & Hinkelmann, R. (2014). Simulation of Wind-Induced Flow and Transport in a Brazilian Bay. *International Conference on Hydroscience & Engineering (ICHE)*, Hamburg, Germany, © 2014 Bundesanstalt für Wasserbau ISBN 978-3-939230-32-8.

Özgen, I., Seemann, S., Candeias, A.L., Koch, H., Simons, F. & Hinkelmann, R. (2013). Simulation of Hydraulic Interaction between Icó-Mandantes Bay and São Francisco River, Brazil. *Sustainable Management of Water and Land in Semiarid Areas,* 28-38.

Selge, F. & Gunkel, G. (2013). Water Reservoirs: Worldwide Distribution, Morphometric Characteristics and Thermal Stratification Processes. *Sustainable Management of Water and Land in Semiarid Areas*, 15-27.

Selge, F., Matta, E., Hinkelmann, R. & Gunkel, G. (2016). Nutrient Load Concept-Reservoir vs. Bay Impacts: a Case Study from a Semi-Arid Watershed. *Water Science and Technology*, 73 (7), 1671-1679.

Siegmund-Schultze, M., Köppel, J. & Sobral, M.C. (2015). Balancing Ecosystem Services and Societal Demands in a Highly Managed Watershed: Setup and Progress of a Comprehensive Research Project. *Revista Brasileira de Ciências Ambientais* 36, 3-18.

Siegmund-Schultze, M., Sobral, M.C., Köppel, J. (2017). INNOVATE's Overall Findings on Sustainable Land Management in a Semi-Arid Watershed in North-East Brazil. *Reg. Environ. Change.* Submitted.

Strickler, A. (1923). *Beitrage zur Frage der Geschwindigheits-formel und der Rauhegkeitszahlen fur Strome, Kanale und geschlossene* Leitungen. Mitt. Eidgeno assischen Amtes Wasserwirtschaft (16), Bern, Switzerland, 77.

Zamani, B., Koch, M., Hodges, B.R. & Fakheri-Fard, A. (2016). Pre-Impoundment Assessment of the Limnological Processes and Eutrophication in a Reservoir using Three-Dimensional Modeling: Abolabbas reservoir, Iran. *Journal of Applied Water Engineering and Research*, 1-14.

SEASONAL WATER QUALITY CHARACTERISTIC OF TROPICAL URBAN AMPANG HILIR LAKE, KUALA LUMPUR, MALAYSIA

SHIN YING ANG[1] & HIN LEE LEE[2]

[1,2] Water Quality and Environment Research Centre
National Hydraulic Research Institute of Malaysia (NAHRIM), Seri Kembangan, Selangor, Malaysia
syang@nahrim.gov.my; hllee@nahrim.gov.my

ABSTRACT

Urban lakes in Malaysia have undergone changes due to urbanization and caused significant deterioration in environment, particularly water quality. This paper is aimed to evaluate the seasonal water quality characteristic of Ampang Hilir Lake, a tropical urban man-made lake in Kuala Lumpur, Peninsular Malaysia. The lake gets its water from rainfall and culvert systems linked to the lakes from the surrounding catchment. Ex-situ and in-situ data collection was performed between November 2014 and July 2015 consisting of Northeast monsoon (wet season), inter-monsoon (April-May) and Southwest monsoon (dry season) seasons at the limnetic and littoral zone of the lake. Water quality of the lake is the worst during Southwest monsoon season compared to inter-monsoon and Northeast monsoon season as rainfall is lower during Southwest monsoon. Water Quality Index (WQI) was Class III at the limnetic zone and Class V at the littoral zone during the dry season. Biological Oxygen Demand (BOD) is at Class V (> 12 mg/l) for both zones during Southwest monsoon season indicating high organic compound in the lake. Chemical Oxygen Demand (COD) was at Class III and Class V at the limnetic and littoral zone, respectively. Ammonia Nitrogen (AN) which is toxic to aquatic life was at Class IV with values of 2.10 ± 0.54 mg/l and 1.67 ± 0.67 mg/l at the limnetic and littoral zone, respectively during dry season. Orthophosphate (OP) which can be absorbed by plants directly, was detected high during inter-monsoon with value of 1,303.33 ± 228.08 µg/l at limnetic zone and 1,203.33 ± 218.53 µg/l at littoral zone. Carlson's Trophic State Index (TSI) revealed that this lake was eutrophic-hypereutrophic with thick layer of algae on the lake surface especially the littoral zone. Systematic lake catchment management plan is necessary to control the pollutant loadings and hydrological runoff within the catchment area.

Keywords: Tropical urban lake; seasonal water quality; eutrophication; limnetic and littoral zone; trophic state index (TSI).

1 INTRODUCTION

Urban lakes are inland bodies of surface water surrounded by an urban environment (Persson, 2012), highly artificial, often hypereutrophic and in contact with more people compared to rural, natural lakes (Birch and McCaskie, 1999). However, well-known features of the modern urban areas significantly threaten the lake ecosystem. Nutrient enrichment has shifted the lake to a phytoplankton dominated environment resulting in the change of ecosystem structure (Naselli-Flores, 2008). Urban lakes in Malaysia, originally from mining activities in ancient times, have also experienced changes due to urbanization. Environmental deterioration especially water quality, is now the major issue and challenge in urban lakes management. Hence, this paper aims to evaluate the seasonal changes of surface water quality and trophic state of urban lake in Malaysia focusing on Ampang Hilir Lake located in Kuala Lumpur, Peninsular Malaysia.

2 METHODOLOGY

2.1 Study Area

Ampang Hilir Lake is a freshwater tropical urban man-made lake near Ampang Hilir, Kuala Lumpur, Malaysia. It is geographically located at 3°9'22"N and 101°44'26"E and covers about 30 acres in Ampang Hilir Lake Garden which is of 40 acres in total area (Said et al., 2012). The lake gets its water from rainfall and from culvert systems surrounding the lake. There are nine (9) culverts with at least three (3) main big culverts that flow into the lake and with one outlet. Ampang Hilir Lake Garden is a recreational park for jogging and fishing under the authority of Kuala Lumpur City Hall. Figure 1 shows the location and aerial view of Ampang Hilir Lake (Google Earth, 2011). Generally, the area is affected by the seasonal monsoon which includes Northeast monsoon (October – March), Southwest monsoon (Jun – September) and inter-monsoon (April – May).

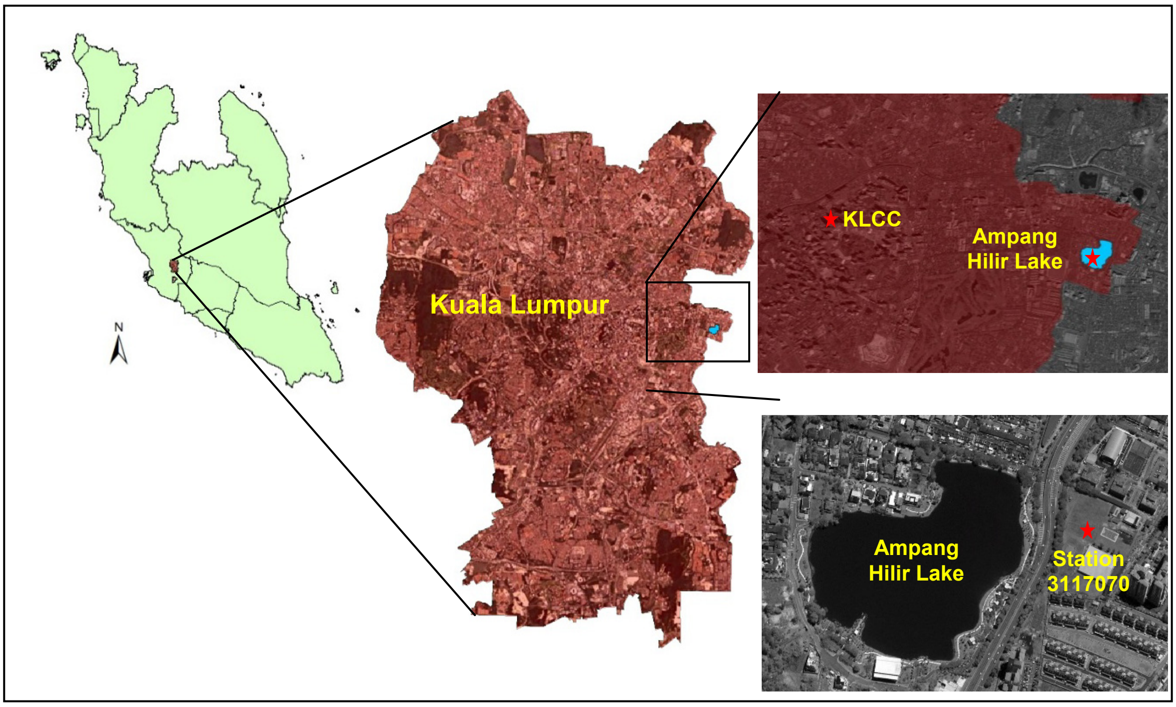

Figure 1. Location of Ampang Hilir Lake, Kuala Lumpur.

2.2 Water Sampling and Data Collection

Water sampling and data collection at Ampang Hilir Lake were performed on November 2014, May 2015 and July 2015 which included wet season (Northeast monsoon), dry season (Southwest monsoon), and inter-monsoon season. All surface water samples were collected in 1000mL polyethylene bottles. A total of three (3) water samples at different locations were taken at the limnetic and littoral zones, respectively. Littoral zone of the lake consisted the main culverts that flowed into the lake. All water samples were sent to accredited laboratory for analyses based on the APHA standard method (2012). Parameters analyzed consisted of Biochemical Oxygen Demand (BOD), Chemical Oxygen Demand (COD), Ammonia Nitrogen (AN), Total Suspended Solid (TSS), Total Phosphorus (TP) and Orthophosphate (OP). In-situ physico-chemical parameters consisted of temperature (T), Dissolved Oxygen (DO), pH and Chlorophyll-a (Chl-a), were also collected using YSI Water Quality Multiparameter Probe Model 6600, 15cm below the water surface. Calibration of the YSI multiparameter probe was conducted in the laboratory before field sampling. 10 years (2006 – 2015) hydrological data was obtained from Department of Irrigation and Drainage (DID) for Station No. 3117070 which was located at DID Ampang, Kuala Lumpur.

2.3 Water Quality Data Analysis

Water quality data obtained was compared with the National Water Quality Standards of Malaysia, NWQS (DOE, 2012), Water Quality Index (WQI) of Malaysia, WQI (DOE, 2012), Department of Environment (DOE) Water Quality Index Classification (DOE, 2012), Trophic State Index, and TSI (Carlson & Simpson, 1996).

3 RESULTS AND DISCUSSION

3.1 Rainfall Pattern

Ampang Hilir, located in Kuala Lumpur at the west coast of Malaysia is also affected by seasonal changes in rainfall. Figure 2 shows the rainfall pattern of Ampang Hilir Lake based on the data obtained from the nearest rainfall station with No. 3117070, located at Department of Irrigation and Drainage (DID), Ampang, Kuala Lumpur from year 2006 to year 2015. It was observed that rainfall was high during inter-monsoon season between April and May and during Northeast monsoon (wet season) between the month of October and March. Rainfall was recorded lower during the Southwest monsoon season between the month of June and September which was considered as the dry season of the year.

3.2 Water Quality

Water quality data collection was performed during the inter-monsoon season (May 2015), Southwest monsoon (July 2015) which was the dry season and Northeast monsoon (November 2014) which was the wet season of the year. Water quality Index (WQI) and its classification at the limnetic zone of Ampang Hilir Lake is as displayed in Figure 3. It was observed that WQI during inter-monsoon was 82.35 ± 0.95 which was in

Class II (range between 76.5 – 92.7) of the Department of Environment (DOE) WQI classification. According to the DOE Water Quality Classification based on WQI, the water quality during the inter-monsoon season was categorized as Clean (ranged between 81 – 100). This might be due to the high rainfall during the month of April that helped to flush out most of the pollutants in the lake. However, during the dry season which was between June and September, it was observed that WQI dropped to Class III (ranged between 51.9 – 76.5) with value of 69.47 ± 2.81 as the rainfall was low during the dry season which was important for the dilution effect in the lake and to flush out the pollutants that flowed into the lake. The water quality during the dry season was classified as Slightly Polluted (ranged between 60 – 80). The water quality slightly improved to Class II during the Northeast monsoon season as rainfall was higher during the wet season. Water Quality Index (WQI) at the limnetic zone of the lake was recorded at 78.38 ± 0.75 which was classified as Slightly Polluted.

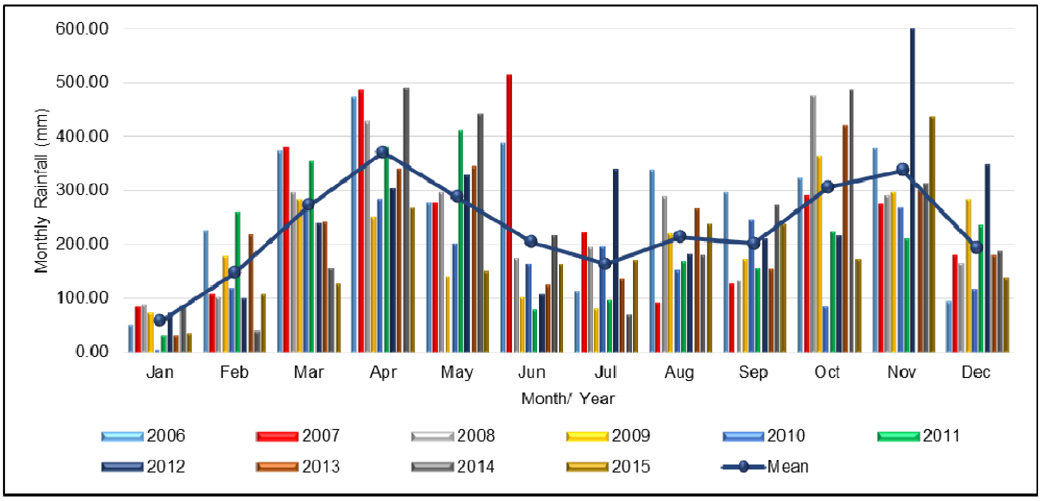

Figure 2. Rainfall pattern at Ampang Hilir Lake based on rainfall station No. 3117070 located at Department of Irrigation and Drainage (DID), Ampang, Kuala Lumpur.

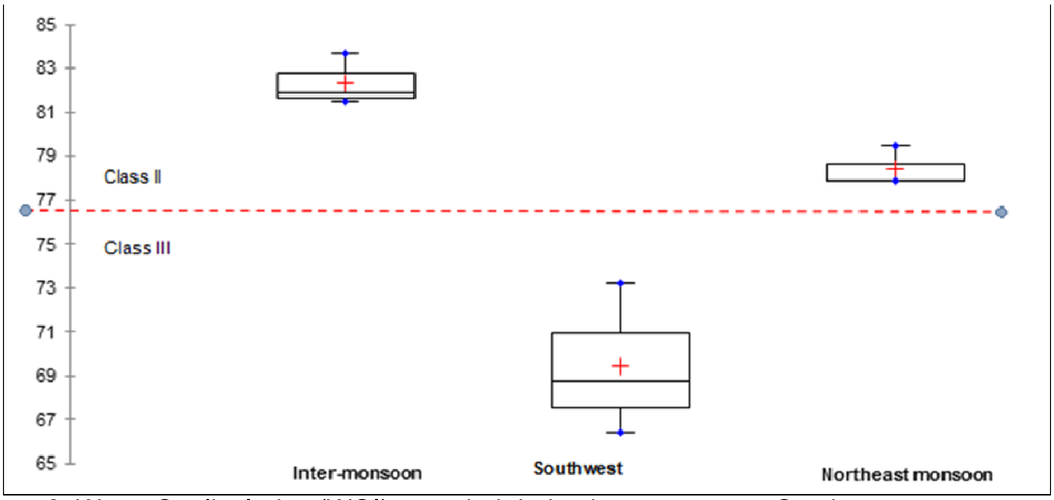

Figure 3. Water Quality Index (WQI) recorded during inter-monsoon, Southwest monsoon and Northeast monsoon season at limnetic zone of Ampang Hilir Lake from year 2014 to 2015.

Figure 4 shows the Water Quality Index (WQI) recorded at the littoral zone of Ampang Hilir during the inter-monsoon, Southwest monsoon and Northeast monsoon season from year 2014 to 2015. Littoral zone of the lake was known to contain higher pollutants as the sullage water from the catchment flowed into the lake through the culverts and have high accumulation of algal scum. It was observed that WQI at the littoral zone during the inter-monsoon season which depicted high rainfall was recorded at Class II with the value of 79.19 ± 1.25 but the water quality was Slightly Polluted. The water quality of Ampang Hilir Lake deteriorated to Class V or 28.74 ± 23.08 which was classified as Polluted under the DOE Water Quality Classification based on WQI. This was due to the lower rainfall and hotter weather with the continuous incoming flow of pollutants into the lake with reduced dilution and flushing out. Thick layer of algal scums were observed at the littoral zone of the lake where the culvert inlets were located. During the Northeast monsoon season, the water quality improved to Class II or 80.90 ± 3.64. This is due to the higher rainfall and higher volume of stormwater discharging from the culverts that gave better dilution in the lake and flushing from the lake.

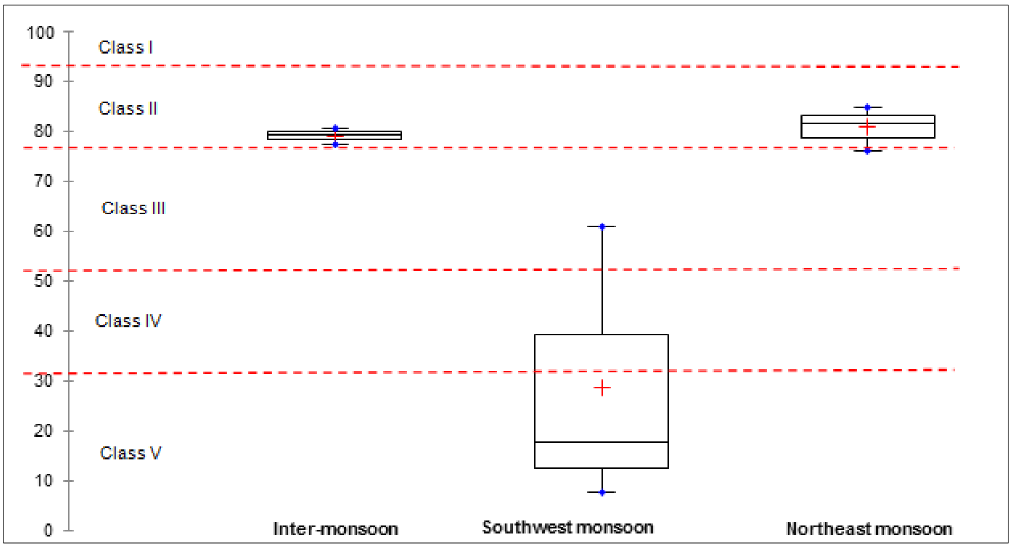

Figure 4. Water Quality Index (WQI) recorded during inter-monsoon, Southwest monsoon and Northeast monsoon season at littoral zone of Ampang Hilir Lake from year 2014 to 2015.

The water quality of Ampang Hilir Lake during inter-monsoon, southwest monsoon and Northeast monsoon season at the limnetic and littoral zone for the period of November 2014 to July 2015 is depicted in Table 1. It was observed that temperature was almost similar between three seasons with value being around 30°C at the limnetic zone of the lake. Temperature was higher at the littoral zone with values recorded between 31.12 ± 0.33 and 32.24 ± 1.24 as the water at this area was shallower compared to the deeper limnetic zone. Increasing water temperature values will lead to increase im evaporation from the water surface of the lake and finally increasing the content of salts (Said et al., 2012).

Table 1. Water quality during inter-monsoon, Southwest monsoon and Northeast monsoon season for limnetic and littoral zone of Ampang Hilir Lake, Kuala Lumpur for the period of November 2014 to July 2015.

No.	Parameters	Limnetic Zone			Littoral Zone			NWQS Class IIB
		Inter-Monsoon	Southwest Monsoon	Northeast Monsoon	Inter-Monsoon	Southwest Monsoon	Northeast Monsoon	
1	Temperature (°C)	30.83 ± 0.12	30.04 ± 0.28	30.21 ± 0.27	32.63 ± 0.74	32.24 ± 1.24	31.12 ± 0.33	-
2	pH	8.65 ± 0.14	7.61 ± 0.32	8.12 ± 0.08	8.99 ± 0.14	9.10 ± 0.37	8.06 ± 0.10	6 – 9
3	Dissolved Oxygen, DO (mg/l)	8.85 ± 1.26	6.22 ± 1.00	6.26 ± 0.28	9.71 ± 1.35	11.76 ± 1.03	6.71 ± 0.44	5 – 7
4	Biochemical Oxygen Demand, BOD (mg/l)	5.83 ± 0.56	12.27 ± 4.60	8.83 ± 0.70	6.30 ± 1.60	470.33 ± 355.98	8.10 ± 3.33	3
5	Chemical Oxygen Demand, COD (mg/l)	19.60 ± 2.26	38.77 ± 14.02	23.37 ± 2.00	22.30 ± 5.37	1,141.33 ± 815.27	21.23 ± 8.89	25
6	Ammonia Nitrogen, AN (mg/l)	0.57 ± 0.23	2.10 ± 0.54	0.72 ± 0.22	0.71 ± 0.20	1.67 ± 0.67	0.58 ± 0.01	0.3
7	Total Suspended Solid, TSS (mg/l)	2.67 ± 0.94	8.67 ± 4.50	3.00 ± 0.82	7.33 ± 2.36	602.00 ± 513.68	6.33 ± 0.47	50
8	Orthophosphate, OP (µg/l)	1,303.33 ± 228.08	466.67 ± 61.82	346.67 ± 4.71	1,203.33 ± 218.53	663.33 ± 129.19	403.33 ± 106.56	-

As for pH, the lake was slightly alkaline with value ranging from 7.61 ± 0.32 to 8.65 ± 0.14 for the limnetic zone, whereas the pH was higher at the littoral zone especially during dry season (Southwest monsoon season) with value recorded as high as 9.10 ± 0.37. Said et al. (2012) also reported that the lake was alkaline with an average of 8.76 during 2010. Typically, pH for a eutrophic lake ranges from 7.7 to 9.6 (Reddy and Vijaykumar, 2005). According to the National Water Quality Standards for Malaysia (NWQS), the pH value for Class IIB which is suitable for recreational body contact is between pH 5 to pH 9.

Dissolved Oxygen (DO) is important for the health and survival of aquatic life. Dissolved Oxygen (DO) recorded at the limnetic zone for 3 different seasons ranged between 6.22 ± 1.00 mg/l and 8.85 ± 1.26 mg/l. The DO at the littoral zone was recorded at a higher value between 6.71 ± 0.44 mg/l and 11.76 ± 1.03 for the

3 different seasons. Higher value of DO recorded at the littoral zone might be due to higher accumulation of green microalgae at this zone that released oxygen during photosynthesis process especially during dry season or Southwest monsoon season. Compared with the NWQS of Class IIB, DO recorded in the lake was within the standard range of 5 – 7 mg/l. However, these DO readings were collected during late morning or near noon with maximum sunlight and due to this; it is assumed thatactive photosynthesis process by green algae in the lake had taken place. Previous preliminary study by Ang et al. (2014) reported that DO was recorded as low as 2.91 mg/L and half of the sampling locations had DO below 4 mg/L which might signify oxygen deficiency. Low concentrations of DO below 5 mg/L may adversely affect the function and survival of biological communities and concentrations below 2 mg/L may lead to the death of most fish (Chapman, 1992) especially during night time where the aquatic organisms including microphytes, microorganisms and fishes, busily competes for DO for respirations and decompositions.

Study revealed that the lake had the highest Biochemical Oxygen Demand (BOD) value during dry season or Southwest monsoon season with value of 12.27 ± 4.60 mg/l followed by 8.83 ± 0.70 mg/l during Northeast monsoon and 5.83 ± 0.56 mg/l during inter-monsoon period. Littoral zone also depicted the same trend as the limnetic zone with BOD reading as high as 470.33 ± 355.98 mg/l during Southwest monsoon or dry season followed by 8.10 ± 3.33 mg/l during Northeast monsoon or wet season and 6.30 ± 1.60 mg/l during inter-monsoon. Higher BOD was observed during dry season due to lower dilution effect in the lake, higher pollutants and higher organic material from microalgae. All values for both zones exceeded the NWQS value for Class IIB of 3 mg/l. The BOD value recorded during the dry season was at Class V in the NWQS. High BOD readings indicate that high amount of available DO will be consumed by microorganisms during decomposition of organic materials, hence robbing dissolved oxygen of other aquatic organisms that is needed for survival especially the fishes in the lake (Ang et al., 2014).

Besides that, it was also observed that Chemical Oxygen Demand (COD) readings exceeded the NWQS for Class IIB of 25 mg/l during Southwest monsoon or dry season with the value of 38.77 ± 14.02 mg/l and 1,141.33 ± 815.27 mg/l at limnetic and littoral zone, respectively. The extremely high COD reading might be due to high oxygen-consuming substances in the chemical breakdown of organic content in water especially algae scum which was in abundance (Ang et al., 2014). Ammonia Nitrogen (AN) concentration was observed high as well during Southwest monsoon with value of 2.10 ± 0.54 mg/l and 1.67 ± 0.67 mg/l at limnetic and littoral zone, respectively, exceeding the NWQS for Class IIB of 0.3 mg/l. The readings observed during dry season were at Class IV (0.9 – 2.7 mg/l) in the NWQS. High ammonia content in the lake will increase the alkalinity of the lake where the pH of the water will increase. Ammonia has been reported to be toxic to freshwater organisms at concentrations ranging from 0.53 to 22.8 mg/L . However, ammonia toxic level is both pH and temperature dependent (Oram, 2014). Toxicity increases as pH increases and as temperature increases (Oram, 2014). Excess in ammonia will cause the death of fishes depending on the ammonia tolerant level of different types of fishes. Total Suspended Solid (TSS) was also reported higher during the dry season compared to the wet and inter-monsoon season. Littoral zone depicted higher TSS value compared to limnetic zone due to high algae accumulation near the edge of the lake.

High algae growth was due to high nutrient enrichment in the lake. Orthophosphate (OP) level in the lake was very high which aided the direct absorption of this nutrient by microphytes and subsequently causing algal bloom or eutrophication. OP was recorded very high during inter-monsoon in the month of May 2015 with value of 1,303.33 ± 228.08 µg/l and 1,203.33 ± 218.53 µg/l at limnetic and littoral zone, respectively. This could be due to high rainfall in April causing high runoff from the lake catchment and the nutrient will be consumed by the microalgae during dry season causing algal bloom and high TSS. During rainy season, the concentration of OP was recorded lower compared to inter-monsoon and dry season.

Physical observation during sampling showed that the lake was green in color with the formation of algal scums on the surface of lake especially at the littoral zone where the algae accumulated. Trophic State Index (TSI) (Table 2) showed that the lake was in eutrophic-hypereutrophic condition. In-situ Chlorophyll-a was almost similar between the 3 seasons at the limnetic zone with value ranging from 24.33 ± 1.65 µg/l to 30.15 ± 4.07 µg/l whereas Chlorophyll-a concentration was observed to be higher during the Southwest monsoon season compared to the other 2 seasons at the littoral zone of the lake with value of 58.61 ± 28.95 µg/l. Chlorophyll-a was lower during the wet season with value of 13.03 ± 5.75 µg/l due to higher dilution rate in the lake. Total Phosphorus (TP) was very high in the lake which will contribute to higher nutrient through phosphorus recycling and causing algal bloom in the lake. Secchi Depth (SD) reading was lower during dry season due to the blooming of algae causing low light penetration. The low light ecological state will shift the phytoplankton structure and composition towards cyanobacteria dominance which may cause sanitary risks since these organisms produce a wide variety of toxic and smelly secondary metabolites which impair all the water uses and represent a health risk for the urban population (Naselli-Flores, 2008).

4 CONCLUSIONS

Water quality study performed during inter-monsoon, Southwest monsoon (dry season), Northeast monsoon (wet season) at Ampang Hilir Lake, Kuala Lumpur revealed that water quality deteriorated during dry season (Class III) compared to inter-monsoon and improved to Class II during wet season at the limnetic zone.

Water quality was at Class V during dry season at the littoral zone and improved to Class II during wet season. Continuous nutrient enrichment from the lake catchment caused the lake to be in eutrophic-hypereutrophic condition with thick layer of algae scums forming on the lake surface. The decomposed algae scum together with the continuous inflow of pollutants into the lake will deteriorate the ecosystem health if proper action is not taken. Thus, systematic lake catchment management plan is necessary to control the pollutant loading and hydrological runoff within the catchment area. Besides, in order to conserve our urban lakes for better future, community involvement in lake conservation and water quality monitoring is essential to cultivate the sense of ownership among the people living within the lake catchment area.

Table 2. Trophic State Index (TSI) for limnetic and littoral zone of Ampang Hilir Lake, Kuala Lumpur during inter-monsoon, Southwest monsoon and Northeast monsoon season from November 2014 to July 2015.

No.	Parameters	Limnetic Zone			Littoral Zone		
		Inter-Monsoon	Southwest Monsoon	Northeast Monsoon	Inter-Monsoon	Southwest Monsoon	Northeast Monsoon
1	Chlorophyll-a (µg/l)	30.15 ± 4.07	24.70 ± 2.82	24.33 ± 1.65	24.46 ± 13.03	58.61 ± 28.95	13.03 ± 5.75
2	$TSI_{Chl\text{-}a}$	63.93 ± 1.28	62.00 ± 1.12	61.89 ± 0.65	60.70 ± 4.83	69.28 ± 5.03	54.92 ± 4.03
3	Total Phosphorus, TP (µg/l)	1,646.67 ± 437.59	560.00 ± 133.67	436.67 ± 4.71	2,063.33 ± 53.12	850.00 ± 85.24	500.00 ± 117.76
4	TSI_{TP}	110.37 ± 4.37	95.00 ± 3.37	91.81 ± 0.16	114.23 ± 0.37	101.35 ± 1.40	93.38 ± 3.30
5	Secchi Depth, SD (m)	0.57 ± 0.02	0.47 ± 0.05	0.82 ± 0.05	0.27 ± 0.12	0.08 ± 0.09	0.48 ± 0.15
6	TSI_{SD}	68.19 ± 0.59	71.06 ± 1.51	62.94 ± 0.85	81.24 ± 8.61	108.64 ± 18.45	71.16 ± 4.33

ACKNOWLEDGEMENTS

The authors sincerely thanks the Kuala Lumpur City Hall for their permission and co-operation in this study. Sincere appreciation to the Government of Malaysia for providing funds and support for the study and the contribution from the technical staffs of Water Quality and Environment Research Centre, National Hydraulic Research Institute of Malaysia (NAHRIM) is greatly acknowledged.

REFERENCES

Ang, S.Y., Ahmad, Z.A.T. & Shapiai, M.A.H. (2014). Assessment of Water Quality and Trophic State of Two Urban Lakes in Malaysia. *13th International Conference on Urban Drainage*, Kuching, Sarawak, Malaysia, 7-12 September 2014.

APHA, AWWA, WEF. (2012). *Standard Methods for the Examination of Water and Wastewater,* 22nd ed. American Public Health Association, Washington DC, USA.

Birch, S. & McCaskie, J. (1999). Shallow Urban Lake: A Challenge for Lake Management. *Hydrobiologia,* 395/396, 365 – 377.

Carlson, R.E. & Simpson, J. (1996). A Coordinator's Guide to Volunteer Lake Monitoring Methods. North American Lake Management Society. The Secchi Dip-In website. Available: http://www.secchidipin.org/tsi.htm [Accessed 16/02/2014].

Chapman, D. (1992). *Water Quality Assessment – A Guide to Use of Biota, Sediments and Water in Environmental Monitoring*. 2nd Ed., Chapman on behalf of UNESCO, WHO and UNEP, Chapman and Hall, London, 585.

DOE. (2012). *Malaysia Environmental Quality Report 2012*, Department of Environment (DOE), Malaysia.

Naselli-Flores, L. (2008). Urban Lakes: Ecosystem at Risk, Worthy of the Best Care. *Proceedings of Taal 2007: The 12th World Lake Conference*, 1333-1337.

Oram, B. (2014). Ammonia in Groundwater and Streams. Water Research Watershed Center. Available: http://www.water-research.net/index.php/ammonia-in-groundwater-runoff-and-streams [Accessed 31/01/2017].

Persson, J. (2012). Urban Lakes and Ponds. *Encyclopedia of Lakes and Reservoirs*, Springer, 836 – 839.

Reddy, M.V. & Vijaykumar, A. (2005). Seasonal Surfacewater Quality and Sediment Characteristics of the Urban Eutrophic Husainsagar Lake in Hyderabad, India. In *Restoration and Management of Trophical Eutrophic Lakes*, 42-45.

Said, K.S.A., Shuhaimi-Othman, M. & Ahmad, A.K. (2012). The Determination of Water Quality and Metal Concentrations of Ampang Hilir Lake, Selangor, Peninsular Malaysia. *Pakistan Journal of Biological Sciences,* 15(9), 437 – 447.

Proceedings of the 37th IAHR World Congress
August 13 – 18, 2017, Kuala Lumpur, Malaysia

ANALYSIS ON COMBINING LANDSCAPE PATTERN WITH HYDROLOGICAL ADJUSTING FUNCTION IN POYANG LAKE AREA

CHENGLIN LIU(1), XIA HU(2), XINGDONG ZHANG(3) & CHENJUN ZENG(4)

(1,2,3) School of Civil Engineering and Architecture, Nanchang University, Nanchang, China,
(4) Center for Eco-environmental Research, Nanjing Hydraulic Research Institute, Nanjing, China,
(4) College of Hydrodynamic and Ecology Engineering, Nanchang Institute of Technology, Nanchang, China,
liucl@qq.com; zhx0406@163.com; 417737835@qq.com; zcjling@163.com

ABSTRACT

With a variety of ecological service functions, Poyang Lake is also the largest freshwater lake in China. This study is based on the fundamental data of landscape pattern in 1990, 2000, 2005 and 2010 and the corresponding hydrological data, build the database in landscape pattern as well as flood storage capacity, and then proceed with further analysis on the change of flood storage capacity. The response relation and mechanism between landscape pattern and hydrological adjusting function is revealed by using grey correlation analysis. The results indicate that both regulation and storage capacity are of great state to protect drainage basin in Poyang Lake area from 1990 to 2010. There was a clear relationship between the landscape pattern and adjusting functions at different degrees, it is demonstrated that landscape plays an important role in economic development and ecological security, influence the function of flood storage at the same time. On the whole landscape, the correlation degree is largest between flood storage capacity and the diversity index (SHDI), which reaches 0.75. It shows that the regulation and storage capacity could be promoted when landscape pattern presented diversity. However, on the single landscape, the correlation degree between flood storage capacity and woodland area is also largest, with the value of 0.85, which explains that woodland would be helpful for water conservation and effective to change distribution around groundwater, soil water, runoff and evaporation.

Keywords: Poyang Lake area; landscape index; gray correlation analysis; flood storage capacity.

1 INTRODUCTION

There are only three freshwater lakes connecting with Yangtze River in China where the largest one is Poyang Lake. Five rivers in Jiangxi province flow into the lake, including Ganjiang, Fuhe, Xinjiang, Raohe and Xiushui. It has characteristics of flowing, swallowing and spiting, seasonality and so on. Meanwhile, it has abundant water resources and biodiversity that contribute to rapid development of the regional economy and contains huge ecological, economic and social value (Chen et al., 2008). The wetland of Poyang Lake plays an irreplaceable part in climatic regulation, purification and maintenance of overwintering habitat. After the research on evaluating importance of its ecological function, it is concluded that function of ecological adjustment is the major ecological function of Poyang Lake (Zhan et al., 2009). Maltby discussed the wetland function would be influenced seriously when ecosystem was being destroyed and the cost would be much more in repairing rather than protecting, so he suggested we should use and protect the wetland scientifically (Maltby, 1991). Besides, William J. Mitsch analyzed wetland was helpful for lakes and rivers to recover their ecological function as a buffer from the perspective of purification (Mitsch, 1995). But for a long time, it was easy to find that unreasonable development and utilization was ubiquitous at the time when humans benefited from Poyang Lake, the ecosystem had fluctuated according to time and wetland functions were in the danger. While each of the functions always connected with the others, the whole ecosystem lost stability eventually. On the other hand, most of the domestic and foreign related research concentrated on hydrological regime and spatial structure, which was on the base of the fact that Poyang Lake was a non-organism (Amoros and Bomette, 2002; Thoms et al., 2005; Kang et al., 2008; Zhang et al., 2012; Robinson et al., 2015). There was relatively less studies on combining landscape structure with hydrological adjusting function and the action process and mechanism of its self-structure, ecological process and ecosystem.

Landscape is the resource for human economic activities with the purpose of development and utilization. Human economic activities are mainly focused on the level of landscape, meanwhile, landscape structure can accurately show all kinds of spatial distribution and gradient variation features affected by ecology. It is possible to prove the effectiveness for various means in spatial structure research. Landscape pattern is a heterogeneous area that is made by interactions of ecological space. There are many remarkable characteristics that belong to landscape pattern such as spatial heterogeneity, regionalism, distinguishability and reproducibility, etc (An et al., 2009) with spatial autocorrelation is the most remarkable characteristic. The highly autocorrelation along a certain direction may foreshow that some kind of ecology process did important work in it (Dong et al., 2015). Landscape pattern influences ecology process (population dynamics, animal behavior, biodiversity, ecological physiology and ecology system process, etc) and we can have a better understanding of ecology process by researching spatial pattern. At present, domestic research about landscape mainly focused on the dynamic changes of landscape pattern with the wetland landscape fragmentation caused by human activities. Researchers especially paid attention to the research on larger spatial scale from the scale larger than basin to analyze the spatial variation characteristics. The depth was really inadequate in researching wetland landscape features and their connected hydrological adjusting function. With the development of "3S" technology, eco-hydrological study have begun to discuss the coupling relationship between hydrological adjusting and landscape pattern, which will become popular on future research as well (Li et al., 2008; Liu et al., 2012).

Therefore, realizing landscape management mode of the functionalized ecology system is likely to become the future development direction of ecological construction in Poyang Lake. This paper chose appropriate landscape index to establish a database. Based on the analysis of the change regulation of hydrological adjusting function for Poyang Lake in 1990, 2000, 2005 and 2010, this paper compared the correlation degree between landscape pattern and hydrological adjusting function, and then analyzed the reasons that correlation came into being. The above research results can provide scientific basis for improving the development of ecological construction of Poyang Lake as well as help for the future research of Poyang Lake and hydraulic project.

2 THE GENERAL SITUATION OF POYANG LAKE AND RESEARCH METHOD

2.1 The general situation of Poyang Lake

Poyang Lake lies in the north of Jiangxi Province and the geographic coordinates are 115°47' to 116°45' east longitude and 28°22' to 29°45' north latitude. Located in the middle and lower reaches of the Yangtze River, Poyang Lake is the largest freshwater lake in China. It adjusts water not only in the rivers of Jiangxi Province, but also in Yangtze River to flow backward. According to the statistics from 1955 to 2003, the runoff in three hydrological stations;Delta, Mei port and Li Jia Du increased rapidly from April to June, and it begun to decrease in July. But at the same time it was the time of flood season in Yangtze River. Affected by this, water in Poyang Lake seem to flow back into Yangtze River and water level rose up rather than having a downward trend (Wang and Pan, 2009).

In this paper, the Poyang Lake area refers to 11 cities and counties, as shown in Figure 1 with a total area of about 20206.10 km^2. In the lake area, it appears annular and layered landform, mountainous, hilly, hillock and plain shows alternately by high and low, and by the edge and inside. At the same time, hills are distributed from Jinxian to Yugan in the south of Lake, as well as the middle area of Duchang and Poyang. Hillock is distributed on both sides of the five rivers and the edge of the new fault basin. Plains are mainly distributed in the downstream river (Huo et al., 2011).

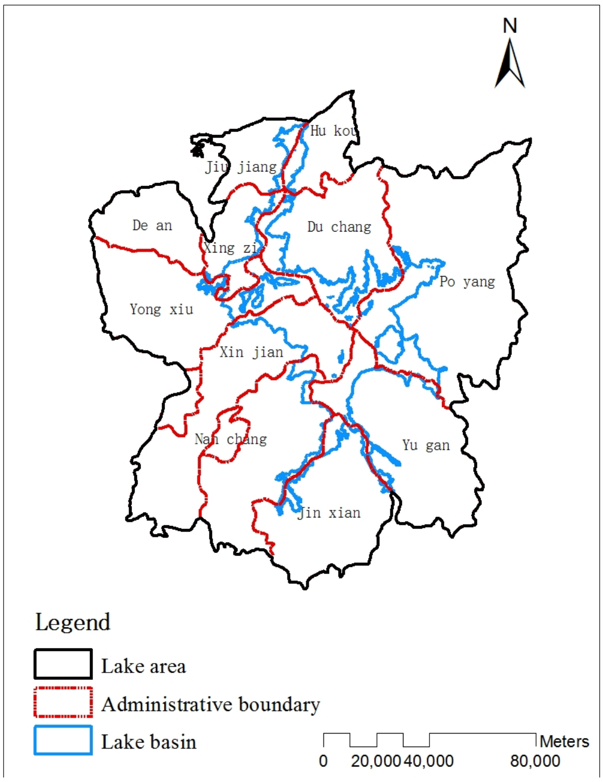

Figure 1. Sketch of Poyang Lake area.

The Poyang Lake area lies in the monsoon region of East Asia and the climate type is subtropical warm and humid climate. It has abundant rainfall, moderate temperatures and abundant light. The frost free period is nearly 300 days and the average annual precipitation is about 1472.2 mm, the average temperature ranges from 16°C to 19°C and the average evaporation is about 1003.7 mm. It's of great benefits for agriculture, forestry, animal husbandry and fishery to develop. Poyang Lake is an important base for producing grain, oil, cotton and fishes in Jiangxi Province and it is also the most developed area in Jiangxi Province.

2.2 Research method

In this paper, we select the relative landscape index and use Fragstats3.3 to build the landscape index database, then analyze the landscape pattern changes in the region in 1990, 2000, 2005 and 2010, respectively, and explored the reasons. At the same time we calculated the real-time flood storage in the four years and built a storage database, analyzed its changes, and then analysis the relationship between landscape pattern and adjusting function by using the gray correlation method. After that we gave the correlation value and made the sort. Finally we discussed the reasons and made the conclusion.

3 DATA SOURCE AND TREATMENT

3.1 Establish landscape pattern base for lake area

3.1.1 Landscape data source and landscape index choice

With the development of remote sensing technology, landscape index is also gradually improving. More and more landscape index and calculation methods are widely applied to land survey and landscape pattern and structure is concentrated and quantified by landscape index. At present, landscape index is the most intuitive and simple mean in landscape ecology study (Jiang et al., 2003; Qiao, 2014). In this paper, we adopted four TM remote sensing images in 1990, 2000, 2005 and 2010 whose resolving power is 30 meters. In China Resources and Environment Database as the basic data of landscape pattern in landscape ecology research, combined with the specific situation, we divided the Poyang Lake landscape into woodland, cultivated land, water area, artificial surface, grassland and unutilized land. Selected landscape indexes include: patch type area (CA), number of patch (NP), largest patch index (LPI), shape index (LSI), diversity index (SHDI), dominance index D, connectivity index (CON) and resolution index (F_i). All of the selected landscape indexes are calculated in Fragstats3.3.

3.1.2 Establish landscape index base

Combined with the landscape index chosen above, then established landscape index base are summarized in Table 1 and Table 2.

As shown in Table 1, the number of patch (NP) of landscape shows a trend of decrease as a whole from 1990 to 2010, which fluctuated lightly from the year 2000 to 2005. Among them, the NP decreased 8175 from 1990 to 2000 and 11782 from 1990 to 2010 if we measure it in a lengthy period of time, which indicates that the landscape in the region had been optimized during these time segment. The publishing policies like "afforestation" and "returning cultivated land to lake" directly contributed to the changes of landscape pattern. For the index of SHDI, it shows the rich degree of landscape type has increased in general. Due to the fact that water in lake area as the most dominant cover type, there was a decline for the dominance index (D) from 0.451 to 0.423 in 1990 and 2010. About value in largest patch index (LPI), the LPI of whole landscape type was consistent to the LPI of waters from Table 2, which illustrated that waters were the most advantageous land cover type. There was a close relationship between the illustration and the chosen in this paper which is the remote sensing image in plentiful water period.

Meanwhile, it can be seen from Table 2 that woodland area increased steadily. The increment from 2000 to 2010 is 2.06 times of that from 1990 to 2000. Although woodland area increased in general and there existed deforestation between 1990 and 2000, the deforestation phenomenon was relieved after 2000 with the policy of enhancing the power of rewards and punishments in "conversion of cropland to forest" and "afforestation'', forest coverage rate improve significantly as a result. The LPI also reflected the same deforestation phenomenon from 1990 and damaged the connection between large areas. The indices of NP, LSI and F_i all decreased during 1990 to 2000 and appear fluctuating later, which shows that interference from human activities has reduced after 2000.

Cultivated area decreased as well, during 1990 to 2000, the value was 547.463 km^2 and 183.652 km^2 during 2000 to 2005 and 472.084 km^2 during 2005 to 2010.The trend was directly related to the policies, especially in "conversion of cropland to forest" and "afforestation''. Besides, the economic development was so rapid that artificial surface obtains extension. The rapid economic development also urged some parts of cultivated areas transform into artificial surface. There was a steadily increasing trend in F_i, which shows that the same quality patches are separated by human interference. We can also know that the boundary of cultivated land suffered from interference by the fluctuating trend of LSI.

Water area decreased 25.57 km^2 during 1990 to 2000, there has been success in protecting Poyang water area by the "leveling embankment for flood running" and "returning cultivated land to lake" projects. The water area in 2005 was the same as that in 2000, but it begun to decrease after 2005 for the rapid extension of artificial surface and the accelerating process of industrialization and urbanization. The NP of water area was consistent with the change of water area, where the NP decreased 866 during 1990 to 2000, mainly because the decrease of water area. The change of NP during 2000 to 2005 was gently inclined and it was smaller than 866 during 2005 to 2010. It could be shown that government focused on green development strategy and rose a serious of ecological restoration engineering after 2005, such as "Green ecological Jiangxi", etc. Poyang Lake was the key construction object and water area achieved more and more attention. The LSI during 2005 to 2010 has decreased such that the boundary of water area tended to be regular. However, the LPI also decreased by 0.65%, so the connectivity of large water area lacked great protection at the time of improving Poyang Lake.

Table 1. Statistics of whole landscape index.

Year	Number of Patch NP	Largest Patch Index LPI (%)	Shape Index LSI (%)	Diversity Index SHDI (%)	Dominance Index D (%)	Connectivity Index CON (%)
1990	60041	21.642	319.111	1.341	0.451	53.702
2000	51866	21.664	302.110	1.357	0.435	53.686
2005	52591	21.662	303.568	1.351	0.441	53.809
2010	48259	21.012	293.319	1.369	0.423	53.394

Table 2. Statistics of landscape index of each land use type.

Land Use Type	Year	Patch Type Area CA (km^2)	Number of Patch NP	Largest Patch Index LPI (%)	Shape Index LSI (%)	Resolution Index F_i (%)
Woodland	1990	5008.786	11084	4.374	134.441	0.149
	2000	5234.608	9096	3.286	122.567	0.129
	2005	5490.031	10888	3.323	128.224	0.135
	2010	5700.639	10511	3.381	127.618	0.128
Cultivated area	1990	8259.04	9609	4.258	201.744	0.084
	2000	7711.577	9831	2.3	197.756	0.091
	2005	7527.925	9450	2.273	198.952	0.092
	2010	7055.841	8637	1.727	191.435	0.094
Water area	1990	5337.624	8984	21.642	88.202	0.126
	2000	5312.053	8118	21.664	79.668	0.121
	2005	5311.113	8110	21.662	79.677	0.121
	2010	5248.098	7570	21.012	76.545	0.118
Artificial surface	1990	895.018	18211	0.351	217.261	1.072
	2000	1500.551	19340	0.591	222.346	0.659
	2005	1491.272	19345	0.532	222.995	0.663
	2010	1894.994	17719	1.58	204.568	0.499
Grassland	1990	463.061	8238	0.032	143.327	1.393
	2000	366.199	4143	0.059	95.549	1.249
	2005	306.05	3519	0.059	87.157	1.378
	2010	226.272	3088	0.059	79.211	1.745
Unutilized Land	1990	242.569	3915	0.057	95.284	1.833
	2000	81.111	1338	0.058	51.355	3.205
	2005	79.707	1279	0.058	49.988	3.189
	2010	80.254	734	0.054	37.624	2.399

Grassland area, patch number and shape index all present downward trend, for the Poyang Lake achieved a certain development and planning. Moreover, unutilized land shows a reasonable planning as a whole.

3.2 Flood storage capacity calculation and analysis on Poyang Lake

Researchers usually measure the size of adjusting function of natural lake by using real-time flood storage capacity. Past study (Wu and Tan, 1996) has discussed the two lakes, Doting Lake and Poyang Lake about calculating the real-time flood storage capacity. It was pointed out that the real-time flood storage capacity was the detained flood volume in one or more periods and these periods had a feature that the inflow runoff is continuously larger than outflow runoff and it could be called regulation and storage period. This is shown in Figure 2 and the following calculation method.

$$W = \sum_{i=1}^{n} W_i \quad [1]$$

$$W_i = \int (Q_{in} - Q_{out}) dt \quad [2]$$

where W is the yearly flood storage capacity, W_i is the flood storage capacity during the period of i, n presents the number of real-time adjusting periods in a whole year, Q_{in} is total inflow water all day during the real-time adjusting period of i and Q_{out} is total outflow water all day during the real-time adjusting period of i.

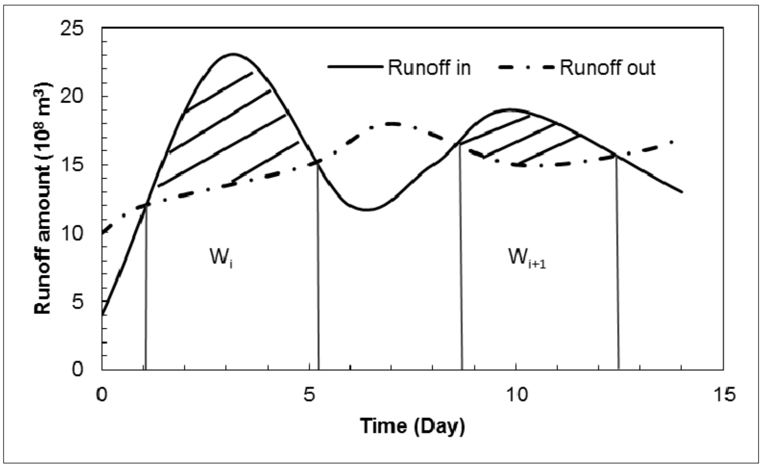

Figure 2. Schematic diagram of real-time storage process of Poyang Lake.

This paper used the mean daily discharge from seven hydrological stations, Changjiang, Anle, Fuhe, Xinjiang, Xiushui, Gangjiang and Liaoshui for statistic inflow runoff where the outflow runoff statistics came from the mean daily discharge of Hukou hydrological station.

After calculating by Eq. [1] and Eq. [2], the sum of real-time flood storage capacity in the years of 1990, 2000, 2005 and 2012 are summarized in Table 3.

Table 3. Statistics of flood storage capacity for four periods.

Year	1990	2000	2005	2010
Sum of real-time flood storage capacity in a year (×10^8 m^3)	181.2119	179.7307	216.4164	228.9976

As shown in Table 3, the flood storage capacity in 1990 is lower than that in 2000, the decrease amplitude is 0.82%. However, in comparison with the value in 2000, it appears clearly an increase in 2005 and the increased amplitude is 20.41%, and then the value in 2010 is even larger. Systematically, there are numerous factors influencing regulation and storage function. The regulation and storage capacity is of great state to protect drainage basin in Poyang Lake at present. It adjusts water not only in the inflow of five rivers, but also in Yangtze River to flow backward.

3.3 Calculating correlation degree between flood storage capacity and landscape structure

Grey correlation analysis can be understood as a method to quantify the correlation degree between factors through the similarity degree of the geometry of changing curve of each factor, also namely the similarity and dissimilarity degree between the development trends of factors. Therefore, this method can express the developing trend in the form of correlation degree. This is very suitable for analysis of dynamic course. Usually there are many kinds of methods for factor analysis, such as regression analysis. However it is quite clear that the study of the regulation and storage capacity of Poyang Lake shows grey system, the regulation and storage capacity is not suitable for regression analysis but suitable for the grey correlation analysis. Take Poyang Lake flood storage capacity as a reference sequence and landscape index as a comparison sequence, first we make standardized processing of each sequences, and then calculate the correlation degree and put them in order. The results are summarized in Table 4 and Table 5.

Table 4. Grey correlation degree between landscape index and flood storage capacity.

Landscape Index	SHDI	LPI	D	CON	NP	LSI
Grey Correlation Degree	0.75	0.60	0.59	0.59	0.55	0.55

Table 5. Grey correlation degree between landscape index of each land cover type and flood storage capacity.

Landscape Index	CA of Woodland	F_i of Grassland	CA of Artificial Surface	LPI of Artificial Surface	F_i of Cultivated Land	LPI of Grassland
Grey Correlation Degree	0.85	0.77	0.76	0.75	0.74	0.69
Landscape Index	NP of woodland	F_i of unutilized land	NP of artificial surface	LSI of woodland	LPI of unutilized land	F_i of woodland
Grey Correlation Degree	0.68	0.63	0.62	0.61	0.59	0.58
Landscape Index	LSI of artificial surface	LPI of water area	LPI of woodland	LSI of cultivated land	CA of unutilized land	CA of water area
Grey Correlation Degree	0.58	0.57	0.55	0.55	0.53	0.52
Landscape Index	NP of unutilized land	LPI of cultivated land	F_i of artificial surface	LSI of water area	LSI of unutilized land	F_i of water area
Grey Correlation Degree	0.52	0.52	0.51	0.51	0.51	0.51
Landscape Index	NP of water area	NP of cultivated land	NP of grassland	LSI of grassland	CA of cultivated land	CA of grassland
Grey Correlation Degree	0.51	0.51	0.50	0.50	0.48	0.47

4 ANALYSIS OF RESULTS AND CONCLUSIONS

(1) Grey correlation analysis between the whole landscape index and flood storage capacity:

As shown in Table 4, there exists a correlation between landscape index and flood storage capacity. As a whole, SHDI had the largest correlation degree with flood storage capacity. Compared to the flood storage capacity in Table 5, we could find that regulation and storage capacity would be promoted when landscape pattern presented diversity. The single landscape pattern was not beneficial for regulation and storage. Kinds of landscape types could complement each other and water achieved conservation at the time of landscape tended to be diverse. There had certain relevance within LPI and flood storage capacity, the largest patched in lake area was water patches. It was obvious that water area was directly related to the size of flood storage capacity. The correlation degrees were all 0.59 between the indices of D and CON and flood storage capacity, combining the two indices could show that a certain or several dominant species have formed great connectivity. The greater connectivity is, the stronger flood channel, flood accommodation and regulation and storage. The correlation degrees between the indices of NP and LSI and flood storage capacity were the lowest, it showed that the more the number of patches is, the more complicated the shape is and the higher the adjusting function, while the improve results were not obvious.

(2) Grey correlation analysis on landscape index of each land cover type and flood storage capacity:

We could also find from Table 5 that the largest correlation degree with flood storage capacity was woodland area, which reached 0.85. Because the woodland was beneficial for water conservation and it could change the distribution of water resources in around groundwater, soil water, runoff and evaporation. The canopy layer and litter layer in forests had high rainfall interception rate, the low sections had high soil infiltration rate, the roots of trees could enhance to absorb the layer water and the canopy layer could interfere the flow path of air, water in area achieved conservation finally. Therefore, the more number of patches is, the more areas are and the more beneficial for water conservation. The correlation degree between LSI and flood storage capacity was 0.61, so the shape of woodland benefited regulation and storage by being complicated. The more complicated the shape, the more complicated the water cycle in area, and then the more the transformation and consumption of water resources. The correlation degree between LPI and flood storage capacity showed the largest patch of woodland could not influence the regulation and storage capacity in the whole lake area totally. In general, woodland could effectively reduce soil and water loss and improve water retention.

In the meantime, the correlation degree between artificial surface area and flood storage capacity was 0.76 and the correlation degree between LPI and flood storage capacity was 0.75. With development and utilization of Poyang Lake, the reserved space in adjusting flood also turned large, while the increased correlation degree between LPI and flood storage capacity reflected that the largest patch area was also one of the most demands for water resources, which was consistent with the reflection of artificial surface area. The correlation degree between NP and flood storage capacity was 0.62, so the increased number of patches presented the increased number of the newly development and utilization areas, it increased the fate and dosage of water as well. Due to the large LSI of polder embankment, flood control project and river regulation works, the correlation degree between LSI and flood storage capacity was 0.58, these projects had obvious function in flood control and regulation and storage.

A part of grassland concentrated near Poyang Lake and it increased with the decrease of water level. The greater resolution is, the more serious water level separated by water area, from the side, it could be explained the larger water area is, the larger volume for water storage. As shown in Table 5, the correlation degree between F_i of grassland and flood storage capacity was 0.77, so we should regulate the land types that hinder ecological connection. But only for regulation and storage period for fear of destroying biotope landscape and wetland ecosystem would not out of balance. It was not remarkable, although grassland would give hydrological process a certain effect, especially the correlation degree between CA of grassland and flood storage capacity, which was only 0.47 and it was smaller than resolution coefficient of grey correlation analysis, so the larger patch area, the smaller regulation and storage capacity.

Most of the cultivated land in the lake area is paddy field and the consume water is mainly from Poyang Lake and its watershed. The correlation degree between F_i of cultivated land and flood storage capacity was very high at 0.74. The larger F_i is, the more scattered water source and more beneficial to storage. Correlation effects of LSI of cultivated land and other index with flood storage capacity was not obvious because paddy field occupied a large proportion in the cultivated land. Although crop needed water for support during its growth period, it wouldn't be like woodland which had a strong influence on hydrological process.

One part of the unutilized land in lake area was mudflat or beach, distributed nearby lake basins. The correlation degree between F_i and flood storage capacity was the largest at 0.63, then the correlation degree between LSI and flood storage capacity was 0.59, the conditions of these two degrees were familiar with grassland above.

Overall, the process of industrialization and urbanization is still deepening. The artificial surface is still in the trend of expansion. Domestic and industrial water demand is still increasing. Therefore, we recommend reasonable planning of artificial surface construction, scientific calculation of water resources consumption. Especially for those large and medium-sized cities and the surrounding areas of Poyang Lake, which relying on the water source of Poyang Lake, they should use the water source in a planned way, try to store water in the regulation and storage period and reduce the overexploitation of water source in dry season. In addition, they should strengthen and harden flood control projects, construct water storage projects, conduct regular inspection and risk mitigation of water conservancy project. If there has been no reasonable utilization and protection of the water source in Poyang Lake, not only the ecosystem will be influenced, but also water supply in the lower Yangtze River will also be threatened.

Landscape pattern of Poyang Lake has an important influence on the hydrological adjusting function in the region. During 1990 to 2010 the landscape pattern of Poyang Lake changed remarkably, reflecting that the human activities intervened greatly in it. There is different relevance between landscape pattern and hydrological adjusting function. According to the relevance, they should develop effective configuration scheme for optimizing Poyang Lake landscape and protect ecological security and ecosystem diversity of Poyang Lake.

ACKNOWLEDGEMENTS

The research reported herein is funded by Graduate Innovative Foundation of Nanchang University.

REFERENCES

Amoros, C. & Bomette, G. (2002). Connectivity and Biocomplexity in Waterbodies of Riverine Floodplains. *Freshwater Biology*, 47(4), 761-776.

An, C., Liu, S.L., Li, X.J. & Qiu, Y. (2009). Application of the Principles of Landscape Ecology on Land Consolidation. *Areal Research and Development*, 28(6), 68-74.

Chen, M.J., Wang, L.Q., Feng, H.L., Dai, X.Q., Huang, C.S. & Wang, G.X. (2008). Theory and Analysis of Wetlands' Eco-hydrological Configuration. *Acta Ecologica Sinica*, 28(6), 2887-2893.

Dong, Y.H., Liu, S.L., An, N.N., Yin, Y.J., Wang, J. & Qiu, Y. (2015). Landscape Pattern in Da'an City of Jilin Province Based on Landscape Indices and Local Spatial Autocorrelation Analysis. *Journal of Natural Resources*, 30(11), 1860-1871.

Huo, Y., Wang, L.C., Chen, X.L. & Meng, H.H. (2011). Long-term Trend and Persistence of Precipitation Over Lake Poyang Basin Since 1950s. *Journal of Lake Sciences*, 23(3), 454-462.

Jiang, X.B., Sun, Y., Zhou, W.C. & Li, A.N. (2003). A Study on the Land Use Dynamic Changes Based on Remote Sensing and GIS. *Resources and Environment in the Yangtze Basin*, 12(2), 130-135. (in Chinese)

Kang, W.X, He, J.N. & Xi, H.Z. (2008). Study on Function of Water Storage and Regulation of Dongting Lake Beaches and Meadow Marsh Wetlands. *Journal of Soil and Water Conservation*, 22(5), 209-216.

Qiao, G.L. (2014). Study on Mountainous Landscape Ecology Assessment Based on GIS -- A Case Study in Sapa district, Laocai province, Vietnam, *Ph.D. Dissertation*. China University of Geosciences.

Li, S.N., Wang, G.X. & Deng, W. (2008) Research advances in wetland landscape pattern and hydrological process. *Chinese Journal of Ecology*, 27(6), 1012-1020.

Liu, N., Wang, K.L. & Duan, Y.F. (2012). Analysis on the Responses of Flood Storage Capacity of Dongting Lake to the Changes of Landscape Patterns in Dongting Lake Area. *Acta Ecologica Sinica*, 32(15), 4641-4650.

Maltby, E. (1991). Wetland Management Goals: Wise Use and Conservation. *Landscape and Urban Planning*, 20, 9-18.

Mitsch, W.J. (1995). Restoration of Our Lakes and Rivers with Wetlands — An Important Application of Ecological Engineering. *Water Science and Technology*, 31(8), 167-177.

Robinson, S.J, Souter, N.J. & Bean, N.G. (2015) Statistical Description of Wetland Hydrological Connectivity to the River Murray in South Australia Under Both Natural and Regulated Conditions. *Journal of Hydrology*, 531, 929-939.

Thoms, M.C., Southwell, M. & McGinness, H.M. (2005). Flood Plain-river Ecosystems: Fragmentation and Water Resources Development. *Geomorphology*, 71(1-2), 126-138.

Wang, H.J. & Pan, W.Y. (2009). A Study on the Causes and the Atmospheric Circulation Characteristics of Abnormal Rainfall in South China during 2008. *Tropical Geography*, 29(3), 213-224.

Wu, D.X. & Tan, Q.F. (1996). Analysis on Calculating Real-Time Storage Capacity of Doting Lake and Poyang Lake. *Yangtze River*, 27(4), 29-32. (in Chinese)

Zhan, J.Y., Shi, N.N. & Deng, X.Z. (2009). Spatial Identification and Representation of the Core Ecosystem Services in Poyang Lake Area. *Geographical Research*, 28(4), 1022-1030.

Zhang, L.L., Yin, J.X., Jiang, Y.Z. & Wang, H. (2012). Relationship between Hydrological Conditions and Vegetation Communities in Poyang Lake National Nature Reserve of China. *Advances in Water Science*, 23(6), 768-775.

